UNIVERSIDAD NACIONAL AUTÓNOMA DE MEXICO

POSGRADO EN CIENCIAS E INGENIERÍA DE MATERIALES
CENTRO DE FÍSICA APLICADA Y TECNOLOGÍA AVANZADA

STUDY OF THE RING-OPENING POLYMERIZATION OF NON-IONIC EUTECTIC MIXTURES FOR THE SYNTHESIS OF MACROPOROUS POLYESTERS BY EMULSION TEMPLATING

TESIS
PARA OPTAR POR EL GRADO DE

DOCTOR EN CIENCIA E INGENIERÍA DE MATERIALES

PRESENTA:
M. en C. MARTÍN CASTILLO SANTILLAN

TUTORES PRINCIPALES
DR. JOSUÉ DAVID MOTA MORALES
CENTRO DE FÍSICA APLICADA Y TECNOLOGÍA AVANZADA
UNIVERSIDAD NACIONAL AUTÓNOMA DE MÉXICO

PROF. KATJA LOOS
ZERNIKE INSTITUTE FOR ADVANCE MATERIALS
UNIVERSITY OF GRONINGEN

MIEMBROS DEL COMITÉ TUTOR

DRA. LARISSA ALEXANDROVA
INSTITUTO DE INVESTIGACIONES EN MATERIALES
UNIVERSIDAD NACIONAL AUTÓNOMA DE MÉXICO

DR. JORGE HERRERA ORDOÑEZ
CENTRO DE FÍSICA APLICADA Y TECNOLOGÍA AVANZADA
UNIVERSIDAD NACIONAL AUTÓNOMA DE MÉXICO

CIUDAD DE MÉXICO. AGOSTO DEL 2023.

Ring-Opening Polymerization of non-ionic eutectic mixtures for the synthesis of macroporous polyesters by emulsion templating

Castillo Santillan Martín

university of groningen / faculty of science and engineering / zernike institute for advanced materials

Study of the Ring-Opening Polymerization of non-ionic eutectic mixtures for the synthesis of macroporous polyesters by emulsion templating

Castillo Santillan Martín

PhD Thesis

University of Groningen

The Netherlands

Zernike Institute PhD thesis

The work described in this thesis is a bilateral collaboration between The University of Groningen and Universidad Nacional Autónoma de México for obtaining a double degree. The research activities were performed at Macromolecular Chemistry and New Polymeric Materials Group, part of the Zernike Institute for Advance Materials (Groningen, The Netherlands), and at the Centro de Física Aplicada y Tecnología Avanzada (Querétaro, México). This work was founded by CONAHCYT, UNAM, the Faculty of Science and Engineering (RUG), and the Executive Board of the University of Groningen.

Cover: design by Dra. Maria Priscila Quiñonez Angulo, Lic. Kaori Sanchez, and M.Sc. Saúl Carrasco Saveedra.

Interior page layout by Martín Castillo Santillán

Printed by: Zernike Institute for Advanced Materials PhD-thesis series 2023.

Supervisors

Dr. Josué David Mota Morales /UNAM
Prof. Katja Ursula Loos /Zernike

Co-supervisors

Dr. Dina Maniar /Zernike

JURADO DE GRADO ASIGNADO

Dr. Ricardo Vera Graciano
Presidente

Dr. Josué David Mota Morales
Primer Vocal

Dr. José Román Torres Lubián
Segundo Vocal

Dra. Lilian Irais Olvera Garza
Tercer Vocal

Dr. Gonzalo Ramírez García
Secretario

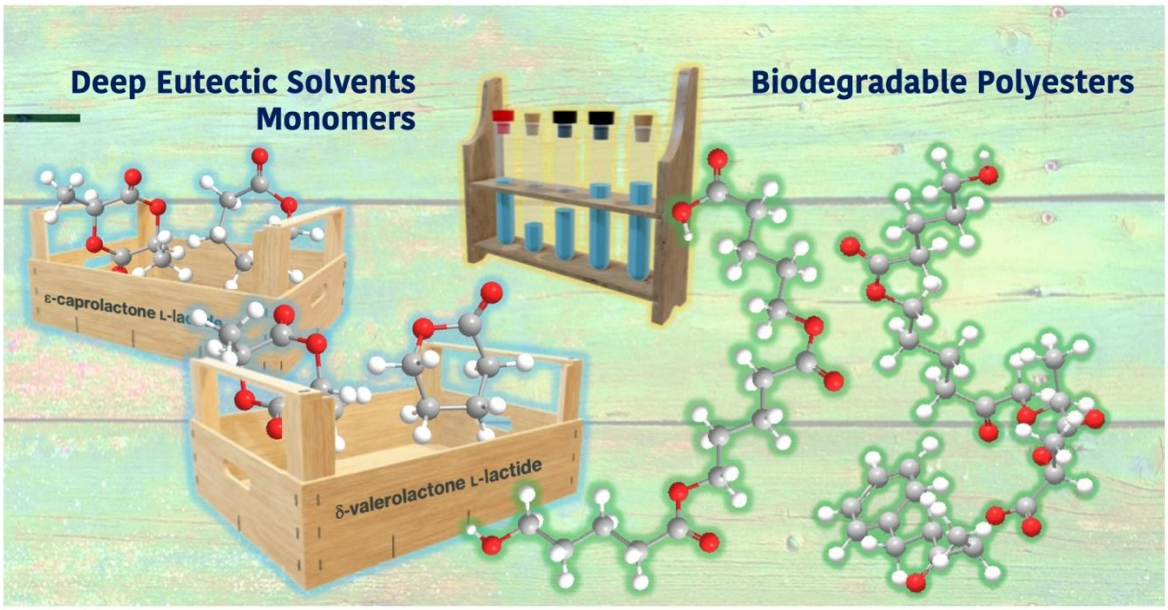

Thesis cover (printed version) will be used for the defense at the University of Groningen.

"The front displays the outer cover used for the printed version of the thesis by the University of Groningen."

The design of the outer cover for the printed book was created by Dr. María Priscila Quiñonez Angulo, Lic. Kaori Sánchez, and M.Sc. Saúl Carrasco Saavedra. The image depicts eutectic blends comprised of lactones and lactides, which, under suitable conditions, can be employed for the synthesis of intrinsically biodegradable polyesters.

To my beloved wife and my wonderful children

With sincere gratitude, I dedicate this thesis to you.

You are my loves, my life, and my guides.

Objectives of the thesis

To study the ring-opening polymerization (ROP) of non-ionic deep-eutectic solvent (DES) monomers composed of different lactones and stereoisomers of lactide, to propose synthetic conditions for fine-tuning polyesters' properties such as molecular weight, architecture, and crystallinity.

To synthesize hierarchical porous polyesters by the ROP of DES monomers composed of lactide and lactones, comprising the continuous phase of nonaqueous high internal phase emulsions, and to study the obtained macroporous interconnected scaffolds' degradation profiles and mechanical properties.

The specific objectives were:

To describe the physicochemical properties of the lactide/lactone non-ionic DES monomers.

To study the impact of different lactide isomers and lactones on their solventless ROP using different organocatalysts.

To modify the polyesters' properties resulting from the ROP of the corresponding DES monomers (lactide isomers or lactones) by adding suitable macroinitiators.

To design stable oil-in-DES, high internal phase emulsions (HIPEs) and to study the conditions for the ROP of the continuous phase.

To synthesize pHIPEs via ROP of DES (lactide and lactone), to modify the molecular weights crystallinity, and architecture of the final 3D polyesters, and to obtain scaffolds with tunable degradation profiles and physicochemical properties.

Propositions

Accompanying the dissertation

Study of the ring-opening polymerization of non-ionic eutectic mixtures for the synthesis of macroporous polyesters by emulsion templating.

Castillo Santillan Martín

1. DES monomers composed of lactones and lactides can be polymerized using organocatalysts at low temperature and a solventless route.

   -Chapters 2-4 of this thesis

2. The production of copolymer and homopolymer blends composed of polylactides and polylactones is achieved through a greener route.

   -Chapters 2-4 of this thesis

3. The final properties of poly-L-lactide and poly-ε-caprolactone can be tuned by modifying parameters in the ring-opening polymerization (ROP) of L-lactide and ε-caprolactone DES monomers.

   -Chapter 2 of this thesis

4. The compositional versatility of non-ionic DES monomers enables the production of copolymers and homopolymers by changing the lactone in the systems.

   -Chapter 3 of this thesis

5. The ROP of non-ionic DES monomers and functional macroinitiators allow obtaining polyesters with controlled molecular weight, crystallinity, molecular architecture, and degradability.

   -Chapter 4 of this thesis

6. Biodegradable macroporous scaffolds can be obtained from the ring-opening polymerization (ROP) of nonaqueous high internal phase emulsions (HIPEs) containing DES monomers.

   -Chapter 4 of this thesis

Contents

CHAPTER 1

Facile and green alternative route to obtain polylactides and polylactones by the ROP of eutectic mixtures composed of lactide/lactones.

This section provides the state-of-the-art for understanding the experimental work done in this thesis. The chapter started with an introduction to polymers and a variety of their applications, including their production around the world, as well as the environmental and health issues that are driving the present situation. Subsequently, the introduction of polylactides and polylactones, which are biodegradable polyesters, are described. The current production of polylactides and polylactones in industry, e.g., by bulk and by ring-opening polymerization (ROP), is also described. This process excludes the use of solvents, albeit it depends on the use of metal catalysts. In this chapter, an understanding of eutectic blends, and previous research on polyester production and applications of DESm are summarized. Finally, the challenges of synthesizing these polyesters using DESm are discussed.

1.1 Polymers and plastics sustainability

Polymers are macromolecules formed by the union of many smaller molecules called monomers. The reaction by which polymers are obtained is called polymerization. A single polymer can be composed of hundreds or thousands of monomers. Polymers are generally used as plastics, rubber, fibers, coatings, adhesives, foams, and films and have been widely used in all aspects of our society.[1,2] Today, polymers have been designed with high quality and versatility, which has given us comfort and well-being.[3] In addition, due to the ease of production and the enabled properties, such as durability, strength, and light weight, they have been applied in areas that have been limiting for other materials.[4]

The words plastics and polymers are often used interchangeably. The word 'Plastics' comes from Latin or Greek words suggesting 'able to be molded'. In practice, the word 'plastics' tends to be used only in the plural by people in the industry to avoid confusion with the adjective 'plastic' used to describe permanent changes of shape or 'plastic deformation' that can occur in any material. Additionally, 'plastics' commonly refer to commercial materials containing not only polymer macromolecules but also additives such as colorants, stabilizers, flow modifiers and other chemicals needed to produce stable commercial materials.[5]

In parallel with petrochemical industry growth and progress in technological development, the demand for polymers is enormous, reaching 368 million metric tons in 2019, and is expected to grow to a total of 1.1 billion metric tons by 2050.[6] In 2017 it was reported that there are 60,000 different plastic formulations and that just six polymer groups account for 90% of total plastic production: polypropylene (PP), high-density and low-density polyethylene (PE), polyethylene terephthalate (PET), polyvinyl chloride (PVC), polystyrene (PS), and polyurethanes (PU).[7] The majority of these plastics are obtained from petroleum-based resources and are also single-use, i.e., once they have fulfilled their purpose, they are disposed of, and this represents losses of 95% of the materials, which are valued at between 80,000 and 120,000 million dollars annually. The increasing consumption of crude oil has an impact on its market price, which is also another issue that has generated considerable concern.[4]

Fossil resources will be rapidly depleted within several hundred years; in parallel to their use as energy, their consumption in the polymer industry poses serious environmental concerns.[4,8] Moreover, environmental concerns in polymer production are increasing, e.g., the use of toxic chemicals, such as metal catalysts and additives.[4,9,10] Organic solvents are also typically used as auxiliaries in polymer production; they account for an estimated 80% of the total chemicals used in polymer synthesis, the vast majority of which are volatile and toxic.[11]

The durability characteristics are intrinsic properties of polymers; most of them have a long period of degradation or decomposition. In 2003, plastics represented a large part of domestic and industrial waste (10-30%).[12] Numerous forms of plastic waste have been found in the ecosystem, including their microscale fragments (microplastics). In addition to environmental pollution, microplastic waste is also known to have a negative impact on human health.[8,13] The handling of plastic waste disposal has not been properly managed for many decades, and there are no appropriate end-of-life strategies for plastics.[14,15] In a substantial majority of countries, the prevalent method of plastic disposal involves depositing plastic waste in landfills, leading to significant adverse environmental impact, and oftentimes, their capacity is insufficient to handle the increasing waste;[3] and their capacity is insufficient. As a result, plastic waste is found in freshwater reservoirs, representing 57% of the total debris.[15] Global plastic production exhibits a recycling rate of only 9%, while approximately 12% of the produced plastic undergoes incineration.[16] Adverse health and environmental effects caused by the current production model of commercial polymers have triggered the demand for more environmentally friendly alternatives and formulations.[17] Therefore, in recent decades, many efforts and studies have been performed on biodegradable, biobased polymers and greener polymer production.[18]

1.2 Biodegradable polymers

Biobased polymers are those obtained from renewable resources or biomass. It is worth noting that not all plastics obtained from natural resources are biodegradable. Plastics themselves can be split into two categories: petroleum-derived and biobased plastics. However, a limited number of them are biodegradable. (See Figure 1).[19]

Bioplastics, as defined by the official European Bioplastics industry association, encompass plastics that are either biobased, biodegradable, or both. Biobased plastics are derived from renewable biomass sources, while biodegradable plastics have the ability to break down through microbial action under specific conditions. Categorizing bioplastics based on their biobased or biodegradable properties is crucial for understanding their characteristics and environmental impact.[6]

Bioplastics are a promising alternative to petroleum-derived plastics, possessing comparable properties that have the potential to reduce environmental impact by diverting challenging-to-degrade single-use plastic waste. However, the biodegradability of bioplastics, while beneficial for addressing plastic pollution, introduces complexities. Variability in biodegradation efficiency and uniformity across diverse environments may lead to incomplete degradation and the release of harmful byproducts. Therefore, maximizing the environmental benefits of biodegradable bioplastics requires meticulous consideration of their inherent characteristics and appropriate disposal strategies. Currently, bioplastics only account for 1% of the 370 million tons of total plastics generated.[21] By 2025, however, annual growth rates of bioplastics are expected to be approximately 30%.[8,17]

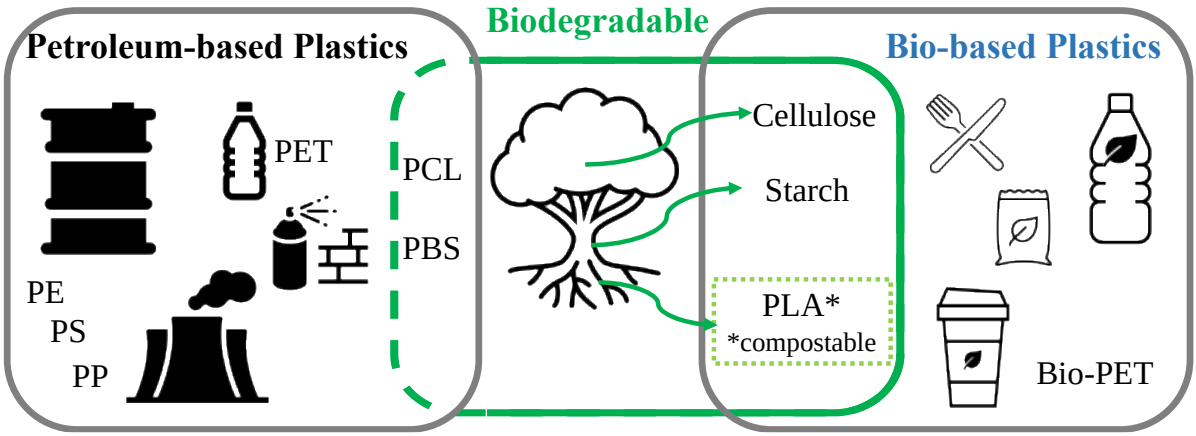

Figure 1. General classification of plastics (petroleum and biobased plastics).[20] Polyethylene terephthalate (PET), polyethylene (PE), polypropylene (PP), polystyrene (PS), polycaprolactone (PCL), polybutylene succinate (PBS), polylactide (PLA).

Some bioplastics, as well biodegradable or compostable polymers, have the ability to degrade in CO_2, water, or biomass due to the action of microorganisms, whereas a specific amount of mass loss needs to be observed in a specific short-term and under specific conditions.[22] Efforts have been made to enhance the production of biodegradable and compostable polymers in order to mitigate the environmental impact of plastic materials, and some of them are in growing demand as alternatives and have reached a stage of development where they offer nearly the same technical properties as plastics of fossil origin.[20] However, despite its advantages, there are still some drawbacks associated with this material. One of the main concerns is its limited mechanical strength, which can make it less suitable for certain applications. Additionally, the use of non-degradable additives to enhance its properties is also a point of concern, as it can contribute to environmental issues.

Hence, the applications of biodegradable polymers still have limitations in being implemented for widespread use.[20,23] In addition, biodegradable polymers have not yet been widely enhanced because of the lack of large-scale manufacturing and, in some cases, the high production cost compared to the production of fossil-based plastics. Moreover, technical limitations in their manufacturing often cause low production yields.[24,25] Nevertheless, there are continuous efforts by academia and industry to overcome these shortcomings. Most biodegradable polymers comprise urethanes, orthoesters, carbonates, anhydrides, amides, and polyesters, as detailed below. The degradation mechanisms of polyesters, for example, are due to the susceptibility to hydrolyze the ester bond.[26]

1.3 Polyesters

Polyesters are considered alternative to certain plastics since some of them are biodegradable or compostable.[27,28] In addition, some polyesters are recyclable; thus, they offer a sustainability advantage in terms of low environmental impact after their disposal.[29] The annual polyester production was estimated at 57.1 million tons in 2020, [30] and is classified into two major groups according to their source of origin: natural and synthetic.[31] Polyesters can also be classified as thermoplastics and thermosetting resins,[31] and based on their monomer structure, polyesters can be classified as either aliphatic, aromatic, or semi-aromatic. The versatility of the properties presented in polyesters depends upon the type of monomers used in their synthesis.[31]

Aliphatic polyesters have a linear chain structure and, for example, are mostly readily biodegradable and have poor mechanical properties. Furthermore, some aliphatic polyesters can be produced from biobased monomers, such as polylactic acid.[32] In comparison to aliphatic polyesters, aromatic polyesters usually possess better mechanical and thermal properties. The incorporation of aromatic structures can improve mechanical properties but also impact their biodegradability.[27] The general structure and example of polyesters are depicted in Figure 2. Some examples of polyesters are polyethylene terephthalate, polylactides, and polylactones, which account for 60% of the overall plastic demand in Europe.[27]

In general, there are two polymerization methods to synthesize them: polycondensation and ring-opening polymerization (ROP).[33] Polycondensation is a common method used in industries; however, extreme conditions such as high temperatures above 150 °C, low pressures, long polymerization times, and metallic catalysts are often needed. Other drawbacks are the reaction's reversibility, which can reduce the yield, and the possibility of monomer evaporation.[33] ROP is preferable due to the greater control obtained in the distribution and molecular weight of the product, fast polymerization time with fewer presence of byproducts. ROP synthesis is typically performed in several steps with metallic catalysts and generated cyclic oligomers as side reactions. Polylactides and polycaprolactone are polyesters that can be synthesized by ROP.[34]

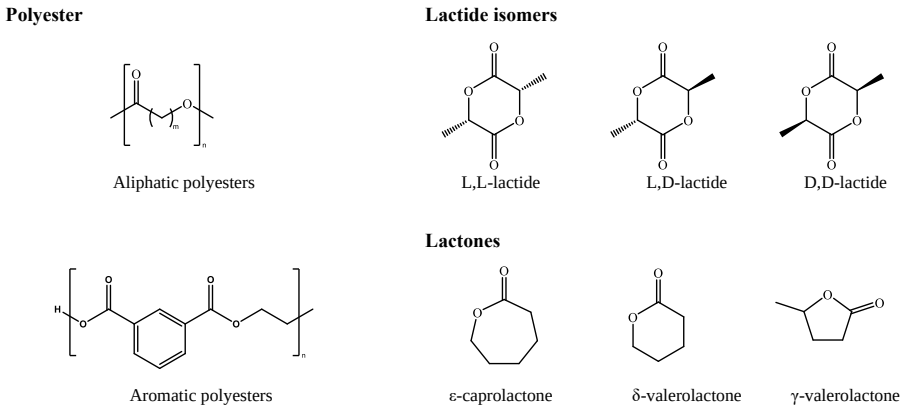

Figure 2. (Left) General chemical structures of aliphatic and aromatic polyesters. (Right) Chemical structure of lactide isomers and lactones.

1.3.1 Polylactides

Polylactide is a biobased, biocompatible, and compostable plastic that has been widely studied.[35,36] Polylactic acid (PLA) use in direct contact with food has been approved by the U.S. Food and Drug Administration (FDA). Their properties, such as innocuity and biocompatibility, enable it to be used in biomedical applications.[28,37] PLA is the most extensively produced biopolymer and is mostly used for packaging, as well as other applications such as toys, automotive, construction, electronics, and agriculture.[4] PLA's properties can be similar to those of commercial petroleum-based polymers such as polyethylene terephthalate (PET) and polystyrene (PS).[36] In addition to its versatile properties, PLA is widely used due to its lower price compared to other biodegradable polymers.[28] However, despite their wide use in modern society, PLA still has some shortcomings to be used as materials, such as brittleness and fragility, and the price is high compared with traditional commodity plastics.[20]

PLA holds a 13.9% share of the bioplastic market, which is projected to increase in production. In 2019, PLA production was reported at approximately 290,000 tons, while in 2024, it is expected to increase to 317,000 tons.[20] PLA is produced from lactic acid, which is obtained through the fermentation of renewable feedstock such as rice, corn, and potato .[19] PLA can be generally produced by two polymerization mechanisms: polycondensation and ring-opening polymerization (ROP). Although polycondensation is a simple and low-cost method, the yields and molecular weights are usually low and require extensive removal of water due to the occurrence of a reversible reaction. Conversely, the production of PLA by ROP has better processing control, and the molecular weights of the product obtained are higher in comparison to polycondensation, although it requires additional reaction steps, catalyst and higher temperatures.[28,38] PLAs are typically produced from the ROP of lactide, of which there are three distinct optical isomers: L-, D- and meso-lactide (L-LA, D-LA and meso-LA, respectively) (See Figure 2). Hence, distinct homopolymer and copolymer structures of PLA can be obtained, such as poly(L-lactide) [PLLA], poly(D-lactide) [PDLA], or poly(L-co-D-lactide) [PLDLA]. The thermal, mechanical, processing and degradation properties of the resulting PLA also rely on the stereochemical sequence in their chains.[39]

1.3.2 Polylactones

Polycaprolactone (PCL) is a hydrophobic and biodegradable polymer with adequate mechanical strength and flexibility for many applications related to the biomedical field. PCL can be obtained from the polymerization of ε-caprolactone (ε-CL), a cyclic monomer (See Figure 2). PCL is a biocompatible polymer, and it has been widely used for some medical applications, as certified by the (FDA) and marked by the European Community.[40] The viscoelastic and mechanical properties of PCL make it a perfect candidate for use in packaging, coatings, adhesives, textiles, and other areas.[41] PCL degradation occurs through to the ester bonds that can be cleaved by hydrolysis under physiological temperature.[42] The biodegradable features of PCL have drawn attention, and over the last decades, their fields of application have diversified.[43] For example, combining PCL with other biopolymers is a way to improve the properties and enhance the sustainability features, providing that the biocompatibility and biodegradability are maintained;[40] PCL blendings with PLA, for example, improve their toughness .[35,40] Copolymerization of ε-caprolactone (ε-CL) with different lactide isomers allows polymers with different crystallinities, mechanical properties, and degradability profiles to be obtained.[35] PCL is typically synthesized via bulk ROP of ε-CL using ionic and metal catalysts,[44] where the mechanism of ROP proceeds depending upon the initiator/catalyst employed.[45] Secondary reactions usually occur during syntheses by ROP, such as transesterification, loss of reaction control, and polydispersity.[45] Such reactions are avoided by using tin [46] or alminium[47] metal-based catalysts, which are widely employed in the industry to produce PCL.

Other cyclic monomers, such as hexadecalactone, δ-valerolactone (see Figure 2), and ω-pentadecalactone, can be polymerized to obtain polylactones, which exhibit similar behavior and mechanical properties to low-density polyethylene glycol.[48] Poly-(δ-valerolactone) [PVL], a member of the lactone family, is a biodegradable polymer that, similar to PCL, has also been used in biomedical applications. [48,49] PVL possesses low mechanical strength, reduced gas permeability, solvent resistance, and degradation profile, which could be useful in other areas similar than PCL [49] or in packaging applications.[50] PVL is obtained from the lactone monomer with 5 methyl groups, namely, δ-valerolactone, via ROP.[49]

1.4 Industrial production of PLLA, PCL, and PVL

1.4.1 Industrial production of PLLA

There are two mechanisms by which PLLA is produced in the industry: polycondensation and ROP. Although polycondensation appears to be the simplest, the throughput is relatively low, the mechanical properties are weak, and its application is limited. Another problem with polycondensation is the high cost of purification.[28] ROP of lactide is the route preferred by the industry since it provides better control in the molecular weight dispersion of PLA and results in high molecular weights. ROP catalyzed by sulfonic acid compounds generally offers high reactivity and selectivity and low product racemization.[51] ROP of lactide is also carried out using anionic and cationic catalysts, and the reaction is generally carried out under solution conditions. However, there are some drawbacks, such as the toxicity of the catalysts as well as the reaction sensitivity to the presence of impurities.[51] Tin-based catalysts are the most common catalyst type used for ROP of lactide in the industry.[38,52] This reaction typically yields a high molecular weight PLA with conversions of approximately 90% and low racemization. ROP of lactide can also be carried out at temperatures below 100 °C using tin octoate as an organocatalyst and tetrahydrofuran (THF) as the solvent.[46] Tin octoate is approved for food and medical applications by the FDA; however, its presence in trace amounts could compromise the corresponding bio-related applications. Therefore, their complete removal is necessary, or at least the concentration in the final product should be less than 10 ppm. For this purpose, they are usually deactivated and extracted from molten polyesters by using aggressive chemicals such as phosphoric acid or acetic anhydride.[28]

1.4.2 Industrial production of PCL and PVL

Similar to PLLA, lactones polymerization via ring-opening polymerization (ROP) are favored over polycondensation polymerization due to offer better control, which yields products with narrow polydispersity and high molecular weight. Typically, this can be achieved by tuning the molar ratio of the monomer and the initiator.[33,53] The initiator and catalyst are the drivers that lead the mechanism of the reaction, either via coordination-insertion or complexation-monomer mechanisms.[33,44]

In industry, polylactones are usually produced in a solvent-free process, with metal catalysts at temperatures between 120-200 °C.[33,54,55] Tin derivatives and aluminum alkoxides are two of the most commonly used catalysts for this reaction. [33,53] Tin-based catalysts are known to perform very well in controlling and obtaining high molecular weight polylactones.[44]

Twin-screw extruders have also been used in the industry to produce polylactones, and ROP can be performed through the appropriate selection of monomers and temperatures. The synthesis of polymers and their extrusion is carried out in a continuous process, which shortens costs and polymerization time and provides high conversions.[56] Nevertheless, in some cases, high temperatures cause secondary reactions such as transesterifications. The most widely used metal catalysts are aluminum alkoxides[56] and titanium alkoxides,[33] which are capable of polymerizing ε-CL. However, tin octoate does not allow reaching a PCLwith high molecular weight due to the longer polymerization time required in the extruder.[33,57] Alternatively, polymerization of ε-CL has been carried out at lower temperatures using aluminum-based catalysts in tetrahydrofuran at 80 °C .[33]

1.5 Organocatalysts in polyester synthesis

Aluminum alkoxide or tin-based metal catalysts are typically used in ROP of polylactones and polylactides, these catalysts have excellent thermal stability and offer good control of the dispersion or molecular weight of the final products.[58] Tin-based catalysts allow the reaction to proceed in a relatively short time with high yields. [59] However, the use of these metal-based catalysts has raised some environmental and health concerns, and removal of the metal residues in the final products is challenging.[38,60] Also, the complexity of removing the remaining catalyst increase the cost of processing,[61,62] In addition, the use of metal catalysts can compromise the polymer's applicability and create new environmental problems at the end of the polymer's lifetime.[38] The toxicity of metals or organometallic catalyst residues also remains a concern for a certain specialized polymeric products, for example, in medical or electrical applications.[62,63]

Additionally, concerns have emerged in the polymer industry due to the forthcoming regulations that limit the use of tin-based catalysts.[38,64] The restrictions to the use of metal catalysts have stimulated the exploration of other (nontoxic) alternative catalysts.[37,65] Considerable research emphasis is being focused on the use of green catalysts, such as enzymes and organocatalysts. Enzymes and organocatalysts have been reported to catalyze ROP, providing metal-free routes for polyester synthesis.[60,62,66–68] However, to date, enzyme catalysis still has some disadvantages, such as a slow polymerization rate, high cost, and less control of the final polymer properties.[53,61] Organocatalysts, on the other hand, have become a powerful method for diverse polymerization routes due to their versatility and easy recovery .[52,69,70]

Organocatalysts have several attractive properties, such as good control and high selectivity in polymerizations, accessibility, and compatibility with several functional groups and monomer structures. Organocatalysts are small organic molecules whose activity can be electrophilic or nucleophilic.[62] Polymer syntheses using organocatalysts include those obtained via ROP, step-growth polymerization, and controlled radical polymerization.[71] Henrick and Waymounth pioneered the organocatalyzed ROP of lactones using N-heterocyclic carbenes.[72] In addition, acids have been studied as organocatalysts; for instance, trifluoromethanesulfonic acids proved highly effective in polymerizing lactides via ROP, which was faster and more controlled .[73] Hoashi, Y. et al. reported a dual organocatalyst combination of amines with thiourea for obtaining polylactides.[74] In general, the organocatalysts used in ROP are classified into two main groups: organic bases and organic acids. Phosphazenes, N-heterocyclic carbenes, pyridines, thioureas/amines, guanidines, and amidines are included in the organic bases category. For example, 1,8-diazobicyclo[5.4.0]undec-7-ene (DBU) is an amidine organocatalyst that is able to catalyze L-lactide polymerization.[60] Sulfonic acids, trifluoromethanesulfonic acid, benzoic acid, and phosphonic acid are examples of acid organocatalysts. Herein, methanesulfonic acid was reported to have excellent control in the ROP of ε-CL.[53]

Despite the advantages that organocatalysts offer, their use in industry is still limited, this is because the typical industrial synthesis of polymers such as PET, polyamides, polyurethane, or polyurethanes is normally conducted in the temperature range of 100-300 °C.[52] While most organocatalysts are quite volatile and subject to thermal decomposition.

Organocatalyst poor thermal stability leads to their degradation during bulk polymerization and remains as an attractive issue to be addressed for future research (see Figure 3).[52] Recently, it was reported that acid and basic organocatalyst combinations retain their catalytic performance and are capable of enduring the high temperature of polymerization.[38] Acids such as phosphonic and sulfonic acid, act as proton carriers for basic oxygen atoms while bases, such as pyridines and guanidine, play the role of a hydrogen bond acceptor. This dual catalyst system has been demonstrated to be stable at temperatures above 400 °C,[38] due to the hydrogen-bond.[60]

Examples of bifunctional organocatalyst systems include sparteine/thiourea, N,N(-dimethylamino)/pyridine, diphenyl phosphate/4-dimethylaminopyridine, imidazole/trifluoroacetic acid, 4-dimethylaminopyridine, and methanesulfonic acid, which have been reported as catalysts for the ROP of lactide.[75–78] It is noteworthy that the latter allowed the polymerization of ε-CL with high control in the absence of side reactions.[38] Similarly, the ROP of ε-CL was also reported by using a combination of sulfonic acids and their conjugated bases, urea, and thiourea, or guanidine-methanesulfonic acid .[53,60,79]

These dual acid-base system organocatalysts proved to be efficient systems with reasonable control and, in some cases, prevent side reactions. However, they still have some drawbacks for industrial applications, such as their commercial availability (e.g., alkyl urea) and high cost, which prevents their potential scale-up.[60,80]

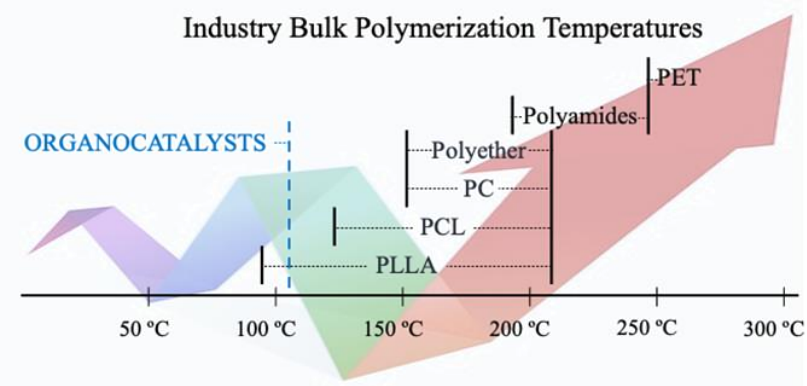

Figure 3. General synthesis temperatures of bulk polymers in the industry.[52]

The efficiency and versatility of the organocatalysts, together with their facile elimination from the final products, aid in enhancing the green character of the synthesis of biodegradable and biocompatible polymers. To prevent organocatalysts thermal degradation during polymerization, it is recommended to develop a dual-system organocatalysts. Another alternative approach is using organocatalysts at low reaction temperatures and in the presence of organic solvents. For example, ROP of L-lactide (LLA) was catalyzed by triazabicyclodecene,[81] or phosphazene-thiourea/urea at room temperature in CH_2Cl_2.[82] However, the use of chlorinated organic solvents is known to causing an environmental problem. Thus, the development of new alternatives for producing polyesters via environmentally friendly routes remains a crucial challenge to be addressed. Therefore, the search for alternatives to volatile organic solvents, high temperatures, and the use of metal-base catalysts in the ROP to produce polyesters will be addressed in this work with the aid of deep eutectic system (DESs).

1.6 Family of green solvents as alternative for polymerizations

1.6.1 Deep eutectic solvent (DES)

Many of the most useful organic solvents in chemical laboratories and industries are volatile, flammable, toxic, and hazardous. They are associated with potentially serious health problems and concerns regarding the safety of handling them and the appropriate use of these chemicals. Volatile organic solvents are derived from petroleum feedstock and are widely used in chemical synthesis processes such as extraction, purification, and cleaning.

In addition, there is a potentially serious environmental impact on polymer production due to the organic solvents used in synthesis and processing, which are primarily responsible for the largest generation of waste in the polymer industry.[83] Thus, there is an increased awareness from academia as well as industry to pursue new routes for more sustainable solvent alternatives, for example, water, glycerol, ionic liquids (ILs), low-transition temperature mixtures, CO_2 tunable solvents, bioderived lignin solvents from oil, and dihydrolevoglucosenone (Cyrene^{TM}).[83,84] However, some of these alternatives have certain limitations in terms of solute dissolution or processes that require a vacuum and temperatures above 100 °C, toxicity in the long term, and price.

In this context, systems known as "deep eutectic solvents" (DESs), more generally deep eutectic systems, have emerged as a new family of green solvents as potential alternatives for replacing traditional organic solvents in biotechnology, chemical, and materials sciences.[83] DES are promising candidates for the substitution of the approximately 600 existing volatile organic compounds (VOCs).[85] A DES is defined as a mixture of different compounds with no reaction between them, which results in a decrease in the freezing point of the final system in comparison with the melting points of the pure compounds. Usually, the compounds are in the solid state, but this is not necessary; the final system is in the liquid phase under operating temperatures.[86–88] DESs were first reported by Abbott et al., who first coined the term to refer to binary mixtures of crystalline urea [($T_m \approx 133$ °C, acting as hydrogen bond donor (HBD)], and choline chloride salt [$T_m \approx 302$ °C, acting as a hydrogen acceptor, (HBA)], at a 2:1 molar ratio composition, which possessed a freezing point of 12 °C.[87] As mentioned before, the resulting DES mixture has a lower melting point in comparison with the melting point of the constituents.[90] The decrease in the melting point is due to the self-associative intermolecular interactions between the components, likely driven by the entropy, van der Waals interactions, hydrogen bonding, and ionic bonding interactions.[87,91] DES are typically clear viscous liquids with varying colors from white to amber to cloudy,[89] they are usually in the liquid phase at room temperature, and their melting point is generally below 100 °C.[92] Properties such as low to negligible vapor pressure, good chemical and thermal stability, and ionic conductivity (when composed of salts) are characteristics of DESs. [93]

Contrary to ionic liquids (ILs), DESs are relatively cheaper and therefore more viable for application on a larger production scale. Another advantage of DESs over ILs is that they tend to be easier to prepare, i.e., the most common method is by simple stirring and heating. The preparation of DES is dependent on several factors, including the equipment's limitations and the water content. Alternative methods of DES synthesis include grinding and mixing until a clear liquid is obtained,[93] evaporation[94] and freeze-drying of solutions with DES counterparts.[95]

The starting materials for DESs are typically inexpensive and ubiquitous, but more sophisticated HBDs and HBAs are growing for new applications. Furthermore, their synthesis is sustainable, and nearly 100% atom economy can be achieved in most cases.[4,83] Purity of DES often only depends on the purity of the starting components, i.e., generally, there are no byproducts. DES can be recycled, from which the respective solvent components can be recovered.[96] They can be considered nontoxic since many of their constituent precursors are nontoxic,[97] although recent concerns have arisen about toxic effects due to acidification and eutrophication of wastewater. To date, the choline/urea combination is the most studied DES. Choline chloride (ChCl) is a component of vitamin B and is currently produced on a scale of megatons per year as a livestock feed supplement, while urea is commonly used in fertilizers.[83,92,98] Even though the constituent components are considered safe, DES cytotoxicity still needs to be further evaluated.[99] Since the initial reports on the principle behind eutectic mixture formation, the research area has broadened, now involving a wide range of novel components. The large diversity of the constituents to produce DES systems is estimated in the range from 10^6 to 10^8 possible binary combinations.[88] Currently, DES systems exhibit an unusually large solvation capacity, and because of their tunable composition, they may include either ionic or nonionic compounds.[84,88]

In general, depending on their compositions, DES can be classified as types I, II, III and IV.[92] Types I and II combine relevant Lewis acids, such as quaternary ammonium base, phosphonium, or sulfonium salts, with their counterparts Lewis bases, such as a metal chloride and a hydrated metal chloride, respectively. Whereas type III encompasses the most extensively studied DESs, they consist of a quaternary ammonium salt and its counterpart, a hydrogen bond donor (HBD), such as alcohols, amines, amides, and carboxylic acids.

Type IV DES comprises a hydrate metal chloride and HBD.[100] Recently, a new class named type V was reported and consists of nonionic components. Hydrogen bonds are particularly predominant in all types of DESs (See Figure 4).[101] The composition of DESs has expanded to include mixtures such as natural deep eutectic solvents (NADES),[102,103] whose components include derivatives of renewable and/or biological raw materials, low-transition-temperature mixtures (LTTM),[89] or even aqueous dilutions of DES.[84]

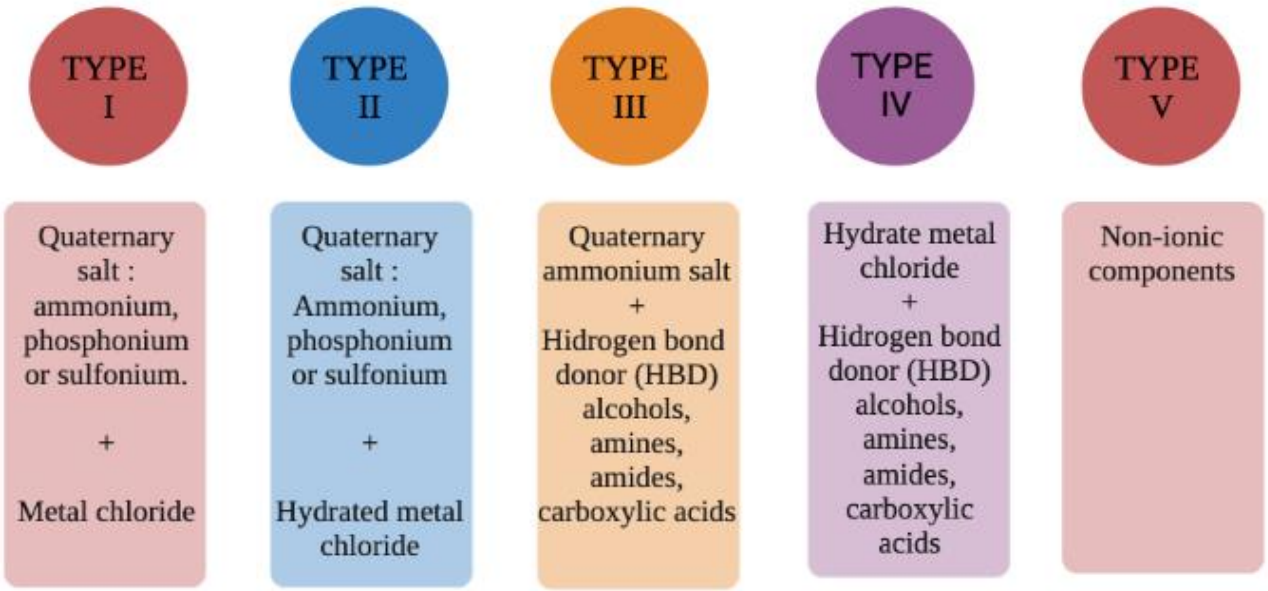

Figure 4. Classification of Deep Eutectic Solvents

DES are typically chemically and thermally stable, however some undesirable reactions during their preparation were reported in literatures, like thermal degradation,[104] or certain reactivity between their constituents such as the formation of ester groups when the DES are mixtures of carboxylic acids and bases or alcohols.[105] Furthermore, DES typically possesses a very high viscosity compared to traditional solvents, up to 100 times higher.[106] This may be considered a significant drawback in regard to handling or dissolution, but pose interesting properties for gels and other topics.[106]

High viscosity results in reduced mobility of molecules and thus hinders the dissolution of compounds, but water addition has solved these problems while also enhancing the ionic conductivity. DESs are in general hydrophilic, therefore the presence of water may be helpful or hampering the applications where viscosity or conductivity is important.[107]

DES has been applied in various fields, with much ongoing investigation in areas such as nanoparticle synthesis,[106] metallurgy and electrodeposition,[107] gas separation and capture,[108] metallic carbon dioxide fixation,[109] energy systems, and battery technologies,[110] biocatalysts and organic chemistry,[109] biomass processing,[111] genomics,[112] and production of polymers which is the focus of the next section.

1.7 Polymerization in DES

DESs can be used in polymer synthesis and may replace conventional organic solvents as well as enables reaction conditions that may not be possible in organic solvents e.g., reaction with vacuum and temperatures above 100 °C, electrochemical deposition, catalysis, or dissolution of resilient biomass.[113] The first polymerization using a eutectic mixture was reported in 1985, where the electrochemical synthesis of polyanilines was obtained by oxidation of aniline in a eutectic mixture with NH_4F in different acid or salt solutions.[114] DES applications go beyond being mere alternative solvent substitutes for reactions. Where typically DES acts as an inert solvent, not participating in polymerization. For instance, in addition to the reaction medium, DESs can enhance the solvation of monomers and initiators, providing an optimized medium and chemical environment for the reactions to proceed.[115] Most DES systems are polar, but hydrophobic DESs have the capability to solubilize aliphatic, aromatic, and nonpolar monomers, e.g., methacrylate and styrene. Polymerization by free radical polymerization of such monomers is beneficial when polymerization is performed in hydrophobic DESs, in which additional co-solvents are required in polar DESs. [83,84]

Other benefits of using DES are the improvement of reaction kinetics to obtain polymeric materials with better thermal and/or mechanical properties.[83] In this regard, Fazende et al. reported that the polymerization rate of methacrylic and methyl methacrylic acid improved five-fold in eutectic mixtures that contained choline chloride when diphenyl (2,4,6-trimethylbenzoyl) phosphine oxide was used as a photoinitiator. They demonstrated that the viscosity and polarity of the mixture were responsible for these results.[83] It is noteworthy that the role of DES in this polymer synthesis is, besides the reaction medium, the precursors or monomers that form the final polymer products.

1.8 Polymers obtained from Deep Eutectic Solvent monomers.

Whenever single or various components comprising a DES system are capable of being polymerized, they are referred to as "polymerizable eutectics mixtures" or "deep eutectic solvent monomers" (DESm).[84] Given suitable conditions, including the appropriate triggering of the initiator of the polymerization, the monomer that forms DESs then polymerizes, creating a unique situation in which the monomer has the dual role of being part of the medium and a reagent at the same time.[84]

Hence, DESs can perform different functions, including solvents, monomers, and templating agents. Cooper et al. reported that if one of the constituents of DESs undergoes a chemical transformation, its counterpart can play the role of a final directing agent of the final material´s structure,[116] A similar scenario occurs in the polymerization of a DESm: the monomer that is part of the DES then polymerizes, whereas its counterpart remains embedded in the resulting output product. Notably, the inert counterpart determines the overall spatial composition of the finished product, such as porosity. Important aspects that are relevant to polymerizable eutectic mixtures and the final spatial composition are the relation between the reaction rate, the separation rate of the DES system components, and its overall viscosity evolution during the reaction.[117]

DES monomers are particularly attractive as sustainable systems because some of their components, which are solid in their original form, are liquid when forming the eutectic mixture, therefore enabling reactions under mild and solvent-free conditions.[83,118 121]Another advantage of eutectic polymerizable mixtures is that the often its gives high yields or atomic economy of ca. 100%, allowing synthesis to be performed at conditions that are impossible in traditional solvents.[83] They also allow for an enhanced rate of polymerization ,[119] and provides better control in the reactions.[120] DESm polymerizations have been reported through several mechanisms of polymerization, such as free radicals, polycondensation, and ring opening, [83] including another methods such as, atom transfer radicals polymerization,[85] and electrochemical.[118].

1.8.1 Free-radical polymerization of eutectic mixtures monomers

The polymerization of vinyl acrylate monomers forming DESm systems has been studied mainly by the free-radical polymerization (FRP) mechanism. For example, Mota-Morales et al.[120] reported the polymerization of DESm comprising acrylic or methacrylic acid with choline chloride. The polymerization was carried out in a column in the presence of benzoyl peroxide as an initiator and ethylene glycol dimethacrylate as a crosslinker. Due to their hydrogen-bonding nature, acrylic monomers play the role of HBD in DES. The high viscosity of DESm stabilizes the polymerization reaction, while ChCl catalyzes the polymerization.[120]

Polymerization of other acrylates, such as acrylamide and N-isopropylacrylamide, which were part of DESm, was also performed by the FRP mechanism.[121] Sánchez-Leija et al. synthesized a polymer-lidocaine complex that was produced from a DESm composed of lidocaine hydrochloride (as ammonium salt) and acrylic acid. The synthesis of polyacrylic acid was carried out by the FRP mechanism, allowing the final polymer to be applied as a drug delivery system.[122] Bednarz et al. reported the copolymerization of a DESm from itaconic acid, ChCl and bisacrylamide.[123] A macroporous polymer composite (carbon nanomaterials or nitrogen-carbon nanotubes, with conversions of approximately 76%) was successfully obtained from FRP of DESm composed of acrylic acid/ChCl.[124,125]

Free-radical enzymatic polymerizations of acrylamide in the ChCl DES system have also been reported. The reaction was conducted at 50 °C using horseradish peroxidase (HRP) enzyme, hydrogen peroxide, and 2,4-pentanedione.[126] Furthermore, the FRP mechanism of DESm, which includes photoinitiators, has been extensively studied in recent years. Fazende et al.,[127] reported the polymerization of DESm composed of acrylic acid, methacrylic acid and ChCl, and the photoinitiator used was diphenyl (2,4,6-trimethylbenzoyl) phosphine oxide. It was observed that the rate of polymerization of acrylates was enhanced by the polarity of its counterpart ChCl in DES and the viscosity of the mixture.[127] Similarly, Mecerreyes et al.,[119] reported the photopolymerization of DESs consisting of 2-cholinium bromide methacrylate and citric acid or amidoxime. The reaction was carried out at room temperature with UV light using 2-hydroxy-2-methylpropiophenone as an initiator, and resulted in poly(ionic) liquids that were applied for CO_2 capture.[119]

In addition, Li Ren'ai et al.,[128] also photopolymerized acrylic acid/ChCl DES using 2-hydroxy-4-(2-hydroxyethoxy)-2-methylpropiophenone (Irgacure 2959®) as a photoinitiator and ethylene glycol diacrylate as a crosslinker. The final product obtained from the polymerization of DESm, poly(DES), was used as inks and deposited on paper via screen-printing into various forms and shapes, enabling the fabrication of origami paper circuits.[128] Similar works were reported by the same groups and applied as conductive paper and strain sensors.[129]

1.8.2 Polycondensation of eutectic mixtures monomers

In addition to other polymerization techniques, polycondensation reactions are also utilized as polymerization methods for deep eutectic mixture monomers. For example, Serrano et al. reported the synthesis of an elastomer polyester obtained from 1,8-octanediol/lidocaine DES and citric acid via polycondensation at 90 °C. Lidocaine degradation occurs at approximately 100°C, and it was prevented by the use of DES, allowing polycondensation at temperatures below 100°C.[130] An example of this is the production of a similar DESm using a combination of 1,8-octanediol and other salts such as tetraethylammonium bromide, hexadecyltrimethylammonium bromide, or methyl triphenylphosphonium bromide. The resulting elastomers possess antibacterial properties due to the presence of nonpolymerizable ammonium or phosphonium salts in the DESm.[131] Moreover, polycondensation of DESm composed of ammonium salts mixed with citric acid, terephthalic acid, or amidoxide has been reported without the need for a catalyst .[119] Del Monte et al. developed carbon monoliths with mesoporosity, narrow pore size distribution, and large surface area through the polycondensation of DESm composed of resorcinol/ChCl or ChCl/urea DES with formaldehyde, followed by carbonization.[124] The same DES system was further explored by adding polymerizable ternary eutectic mixtures, i.e., resorcinol/3-hydroxypyridine/ChCl;[132,133] 3-hydroxypyridine/tetraethylammonium bromide;[134] and, 4-hexylresorcinol/ tetraethylammonium bromide.[135] The advantages of the synthesis of such materials were high yields, low cost, and exclusion of additives. The carbon surface was functionalized with nitrogen to enhance the adsorption of carbon dioxide,[134,136] or included iron acetate,[134] to provide electrical conductivity. Finally, a phosphorus-doped carbon composite was obtained from polycondensation of triethyl phosphate/*p*-toluene sulfonic acid/furfural alcohol DES and carbon nanotubes.[137]

1.8.3 Ring--opening polymerization (ROP) of eutectic mixtures monomers

More recently, DES monomers composed of lactides, carbonates, and lactones were studied as alternatives to traditional ROP in bulk or solution. Under suitable conditions, it is possible to polymerize these DESm to produce polyesters under mild temperature conditions and through a simple and overall sustainable route, i.e., it allows them to be produced in a solvent-free method.

Coulembier et al.[138] carried out a pioneering study in which they prepared a nonionic DESm consisting of an equimolar combination of L-lactide (LLA) and trimethylene carbonate (TMC). They performed ring-opening polymerization (ROP) in this nonionic DES at 23 °C using 1,8-diazabicyclo [5.4.0]undec-7-ene (DBU) as the organocatalyst and benzyl alcohol as the initiator. LLA was able to polymerize first due to its liquid phase at room temperature, and the selectivity of DBU, allowing mild temperature conditions and the absence of organic solvents. Subsequent polymerization of TMC onto the blend led to a final poly(LLA-*g*-TMC) copolymer with a gradient composition.[138] Similarly, Pérez-García et al. produced a eutectic mixture composed of L-lactide (LLA) and ε-caprolactone (CL) in a molar ratio of 3:7, respectively. The melting point of the mixture was -19 °C, which is below the melting point of the constituents. Taking advantage of the liquid nature of LLA, polymerization was possible under mild temperature conditions (37°C) through sequential ROP, resulting in a blend of poly(L-lactide) and polycaprolactone homopolymers with high crystallinity.[139]

1.9 Polymers from the eutectic mixture and their applications

Utilizing DES monomers presents an attractive approach to replace volatile organic solvents, achieve high yields, or enhance the rate of polymerization when synthesizing various polymers. As previously discussed, polymers can be produced by different mechanisms from DESm with several advantages over conventional systems. Furthermore, the benefits of implementing DES monomers are not restricted to polymer synthesis applications; they can also be employed to create diverse materials, including supramolecular hydrogels, porous monoliths, and molecular imprinted polymers.

Bernardz et al. reported the production of a poly(itaconic acid-co-N,N'-methylenebisacrylamide (BIS) hydrogel obtained from DESm consisting of itaconic acid and ChCl.[123] Wu et al. produced a deep eutectic supramolecular polymer gel from cyclodextrin/natural acids DES.[140] Li et al. mixed glycerol with urea to prepare acrylamide polymers for molecular printing.[129] Ndizeye et al., used non-ionic DESs as a porogen in the synthesis of porous polymer monoliths.[141]

Porous polymers have garnered significant interest due to their potential applications in fields like biomedicine, separation processes, and energy storage. The morphology, size, and connectivity of the pores in these polymers are directly linked to their intended use. To achieve these properties, various pore-generation methodologies have been developed, including macromolecular design, self-assembly, phase separation, solid-liquid melt, sol-gel, and foam formation. [142]

Recently, emulsion templates have become a popular choice for developing porous materials, and they can be further extended to fabricate interconnected macroporous polymeric monoliths by utilizing a high internal phase emulsion (HIPE) as a template, where a DES monomer comprises the continuous phase.[122] HIPE is a packed emulsion that has a higher internal phase of 74% v/v and is stabilized by surfactants. The closed-pack emulsion droplets provide the template where the subsequent polymerization of the continuous phase followed by the elimination of the internal phase gives rise to a macroporous polymer with interconnected pores. Pérez García et al. exploited the liquid nature of the mixture of L-lactide and ε-caprolactone monomers at room temperature, which otherwise are separately solid and liquid, respectively. To prepare the HIPE, the eutectic mixture of L-lactide and ε-caprolactone, liquid at RT, was mixed with nonpolar solvents and stabilized with nonionic surfactants. Polymerization of the DESm in the continuous phase was performed at 37 °C, and the resulting polyHIPE (pHIPE) was reported to possess pores with a diameter close to 20 μm.[139] pHIPES has found numerous applications in biomedical applications, separations, or catalyst supports.[83]

The polymerization of DESm and eutectic systems has flourished over the last decade with exciting results that have translated into new materials and applications. Nevertheless, in the case of other methods of polymerization, apart from free radicals, the literature is scarce, with only a handful of works published concerning polycondensation and ROP, for instance. Hence, this work aims to fill the gap in understanding and exploring the ROP of eutectic mixtures composed of lactones for the synthesis of biodegradable polyesters through a sustainable approach. The synthesis of porous polyesters with properties that can be tailored to adjust their biodegradability is one of the expected results. Such materials will add to the existing toolbox for applications in areas such as biomedicine and separation processes.

1.10 Scope and Outline of the Thesis

Chapter 2 provides a fundamental study on the Ring Opening Polymerization (ROP) of deep eutectic solvent monomers (DESm) composed of L-lactide and ε-caprolactone, leading to the synthesis of polymer blends and a block copolymer. The Chapter discusses the influence of various parameters in producing polyesters with tunable number average-molecular weight (in the range of 2000 to 6900 g/mol^{-1}), crystallinity (from 37% to 70 %), and polymer architectures with controlled degradation profiles. The outcome strongly depends on the selection of organocatalysts, including 1,5-Diazabicyclo (4.3.0) non-5-ene (DBN), a new catalyst for the ROP of L-lactide/ε-caprolactone DESm. The use of this organocatalyst not only allows an increase in the polymerization temperature (up. to 92 °C) but also facilitates the formation of a block copolymer P(LLA-*b*-CL) for the first time using this methodology. Additionally, the Chapter discusses the influence of the stereoisomer D-lactide in the DESm and water content (ca. 0.2 wt.%) during the ROP process.

Chapter 3 introduces new DESm capable of undergoing ROP to produce biodegradable polyesters by mixing various lactones with L-lactide. These lactones encompass a range of molecular weights and structures, including δ-valerolactone and δ-decalactone. The Chapter provides fundamental insights into ROP kinetics and explores the impact of different organocatalysts, benzyl alcohol initiator concentration, and reaction temperatures (37 and 60°C).

These factors significantly influence the achieved number average molecular weight (in the range of 2400 to 8700 g/mol^{-1}), crystallinity, and polymer architectures of the resulting polyesters, including blends and block copolymers.

Chapter 4 investigates the incorporation of multifunctional macroinitiators in the ROP of a DESm composed of L-lactide and ε-caprolactone to enhance the properties of the resulting polyesters. These macroinitiators include polycaprolactone triol (PCL segments of 900 g/mol^{-1}) and polyethylene glycol (6000 g/mol^{-1}), both OH-terminated. The thorough understanding of the ROP kinetics of the DESm, considering factors such as hydrophobicity and molecular weight of the final bulk polyesters (from M_n 2400 to 9500 g/mol^{-1}), serves as the basis for the synthetic conditions applicable to the design and synthesis of high internal phase emulsions (HIPEs).

These HIPEs consist of highly viscous emulsions of tetradecane-in-DESm, which are stabilized by Pluronic F-127 surfactant, and acts as a template for the ROP of the continuous (external) phase. The macroinitiators enable precise control over the hydrophilic characteristics of the polyesters, whether in bulk or polyHIPEs, providing control over the degradability, average-molecular weight, and polymer architectures of the resulting polymers. Notably, the macroporous polyHIPEs (with pores in the range of 33 to 42 μm) exhibit excellent crude oil sorption capabilities, with a competitive sorption capacity of 2 grams of oil per gram of sorbent.

These chapters provide a comprehensive exploration of a solventless ROP process at low temperatures (e.g., 37°C), using organocatalysts to synthesize biodegradable polyesters with tailored properties. The research contributes to the development of alternative protocols in polymer synthesis and offers valuable insights for sustainable development. The solvent-free ROP of lactide and lactones in the form of DESm, conducted under mild temperature conditions without metal catalysts and volatile organic solvents, demonstrates a versatile process for polyester synthesis with rapid degradability and controllable properties. The use of mild temperatures and organocatalysts in preparing polyesters with programmable degradation profiles represents important environmentally friendly features for the development of new materials.

These findings are expected to have significant implications for biomaterials science and polymer chemistry, enabling the exploration of sustainable materials engineering or degradable biomaterials. Such materials, with controllable degradation profiles, hold potential applications in separation processes, cell culture scaffolds, and drug delivery. Overall, this research lays the foundation for an alternative, greener methodology for polyester production, opening new avenues for sustainable materials development in the field of biomaterials and beyond.

1.11 References

1 D. I. Bower, *An Introduction to Polymer Physics*, Cambridge University Press, 2002.

2 G. Odian, in *Principles of Polymerization*, John Wiley & Sons, Ltd, New York, 3rd edn., 2004, pp. 1–38.

3 S. Thakur, J. Chaudhary, B. Sharma, A. Verma, S. Tamulevicius and V. K. Thakur, *Curr. Opin. Green Sustain. Chem.*, 2018, **13**, 68–75.

4 E. M. Melchor-Martínez, R. Macías-Garbett, L. Alvarado-Ramírez, R. G. Araújo, J. E. Sosa-Hernández, D. Ramírez-Gamboa, L. Parra-Arroyo, A. G. Alvarez, R. P. B. Monteverde, K. A. S. Cazares, A. Reyes-Mayer, M. Y. Lino, H. M. N. Iqbal and R. Parra-Saldívar, *Polymers*, 2022, **14**, 1–32.

5 N. Mills, M. Jenkins and S. Kukureka, eds. N. Mills, M. Jenkins and S. B. T.-P. (Fourth E. Kukureka, Butterworth-Heinemann, 2020, pp. 1–11.

6 N. Döhler, C. Wellenreuther and A. Wolf, *EFB Bioeconomy J.*, 2022, **2**, 100028.

7 R. Geyer, J. R. Jambeck and K. L. Law, *Sci. Adv.*, 2017, **3**, 1700782.

8 T. D. Moshood, G. Nawanir, F. Mahmud, F. Mohamad, M. H. Ahmad and A. AbdulGhani, *Curr. Res. Green Sustain. Chem.*, 2021, **5**, 100273.

9 A. Pellis, M. Malinconico, A. Guarneri and L. Gardossi, *N. Biotechnol.*, 2021, **60**, 146–158.

10 C. Campanale, C. Massarelli, I. Savino, V. Locaputo and V. F. Uricchio, *Int. J. Environ. Res. Public Health*, 2020, **4**, 1212.

11 C. J. Clarke, W.-C. Tu, O. Levers, A. Bröhl and J. P. Hallett, *Chem. Rev.*, 2018, **118**, 747–800.

12 M. Kolybaba, L. G Tabil, S. Panigrahi, W. J Crerar, T. Powell and B. Wang, *Trends Food Sci Technol*. 2003, **14**, 71-78.

13 P. Li, X. Wang, M. Su, X. Zou, L. Duan and H. Zhang, *Bull. Environ. Contam. Toxicol.*, 2021, **107**, 577–584.

14 J. E. Weinstein, J. L. Dekle, R. R. Leads and R. A. Hunter, *Mar. Pollut. Bull.*, 2020, **160**, 111518.

15 F. D. B. de Sousa, *Environ. Sci. Pollut. Res. Int.*, 2021, **28**, 46067–46078.

16 I. Notaro, E. Lovera and A. Paletto, *J. For. Sci.*, 2022, **68**, 121–135.

17 H. Kawaguchi, K. Takada, T. Elkasaby, R. Pangestu, M. Toyoshima, P. Kahar, C. Ogino, T. Kaneko and A. Kondo, *Bioresour. Technol.*, 2022, **344**, 126165.

18 C. Lim, S. Yusoff, C. G. Ng, P. E. Lim and Y. C. Ching, *J. Environ. Chem. Eng.*, 2021, **9**, 105895.

19 T. Narancic and K. E. O'Connor, *Microb. Biotechnol.*, 2017, **10**, 1232–1235.

20 T. Narancic, F. Cerrone, N. Beagan and K. E. O'Connor, *Polymers.*, 2020, **12,** 920.

21 G. Coppola, M. T. Gaudio, C. G. Lopresto, V. Calabro, S. Curcio and S. Chakraborty, *Earth Syst. Environ.*, 2021, **5**, 231–251.

22 J. Wang, Z. Tan, J. Peng, Q. Qiu and M. Li, *Mar. Environ. Res.*, 2016, **113**, 7–17.

23 J. Yang, Y. C. Ching and C. H. Chuah, *Polymers.*, 2019, **11**, 751.

24 J. Brizga, K. Hubacek and K. Feng, *One Earth*, 2020, **3**, 45–53.

25 G. Bhagwat, K. Gray, S. P. Wilson, S. Muniyasamy, S. G. T. Vincent, R. Bush and T. Palanisami, *J. Polym. Environ.*, 2020, **28**, 3055–3075.

26 R. Shi, D. Chen, Q. Liu, Y. Wu, X. Xu, L. Zhang and W. Tian, *Int. J. Mol. Sci.*, 2009, **10**, 4223–4256.

27 J. Rydz, W. Sikorska, M. Kyulavska and D. Christova, *Int. J. Mol. Sci.*, 2015, **16**, 564–596.

28 L. T. Sin and B. S. Tueen, *Polylactic Acid*, Second Ed., William Andrew Publishing, Oxford, United Kingdom 2019, pp 53-95.

29 M. A. Hillmyer and W. B. Tolman, *Acc. Chem. Res.*, 2014, **47**, 2390–2396.

30 Production of polyester fibers worldwide from 1975 to 2020., https://www.statista.com/statistics/912301/polyester-fiber-production-worldwide/,.

31 S. M. Satti and A. A. Shah, *Lett. Appl. Microbiol.*, 2020, **70**, 413–430.

32 L. Filiciotto and G. Rothenberg, *ChemSusChem*, 2021, **14**, 56–72.

33 C. Jérôme and P. Lecomte, *Adv. Drug Deliv. Rev.*, 2008, **60**, 1056–1076.

34 B. L. Deopura, R. Alagirusamy, M. Joshi and B. B. T. P. and P. Gupta, *Polyesters and Polyamides*, Woodhead Publishing InTextiles, 2008, pp. 41–61.

35 G. Fredi and A. Dorigato, *Adv. Ind. Eng. Polym. Res.*, 2021, **4**, 159–177.

36 W. Abdelmoez, I. Dahab, E. M. Ragab, O. A. Abdelsalam and A. Mustafa, *Polym. Adv. Technol.*, 2021, **32**, 1981–1996.

37 J. Payne and M. D. Jones, *ChemSusChem*, 2021, **14**, 4041–4070.

38 A. Basterretxea, E. Gabirondo, C. Jehanno, H. Zhu, O. Coulembier, D. Mecerreyes and H. Sardon, *Macromolecules*, 2021, **54**, 6214–6225.

39 L. Feng, B. Zhang, X. Bian, G. Li, Z. Chen and X. Chen, *Macromolecules*, 2017, **50**, 6064–6073.

40 V. Guarino, G. Gentile, L. Sorrentino and L. Ambrosio, in *Encyclopedia of Polymer Science and Technology*, 2017, pp. 1–36.

41 R. Sachan, S. G. Warkar and R. Purwar, *Polym. Technol. Mater.*, 2023, **62**, 327–358.

42 L. S. Nair and C. T. Laurencin, *Prog. Polym. Sci.*, 2007, **32**, 762–798.

43 P. Mandal and R. Shunmugam, *J. Macromol. Sci. Part A*, 2021, **58**, 111–129.

44 M. A. Woodruff and D. W. Hutmacher, *Prog. Polym. Sci.*, 2010, **35**, 1217–1256.

45 M. Labet and W. Thielemans, *Chem. Soc. Rev.*, 2009, **38**, 3484–3504.

46 A. Kowalski, A. Duda and S. Penczek, *Macromolecules*, 2000, **33**, 7359–7370.

47 M. Okada, *Prog. Polym. Sci.*, 2002, **27**, 87–133.

48 J. Fernández, A. Etxeberria and J.-R. Sarasua, *J. Appl. Polym. Sci.*, 2015, **37**, 42534.

49 H. Lee, F. Zeng, M. Dunne and C. Allen, *Biomacromolecules*, 2005, **6**, 3119–3128.

50 A. Sangroniz, L. Sangroniz, S. Hamzehlou, N. Aranburu, H. Sardon, J. R. Sarasua, M. Iriarte, J. R. Leiza and A. Etxeberria, *Polymers.*, 2022, **14**, 1–14.

51 D. Garlotta, *J. Polym. Environ.*, 2001, **9**, 63–84.

52 A. Basterretxea, C. Jehanno, D. Mecerreyes and H. Sardon, *ACS Macro Lett.*, 2019, **8**, 1055–1062.

53 S. García-Argüelles, C. García, M. C. Serrano, M. C. Gutiérrez, M. L. Ferrer and F. del Monte, *Green Chem.*, 2015, **17**, 3632–3643.

54 W. Punyodom, W. Limwanich, P. Meepowpan and B. Thapsukhon, *Des. monomers Polym.*, 2021, **24**, 89–97.

55 R. F. Storey and A. E. Taylor, *J. Macromol. Sci. Part A*, 1998, **35**, 723–750.

56 Hostottler, F. US3663515A, 5,468,837, 1995.

57 Y. Shibasaki, H. Sanada, M. Yokoi, F. Sanda and T. Endo, *Macromolecules*, 2000, **33**, 4316–4320.

58 R. E. Drumright, P. R. Gruber and D. E. Henton, *Adv. Mater.*, 2000, **12**, 1841–1846.

59 Y. Yu, G. Storti and M. Morbidelli, *Ind. Eng. Chem. Res.*, 2011, **50**, 7927–7940.

60 A. Dzienia, P. Maksym, B. Hachuła, M. Tarnacka, T. Biela, S. Golba, A. Zięba, M. Chorążewski, K. Kaminski and M. Paluch, *Polym. Chem.*, 2019, **10**, 6047–6061.

61 C. Jehanno, L. Mezzasalma, H. Sardon, F. Ruipérez, O. Coulembier and D. Taton, *Macromolecules*, 2019, **52**, 9238–9247.

62 V. D. Oliveira, M. F. Cardoso and L. D. Forezi, *Catalysts*, 2018, 8, 605.

63 Y. Liang, M. Sui, M. He, Z. Wei and W. Zhang, *Polymers.*, 2019, **5**, 790.

64 A. Bossion, K. V Heifferon, L. Meabe, N. Zivic, D. Taton, J. L. Hedrick, T. E. Long and H. Sardon, *Prog. Polym. Sci.*, 2019, **90**, 164–210.

65 A. Nachtergael, O. Coulembier, P. Dubois, M. Helvenstein, P. Duez, B. Blankert and L. Mespouille, *Biomacromolecules*, 2015, **16**, 507—514.

66 S. Kobayashi, H. Uyama and S. Kimura, *Chem. Rev.*, 2001, **101**, 3793–3818.

67 M. Nikulin and V. Švedas, *Molecules*, 2021, **9**, 2750.

68 K. Schröder, K. Matyjaszewski, K. J. T. Noonan and R. T. Mathers, *Green Chem.*, 2014, **16**, 1673–1686.

69 C.-J. Zhang, X. Zhang and X.-H. Zhang, *Sci. China Chem.*, 2020, **63**, 1807–1814.

70 P. Pladis, K. Karidi, T. Mantourlias and C. Kiparissides, *Macromol. React. Eng.*, 2014, **8**, 777.

71 A. Dove, H. Sardon and S. Naumann, Eds., *Organic Catalysis for Polymerisation*, The Royal Society of Chemistry, 2018.

72 M. K. Kiesewetter, E. J. Shin, J. L. Hedrick and R. M. Waymouth, *Macromolecules*, 2010, **43**, 2093–2107.

73 H. R. Kricheldorf and R. Dunsing, *Die Makromol. Chemie*, 1986, **187**, 1611–1625.

74 Y. Hoashi, T. Yabuta and Y. Takemoto, *Tetrahedron Lett.*, 2004, **45**, 9185–9188.

75 A. P. Dove, R. C. Pratt, B. G. G. Lohmeijer, R. M. Waymouth and J. L. Hedrick, *J. Am. Chem. Soc.*, 2005, **127**, 13798–13799.

76 J. Kadota, D. Pavlović, J.-P. Desvergne, B. Bibal, F. Peruch and A. Deffieux, *Macromolecules*, 2010, **43**, 8874–8879.

77 K. Makiguchi, S. Kikuchi, K. Yanai, Y. Ogasawara, S. Sato, T. Satoh and T. Kakuchi, *J. Polym. Sci. Part A Polym. Chem.*, 2014, **52**, 1047–1054.

78 O. Coulembier, T. Josse, B. Guillerm, P. Gerbaux and P. Dubois, *Chem. Commun.*, 2012, **48**, 11695–11697.

79 N. Susperregui, D. Delcroix, B. Martin-Vaca, D. Bourissou and L. Maron, *J. Org. Chem.*, 2010, **75**, 6581–6587.

80 L. Mezzasalma, A. P. Dove and O. Coulembier, *Eur. Polym. J.*, 2017, **95**, 628–634.

81 R. C. Pratt, B. G. G. Lohmeijer, D. A. Long, R. M. Waymouth and J. L. Hedrick, *J. Am. Chem. Soc.*, 2006, **128**, 4556–4557.

82 M. S. Zaky, A.-L. Wirotius, O. Coulembier, G. Guichard and D. Taton, *Chem. Commun.*, 2021, **57**, 3777–3780.

83 Y. Nahar and S. C. Thickett, *Polymers.*, 2021, **3**, 447.

84 J.D. Mota-Morales, in: Diego J. Ramon, Gabriela Guillena (Eds.), Deep Eutectic Solvents, Shyntesis, Properties, and Applications, vol. 9, Wiley-VCH, Weinheim, Germany, 2020, pp. 70–71. Polymerizations, 187–216.

85 P. Pollet, E. A. Davey, E. E. Ureña-Benavides, C. A. Eckert and C. L. Liotta, *Green Chem.*, 2014, **16**, 1034–1055.

86 A. P. Abbott, G. Capper, D. L. Davies, R. K. Rasheed and V. Tambyrajah, *Chem. Commun.*, 2003, 70–71.

87 M. A. R. Martins, S. P. Pinho and J. A. P. Coutinho, *J. Solution Chem.*, 2019, **48**, 962–982.

88 B. B. Hansen, S. Spittle, B. Chen, D. Poe, Y. Zhang, J. M. Klein, A. Horton, L. Adhikari, T. Zelovich, B. W. Doherty, B. Gurkan, E. J. Maginn, A. Ragauskas, M. Dadmun, T. A. Zawodzinski, G. A. Baker, M. E. Tuckerman, R. F. Savinell and J. R. Sangoro, *Chem. Rev.*, 2021, **121**, 1232–1285.

89 M. Francisco, A. van den Bruinhorst and M. C. Kroon, *Angew. Chemie Int. Ed.*, 2013, **52**, 3074–3085.

90 D. J. G. P. van Osch, C. H. J. T. Dietz, J. van Spronsen, M. C. Kroon, F. Gallucci, M. van Sint Annaland and R. Tuinier, *ACS Sustain. Chem. Eng.*, 2019, **7**, 2933–2942.

91 M. K. Banjare, K. Behera, M. L. Satnami, S. Pandey and K. K. Ghosh, *RSC Adv.*, 2018, **8**, 7969–7979.

92 E. L. Smith, A. P. Abbott and K. S. Ryder, *Chem. Rev.*, 2014, **114**, 11060–11082.

93 A. P. Abbott, D. Boothby, G. Capper, D. L. Davies and R. K. Rasheed, *J. Am. Chem. Soc.*, 2004, **126**, 9142–9147.

94 C. L. Yiin, A. T. Quitain, S. Yusup, M. Sasaki, Y. Uemura and T. Kida, *Bioresour. Technol.*, 2016, **199**, 258–264.

95 M. C. Gutiérrez, M. L. Ferrer, C. R. Mateo and F. del Monte, *Langmuir*, 2009, **25**, 5509–5515.

96 K. M. Jeong, M. S. Lee, M. W. Nam, J. Zhao, Y. Jin, D.-K. Lee, S. W. Kwon, J. H. Jeong and J. Lee, *J. Chromatogr. A*, 2015, **1424**, 10–17.

97 M. Hayyan, M. A. Hashim, A. Hayyan, M. A. Al-Saadi, I. M. AlNashef, M. E. S. Mirghani and O. K. Saheed, *Chemosphere*, 2013, **90**, 2193–2195.

98 K. L. Marsh, G. K. Sims and R. L. Mulvaney, *Biol. Fertil. Soils*, 2005, **42**, 137–145.

99 D. Jung, J. B. Jung, S. Kang, K. Li, I. Hwang, J. H. Jeong, H. S. Kim and J. Lee, *Green Chem.*, 2021, **23**, 1300–1311.

100 A. P. Abbott, J. C. Barron, K. S. Ryder and D. Wilson, *Chemistry*, 2007, **13**, 6495–6501.

101 D. O. Abranches, M. A. R. Martins, L. P. Silva, N. Schaeffer, S. P. Pinho and J. A. P. Coutinho, *Chem. Commun.*, 2019, **55**, 10253–10256.

102 C. D'Agostino, L. F. Gladden, M. D. Mantle, A. P. Abbott, E. I. Ahmed, A. Y. M. Al-Murshedi and R. C. Harris, *Phys. Chem. Chem. Phys.*, 2015, **17**, 15297–15304.

103 C. Florindo, F. S. Oliveira, L. P. N. Rebelo, A. M. Fernandes and I. M. Marrucho, *ACS Sustain. Chem. Eng.*, 2014, **2**, 2416–2425.

104 M. A. Kareem, F. S. Mjalli, M. A. Hashim and I. M. AlNashef, *J. Chem. Eng. Data*, 2010, **55**, 4632–4637.

105 D. J. G. P. van Osch, L. F. Zubeir, A. van den Bruinhorst, M. A. A. Rocha and M. C. Kroon, *Green Chem.*, 2015, **17**, 4518–4521.

106 H.-G. Liao, Y.-X. Jiang, Z.-Y. Zhou, S.-P. Chen and S.-G. Sun, *Angew. Chemie Int. Ed.*, 2008, **47**, 9100–9103.

107 R. Bernasconi, G. Panzeri, A. Accogli, F. Liberale, L. Nobili and L. Magagnin, ed. S. Handy, IntechOpen, Rijeka, 2017, p. Ch. 11.

108 G. García, S. Aparicio, R. Ullah and M. Atilhan, *Energy & Fuels*, 2015, **29**, 2616–2644.

109 A. Zhu, T. Jiang, B. Han, J. Zhang, Y. Xie and X. Ma, *Green Chem.*, 2007, **9**, 169–172.

110 D. Di Marino, D. Stöckmann, S. Kriescher, S. Stiefel and M. Wessling, *Green Chem.*, 2016, **18**, 6021–6028.

111 K. H. Kim, A. Eudes, K. Jeong, C. G. Yoo, C. S. Kim and A. Ragauskas, *Proc. Natl. Acad. Sci. U. S. A.*, 2019, **116**, 13816–13824.

112 I. Mamajanov, A. E. Engelhart, H. D. Bean and N. V. Hud, *Angew. Chemie Int. Ed.*, 2010, **49**, 6310–6314.

113 Q. Zhang, K. De Oliveira Vigier, S. Royer and F. Jérôme, *Chem. Soc. Rev.*, 2012, **41**, 7108–7146.

114 E. M. Genies and C. Tsintavis, *J. Electroanal. Chem. Interfacial Electrochem.*, 1985, **195**, 109–128.

115 D. Carriazo, M. C. Serrano, M. C. Gutiérrez, M. L. Ferrer and F. Del Monte, *Chem. Soc. Rev.*, 2012, **41**, 4996–5014.

116 E. R. Cooper, C. D. Andrews, P. S. Wheatley, P. B. Webb, P. Wormald and R. E. Morris, *Nature*, 2004, **430**, 1012–1016.

117 G. Carrasco-Huertas, R. J. Jiménez-Riobóo, M. C. Gutiérrez, M. L. Ferrer and F. del Monte, *Chem. Commun.*, 2020, **56**, 3592–3604.

118 K. F. Fazende, M. Phachansitthi, J. D. Mota-Morales and J. A. Pojman, *J. Polym. Sci. Part A Polym. Chem.*, 2017, **55**, 4046–4050.

119 M. Isik, F. Ruiperez, H. Sardon, A. Gonzalez, S. Zulfiqar and D. Mecerreyes, *Macromol. Rapid Commun.*, 2016, **37**, 1135–1142.

120 J. D. Mota-Morales, R. J. Sánchez-Leija, A. Carranza, J. A. Pojman, F. del Monte and G. Luna-Bárcenas, *Prog. Polym. Sci.*, 2018, **78**, 139–153.

121 J. D. Mota-Morales, M. C. Gutiérrez, M. L. Ferrer, I. C. Sanchez, E. A. Elizalde-Peña, J. A. Pojman, F. Del Monte and G. Luna-Bárcenas, *J. Polym. Sci. Part A Polym. Chem.*, 2013, **51**, 1767–1773.

122 R. J. Sánchez-Leija, J. A. Pojman, G. Luna-Bárcenas and J. D. Mota-Morales, *J. Mater. Chem. B*, 2014, **2**, 7495–7501.

123 S. Bednarz, M. Fluder, M. Galica, D. Bogdal and I. Maciejaszek, *J. Appl. Polym. Sci.*, 2014, ***131***, 40608.

124 D. Carriazo, M. C. Gutiérrez, M. L. Ferrer and F. del Monte, *Chem. Mater.*, 2010, **22**, 6146–6152.

125 J. D. Mota-Morales, M. C. Gutiérrez, M. L. Ferrer, R. Jiménez, P. Santiago, I. C. Sanchez, M. Terrones, F. Del Monte and G. Luna-Bárcenas, *J. Mater. Chem. A*, 2013, **1**, 3970–3976.

126 R. J. Sánchez-Leija, J. R. Torres-Lubián, A. Reséndiz-Rubio, G. Luna-Bárcenas and J. D. Mota-Morales, *RSC Adv.*, 2016, **6**, 13072–13079.

127 K. F. Fazende, D. P. Gary, J. D. Mota-Morales and J. A. Pojman, *Macromol. Chem. Phys.*, 2020, **221**, 1900511.

128 L. Ren'ai, K. Zhang, G. Chen, B. Su, J. Tian, M. He and F. Lu, *Chem. Commun.*, 2018, **54**, 2304–2307.

129 R. Li, G. Chen, M. He, J. Tian and B. Su, *J. Mater. Chem. C*, 2017, **5**, 8475–8481.

130 M. C. Serrano, M. C. Gutiérrez, R. Jiménez, M. L. Ferrer and F. del Monte, *Chem. Commun.*, 2012, **48**, 579–581.

131 S. García-Argüelles, M. C. Serrano, M. C. Gutiérrez, M. L. Ferrer, L. Yuste, F. Rojo and F. del Monte, *Langmuir*, 2013, **29**, 9525–9534.

132 J. Dou, Y. Zhao, H. Li, J. Wang, A. Tahmasebi and J. Yu, *ACS Omega*, 2020, **5**, 31220–31226.

133 D. Carriazo, M. C. Gutiérrez, R. Jiménez, M. L. Ferrer and F. del Monte, *Part. Part. Syst. Charact.*, 2013, **30**, 316–320.

134 J. Patiño, M. C. Gutiérrez, D. Carriazo, C. O. Ania, J. L. G. Fierro, M. L. Ferrer and F. del Monte, *J. Mater. Chem. A*, 2014, **2**, 8719–8729.

135 J. Patiño, M. C. Gutiérrez, D. Carriazo, C. O. Ania, J. B. Parra, M. L. Ferrer and F. del Monte, *Energy Environ. Sci.*, 2012, **5**, 8699–8707.

136 M. C. Gutiérrez, D. Carriazo, C. O. Ania, J. B. Parra, M. L. Ferrer and F. del Monte, *Energy Environ. Sci.*, 2011, **4**, 3535–3544.

137 J. Patiño, N. López-Salas, M. C. Gutiérrez, D. Carriazo, M. L. Ferrer and F. del Monte, *J. Mater. Chem. A*, 2016, **4**, 1251–1263.

138 O. Coulembier, V. Lemaur, T. Josse, A. Minoia, J. Cornil and P. Dubois, *Chem. Sci.*, 2012, **3**, 723–726.

139 M. G. Pérez-García, M. C. Gutiérrez, J. D. Mota-Morales, G. Luna-Bárcenas and F. Del Monte, *ACS Appl. Mater. Interfaces*, 2016, **8**, 16939–16949.

140 S. Wu, C. Cai, F. Li, Z. Tan and S. Dong, *Angew. Chemie Int. Ed.*, 2020, **59**, 11871–11875.

141 N. Ndizeye, S. Suriyanarayanan and I. A. Nicholls, *Polym. Chem.*, 2019, **10**, 5289–5295.

142 M. S. Silverstein, *Isr. J. Chem.*, 2020, **60**, 140–150

CHAPTER 2

From polymer blends to a block copolymer: ring-opening polymerization of L-lactide/ε-caprolactone eutectic system

In this work, we provide new insights into the ring-opening polymerization (ROP) of eutectic mixtures of L-lactide and ε-caprolactone that lead to the synthesis of polymer blends and a block copolymer. The influence of a set of parameters is studied to produce polyesters with tunable average-molecular weight, crystallinity, and polymer architectures with controlled degradation profiles. The outcome depends on the selection of organocatalysts, including 1,5-diazabicyclo (4.3.0) non-5-ene (DBN), a new catalyst for the L-lactide/ε-caprolactone eutectic mixture ROP that enabled increasing the polymerization temperature. The mild polymerization temperatures and solventless conditions stand as green features of the ROP here described to prepare resorbable biomaterials with programmable degradation profiles.

This Chapter was published in Polymer, **2022**, 262, 125432. https://doi.org/10.1039/D0GC02274H

2.1 Introduction

Poly(L-lactide) (PLLA) and poly(ε-caprolactone) (PCL) represent two of the most important biodegradable and biocompatible commercial polyesters, being critical components in materials applied in areas such as packaging, biomedicine, and 3D printing.[1] These polyesters are obtained by the catalytic ring-opening polymerization (ROP) of their respective monomers, L-lactide (LLA) and ε-caprolactone (CL). [2]

PLLA and PCL synthesis via ROP mechanism is preferred over other mechanisms such as polycondensation due to better control on the molecular weight and polydispersity of the resulting polymers.[3] Although these two polymers represent biodegradable alternatives to other synthetic polymers, their production typically requires high temperatures, in bulk or in solution, and avoiding undesired side reactions in these conditions is challenging. Industrial synthesis of these polyesters are typically carried out by melting (150-200ºC) due to lower environmental impact and cost.[4–6] It also includes the use of metal-based catalysts which are reported to be the most efficient in their production,[7,8] e.g., tin-based catalysts allow obtaining polyesters with high molecular weights,[5] and is approved by the FDA.[8] However, it demands an additional purification step, which may generate environmental issues and compromises some applications.[9] In addition, some upcoming regulations will be limiting their use.[4,5,8] Thus, the search for catalytic alternatives to produce PLLA and PCL, excluding the use of toxic solvents, is a current challenge.

Greener routes for PLLA and PCL synthesis also mean new possibilities to apply them in diverse areas in simple manners, for instance, without demanding purification steps post-synthesis while expanding their properties. The use of organocatalysts has been proposed as a greener alternative to produce PLLA and PCL. Compared to metal catalysts, some advantages of organocatalysts include their environmentally friendly character, less toxicity, and ease of removal with greener solvents (e.g., ethanol).[2,5,10,11] In this line, the amidine organocatalysts such as [1,8-diazabicyclo 5.4.0] undec-7-ene (DBU), which is a strong base, has been used in the ROP of LLA due to its high selectivity.[12]

As for the ROP of CL, acid organocatalysts such as methanesulfonic acid (MSA) are commonly used to provide faster reactions and excellent control in the ROP.[11] The type of organocatalyst and their structure determines the mechanism by which the ROP operates, for instance, by a nucleophilic attack [12] or monomer activated chain pathway [11], in the case of DBU and MSA, respectively. The ROP of LLA and CL using organocatalysts can be performed in bulk and in solution. The use of organocatalysts presents some drawbacks, such as high costs and low operational temperatures resulting in low molecular weights. [2,3,6,12] However, low molecular weight polymers can lead to programmable degradation profiles in resorbable biomaterials.

Substantial efforts have been made to reduce the use of volatile organic solvents in polymer production, especially those regarded as toxic. In this context, the deep eutectic solvents (DESs) have emerged as a new family of designer solvents, many of them with notable green features. DESs comprised combinations of two or more components capable of self-associating through hydrogen bond interactions, with a resulting melting point lower than their individual components.[13,14] DESs implementation in polymer science goes beyond its functioning as inert solvents; they can also play the role of monomers that can polymerize in bulk for instance. These types of DESs are known as DES monomers (DESm), which exhibit greener features, meaning polymerizations are possible in solventless conditions and with a 100% atom economy. [15]

Coulembier et al. first reported the ROP at 23 °C of a non-ionic DESm composed of an equimolar mixture of LLA and trimethylene carbonate using DBU organocatalyst and benzyl alcohol (BnOH) as initiator. The sequential polymerization of the eutectic mixture yielded a copolymer with a gradient composition.[16] Later, our group demonstrated the ROP at 37 °C of a eutectic mixture composed of LLA and CL in a 3:7 molar ratio, respectively, using DBU and MSA organocatalysts, and BnOH as initiator. A blend of homopolymers with high crystallinity and high conversion in solventless conditions was obtained. It should be noted that a sequential polymerization took place, the homopolymerization of LLA catalyzed by DBU using BnOH as initiator first, followed by the addition of MSA for the ROP of CL.[17]

Taking advantage of this approach, it was possible to functionalized hierarchical macroporous polyesters composed of PLLA and PCL applied for hydrocarbon separation processes. The synthesis was carried out by using high internal phase emulsions (HIPEs) as templates, where polymerization of the continuous phase composed of LLA/CL (3:7 molar ratio respectively) affords macroporous polymers.[17] In the same line, it was possible to functionalized the internal walls of macroporous polyesters with non-functionalized nanohydroxyapatite, by polymerization of the continuous phase of a HIPE, to obtain polyester-hydroxyapatite composites with prospect applications in tissue engineering.[18]

Polyesters are limited in some applications due to their mechanical properties, for instance, PLLA and PCL exhibit poor elasticity and toughness, respectively.[2] These properties can be improved by increasing their molecular weight and modifying their crystallinity. Strategies such as blending, synthesis of copolymers, stereocomplexation, or incorporation of nanofillers, are some alternatives.[19,20]

Herein, we present advances in obtaining a series of blends and copolymers of PLLA and PCL through a sustainable synthetic protocol in solventless conditions and without metal-based catalysts. This approach is based on the eutectic composition of LLA and CL monomers mixture, which upon ROP at various temperatures and with the aid of strong bases (e.g., amidines) and an acid organocatalyst, resulted in a series of polyesters with tunable molecular weight, crystallinity, and molecular architecture. For this purpose, we took advantage of using a DESm, thus excluding organic solvents in the ROP and substituting metal-based catalysts with organocatalysts such as DBU and MSA at similar concentrations as reported on literature.[8,12,21,22] Additionally, we propose using 1,5-diazabicyclo (4.3.0) non-5-ene (DBN) as a suitable organocatalyst towards the ROP of LLA in the DESm for the first time. DBN is a strong base [12] employed in the synthesis of carbolines or acylation of pyrroles and indoles. [23] Altogether, these green features open the possibility of exploring new applications for PLLA and PCL blends and copolymers in areas such as biomaterials with programmable biodegradability.

2.2 Experimental section

2.2.1 Materials

ε-Caprolactone (CL, 97%), L-lactide (LLA, 98%), 1,8-diazabicyclo [5.4.0] undec-7-ene (DBU, 98%), 1,5-diazabicyclo (4.3.0) non-5-ene (DBN, 99%), methanesulfonic acid (MSA, 99.5%), and benzyl alcohol (BnOH, 99%) were obtained from Sigma-Aldrich.

2.2.2 Synthesis

The DES monomer was obtained by mixing LLA and CL with a 3:7 molar ratio at 90 °C until a clear homogeneous liquid was observed; the mixture remained liquid upon cooling to room temperature. It is important to mention that LLA and CL did not require further purification.

Next, the sequential ROP of the DESm (LLA/CL, 3:7 molar ratio, respectively) was carried out by adding a mixture of DBU or DBN, 2.92 wt.%, (organocatalyst) and BnOH, 2.08 wt.%, as the initiator (1:1 molar ratio, organocatalyst: initiator), both accounting 5 wt.% with respect to the eutectic mixture, at different temperatures (37, 60, 80 and 92 °C). Subsequently, a second organocatalyst, MSA, was added to the reaction mixture (3 wt.% to the eutectic mixture). The synthesized polyesters were named according to the first organocatalyst used (BU for DBU and BN for DBN), followed by the polymerization temperature.

The reaction was maintained for 12 hours to ensure that the polymerization reached high conversions. This duration was proposed based on a previous report that indicated that the ROP of DES LLA/CL at 37ºC, with DBU and MSA as organocatalysts, and BnOH as initiator were carried out within 6 hours.[17] Thus, after 12 hours it was ensured that the polymerization reached high conversions. Then, the samples were washed with ethanol to remove the organocatalysts and all residual monomers and oligomers, considering that in future applications in tissue engineering, the release of acidic oligomers may trigger the accelerated hydrolysis of the polyesters and cause toxic effects. Experimental conversions were determined by gravimetry, i.e., the ratio between the final polymer's mass and the initial mass of monomers. The experimental conversions in all the samples were *ca.* 88%.

The eutectic mixture composed of an isomer of lactide, and CL, were prepared similarly to the DESm of LLA/CL but in different molar ratios 20:80; 25:75, 30:70 (lactide in the eutectic mixture possesses the same proportion of D-LA and L-LA). Although these new eutectic mixtures were unstable compared with DES composed of LLA and CL, it was possible to stabilize them by heating the eutectic mixture at 60 ºC and mixing at 2500 rpm for 1 minute, previously to the polymerizations at temperatures of 37 and 60 ºC.

2.2.3 Characterizations

^{1}H (400 MHz), NMR spectra were obtained at room temperature with a 400 MHz Bruker Avance III HD 400N spectrometer (with a 5 mm multinuclear BBI-decoupling probe with Z grad). Chemical shifts (ppm) are relative to the remaining non-deuterated chloroform signal (from $CDCl_3$) and used as an internal reference for ^{1}H NMR spectroscopy.

Differential scanning calorimetry (DSC) measurements were carried out using a Mettler Toledo calorimeter model DSC3+ previously calibrated with indium. Scans were carried out at 10 ºC min^{-1} under nitrogen flow. First, the samples were cooled from room temperature to −20 °C, then the temperature was maintained at −20 °C for 10 min, after the temperature were raised to 140 °C, and finally decreased from 140 °C to room temperature.

The X-ray diffraction patterns were obtained using a diffractometer Rigaku (Ultima IV model, Texas-USA), with a detector D/tex ultra (35 kV and 15 mA) and using a CuKα radiation wavelength (λ = 0.15406 nm).

DOSY (Diffusion Order Spectroscopy) data were acquired using the pulse program ledbpgp2s installed in the topspin 3.6.2 software from Bruker with 95 gradient levels with a linear increase from 2% to 95% using a gradient of strengths up to 54 G/cm and 8 transients. The diffusion delay (Δ) was 150 ms, and the length of the square diffusion encoding gradient pulse (δ) was 0.6 ms. Laplace transformations for generating the diffusion dimensions were obtained with the Bruker Biospin Dynamics Center using a least-squares fitting routine with Monte Carlo error estimation analysis.

Size exclusion chromatography (SEC). The molecular weight characteristics of polymers were determined by SEC using a Hewlett-Packard instrument (HPLC series 1100) equipped with UV light and refractive index detectors. A PLGel mixed column was used (1-PL Gel 10 6A− 400,000-40,000,000; 2-PL Gel mixed C 200-3,000,000), with refractive index at 40 °C. Calibration was carried out with polystyrene standards and THF (HPLC grade) was used as eluent at a flow rate of 1 mL/min.

The PLLA/PCL blends and copolymers were also analyzed by matrix-assisted laser desorption/ionization time-of-flight mass spectrometry (MALDI/TOF-MS). MALDI/TOF-MS measurements were performed on a BRUKER ULTRAFLEX III (MALDI-TOF/TOF) mass spectrometer equipped with a pulsed NdYAG laser (λ = 355 nm) and a delayed extraction ion source. Mass spectra were obtained over the m/z range of 500−10000 Da in the reflector positive ion mode. External mass calibration was applied. Trans-2-[3-(4-tert-butylphenyl)-2-methyl-2-propenylidene] malononitrile (DCTB) at 8 mg mL^{-1} in dichloromethane (DCM) was used as the matrix. Samples were dissolved at a concentration of 2 mg mL^{-1} in DCM, being 5 mL mixed with the matrix at a ratio of 1:4 (v/v) and 0.5 μL of sodium iodide (2 mg mL^{-1}). Then, 0.5 μL of this solution was spotted onto a flat stainless-steel sample plate and dried in air.

The optical transmittance measurements were carried out with a UV–Vis Hitachi U-1800 spectrophotometer using a 1 cm path length quartz cell, in a wavelength range from 300 to 800 nm at 20 °C.

2.3 Results and discussion

2.3.1 Synthesis of homopolymers and copolymer

The sequential ROP of the LLA/CL DESm is described in Scheme 1. First, the nucleophilic organocatalysts (DBU or DBN) allow the selective ROP of LLA using the BnOH as initiator at temperatures ranging from 37 to 92 °C, depending upon the use of DBU or DBN. At this point, the composition of the medium comprises PLLA chains dispersed in the liquid CL, which was released from the liquid eutectic composition as LLA was consumed.

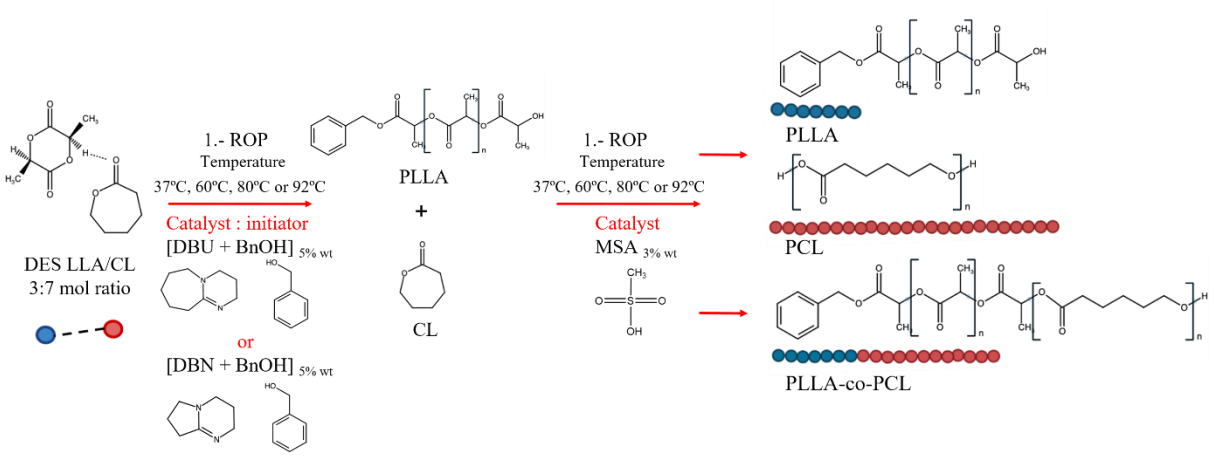

Scheme 1. Sequential Ring-Opening Polymerization of the DESm composed of LLA/CL (3:7 molar ratio) at different temperatures. DBU and DBN organocatalyst were used for the selective ROP of LLA in the first step, and they were added together with the initiator BnOH (1:1, molar ratio). MSA was used as a second organocatalyst to start the ROP of CL in the presence of the already formed PLLA.

Under these temperature conditions, pure LLA is solid (melting point of LLA is ca 98.3 °C) and thus not available to polymerize. Subsequently, MSA (second organocatalyst) was added to the reaction mixture promoting the ROP of CL. In this second ROP, the hydroxyl groups from either lactidyl previously formed or the residual water played the role of initiator,[17] depending on the temperature and organocatalyst. As a result, PLLA/PCL blends, or a P(LLA-*b*-CL) copolymer were obtained.

It is worthy of mentioning two critical aspects of the new nucleophilic organocatalyst proposed for the LLA/CL DESm ROP: 1) the DBN was able to selectively polymerize the LLA present in the eutectic mixture, similarly to DBU, and 2) it was possible to carry out the ROP at higher temperatures (e.g., 80 and 92 °C), temperatures at which DBU readily degrades, [8] thus expanding the polymerization conditions for this type of polymerization. The general procedure is described in detail in the experimental section.

2.3.2 Characterization of PLLA, PCL and p(LLA-*b*-CL)

The ROP of LLA and CL was confirmed by ^{1}H NMR spectroscopy, where typical peaks for PLLA were found at 1.60 ppm and 5.19 ppm assigned to (-**CH$_3$**) and (-**CH**-) groups, respectively in all samples. The appearance of the terminal peak at 4.39 ppm was related to the methine end group (-CH$_3$**CH**OH). The ROP of CL was confirmed by the presence of the peak at 3.68 ppm assigned to the terminal methylene group -**CH$_2$**OH: note the very low intensity of the peak in the copolymer at 4.39 ppm (BN37) in Figure 1, inset b), which will be further discussed below. The average molecular weight (M_n) was calculated by ^{1}H NMR spectroscopy.

The M_n of PLLA was obtained by the integration ratio of peaks that correspond to the repeating methine groups (δ= 5.19 ppm) and the terminal aromatic group from BnOH (δ= 7.34 ppm).[16] The aromatic terminal group from BnOH alcohol initiation could be presented in both the PLLA homopolymer and the PLLA block in the copolymer, so it is possible to calculate the PLLA M_n in both cases.

The same process was applied to determine the M_n of PCL. In this case, the signals were attributed to the repeating ε-methylene groups at δ= 4.08 ppm and the terminal methylene group at δ= 3.67 ppm.[17] The absence of peaks at 3.0 and 3.2 ppm which corresponded to the methylene and methyl groups for MSA and DBU, respectively, ensured that they were removed during the purification process.

The M_n of PLLA ranged from 1736 g mol^{-1} at 80 ºC to 2182 g mol^{-1} at 60 ºC (Table 1). As mentioned before, LLA polymerized in a first step in the eutectic mixture of LLA/CL[17] (having a constant molar ratio of CL of 0.7). Thus, the polymerization temperatures and type of organocatalyst (DBU or DBN) did not strongly affect its molecular weight. It is important to mention that DBU and DBN belong to the amidine family. However, while DBU has been widely reported in the synthesis of PLLA, [12] there is no information about DBN use as an organocatalyst for similar ROP of LLA as in this work.

We propose using DBN in the ROP of the eutectic mixture LLA/CL to expand the polymerization temperatures for the first time. The DBN organocatalyst possesses selectivity for the LLA in the eutectic mixtures similarly to DBU but exhibits a higher operating temperature range. Thus, the ROP was possible above 79 °C (DBU degrades at 79 °C [8]). On the other hand, by increasing the temperature above 60 ºC in the sequential ROP, i.e., just above the melting point of PCL, PCL formation takes place in unreacted CL and the molten polymer containing PLLA. Here, the viscosity of the medium decreased as compared with ROP at 37 °C, promoting the diffusion of CL available for the ROP, similarly to the ROP of trimethylene carbonate-based DESm.[16] Therefore, the M_n of PCL in the resulting polyesters increased from 4013 at 37 °C to *ca*. 6988 g mol^{-1} at 92 °C, see Table 1.

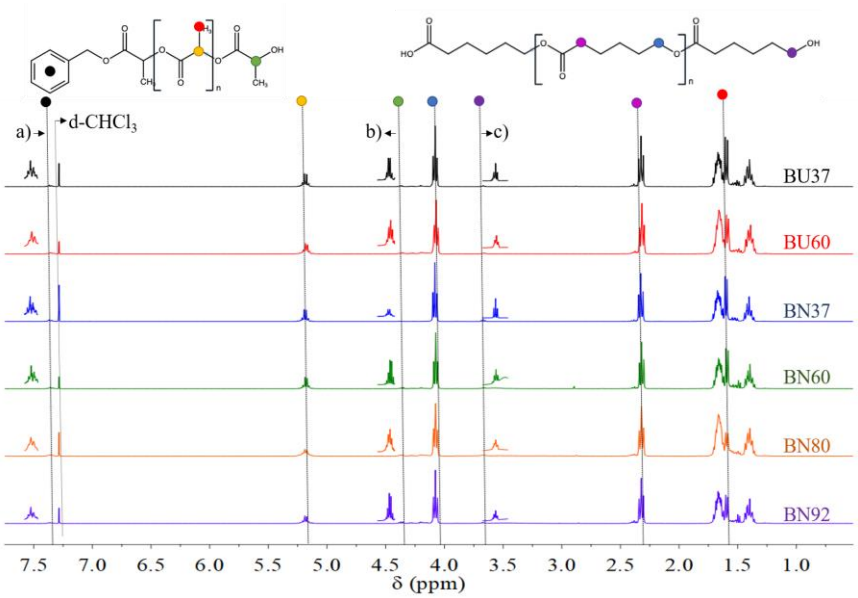

Figure 1. ^{1}H NMR spectra of synthesized polyesters: **BU37** (black), **BU60** (red), **BN37** (blue), **BN60** (green), **BN80** (orange), and **BN92** (purple). (Insets, zoom of the signals for a) δ= 7.34 ppm and b) 4.39 ppm of PLLA, and c) δ= 3.68 ppm of PCL).

Table 1. Summary of the ROP of LLA/CL DESm. ROP temperature, experimental conversion, experimental PLLA/PCL molar ratio, number-average molecular weight (M_n), melting point (Tm), crystallinity (Xc), and architecture of polyesters resulted from the ROP of DESm composed of LLA/CL (3:7 molar ratio) at the indicated conditions.

Sample[a]	ROP Temp (ºC)	Conv (%)[b]	PLLA/PCL[c]	$M_{n,NMR\ PLLA}$[d] (g mol^{-1})	$M_{n,NMR\ PCL}$[d] (g mol^{-1})	$T_{m,PLLA}$[e] (ºC)	$X_{c,PLLA}$[e] (%)	$T_{m,PCL}$[e] (ºC)	$X_{c,PCL}$[e] (%)	Polymer architecture[f]
BU37	37	89	38 : 62	1964	4013	116.5	30	60	69	Blend
BU60	60	88	39 : 61	2182	5444	116.6	30	58	62	Blend
BN37	37	88	38 : 62	1835	4490	105.3	37	60	73	Copolymer
BN60	60	88	40 : 60	1867	5746	116.7	30	58	60	Blend
BN80	80	88	35 : 65	1736	5918	105.3	20	60	63	ND [g]
BN92	92	86	33 : 67	1962	6988	94.2	13	50	44	ND [g]

[a] Organocatalysts:initiator, DBU:BnOH:MSA or DBN:BnOH:MSA, used for the ROP of LLA. The molar ratio of catalyst (DBU or DBN): initiator (BnOH) was [1:1], respectively, and they represented 5 wt.% with respect to the eutectic mixture. The weight of MSA was 3 wt.% with respect to the eutectic mixture. The polymerization temperature was added to the second column,

[b] experimental conversions obtained by gravimetry, [c] molar ratio and [d] number-average molecular weight obtained by ^{1}H NMR, [e] thermal properties calculated by DSC, [f] obtained by ^{1}H NMR diffusion-ordered spectroscopy, [g] ND not determined.

The thermal properties of the synthesized polyesters were analyzed by DSC. Figure 2-A shows the corresponding thermograms, where two endothermic peaks were observed. The first one corresponds to the melting point of PCL identified from 58 to 60 ºC (peak a), and the second small one corresponds to the melting point of PLLA identified from 94.2 to 116.7 ºC (peak b).[17] The samples' crystallinity was determined considering the ratio of the melting enthalpy of each compound obtained by DSC (PLLA or PCL), with respect to the compound reference with 100% crystallinity (106 J g^{-1} for PLLA, and 135 J g^{-1} for PCL, see details in equation 1).[24,25]

A closer analysis of the DSC traces reveals that, as the temperature of polymerization increases from 60 to 92 °C, using DBN as organocatalyst for LLA ROP, the Tm of PLLA decreased, as shown in Table 1. A possible scenario is that PLLA Tm decrease results from PLLA domains being in a glassy state when the ROP of CL started (the PLLA glass transition temperature is around 50 °C).[26] At these temperatures, PLLA reorganization in a molten media could be restrained, as reported by Lv et al. during the annealing of PLLA/PCL blends, causing the reduction of their Tm and crystallinity.[27]

Equation 1. Degree of crystallization equation

$$x_c^a = \frac{100}{X^a}\left(\frac{\Delta H_m^a}{\Delta H_{mo}}\right)$$

x_c^a = *Degree of crystallinity of componente a*

X^a = *Mass fraction of component a in eutectic mixture*

ΔH_m^a = *Melting enthalpy of component a, obtained by DSC*

ΔH_{mo} = *Melting enthalpy of component with* 100% *of crystallinity* ($PLLA$ 106 $g\ mol^{-1}$; PCL 135 $g\ mol^{-1}$)

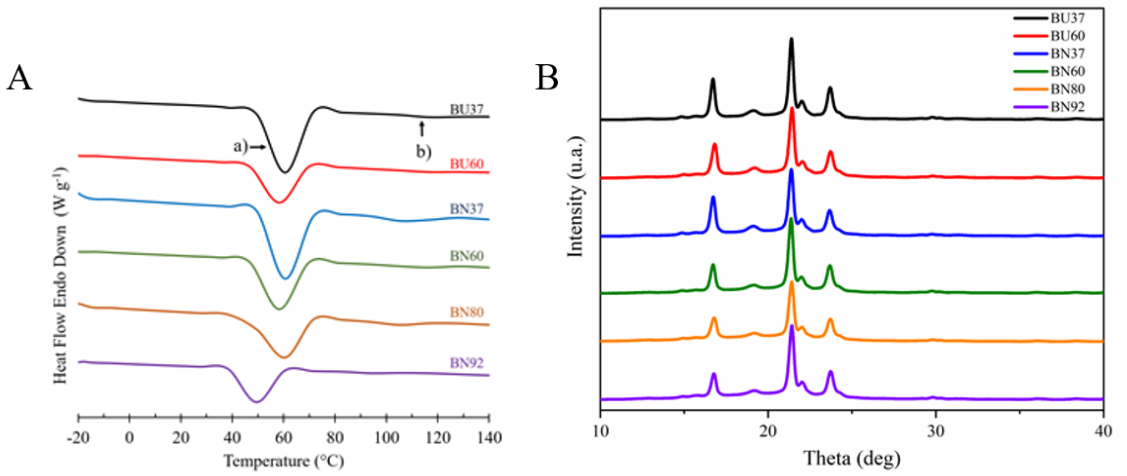

Figure 2-A. DSC scans of polyesters. Figure 2-B. XRD scans of polyesters of **BU37** (black), **BU60** (red), **BN37** (blue), **BN60** (green), **BN80** (orange), and **BN92**.

On the other hand, it was reported that the rate of polymerization of racemic lactide in the absence of an initiator in CH_2Cl_2 or THF/ CH_2Cl_2 at room temperature is lower with DBN than DBU.[28]

Thus, it is possible that the lower polymerization rates (e.g., at 37 ºC) enable PLLA chains to organize, improving their crystallinity, mainly in the solventless polymerization conditions like in this work. This effect was observed in sample BN37 which showed a higher crystallinity (37%) than sample BU37 (30%) obtained under the same conditions. Han et al. reported that when the ratio of PLLA exceeded 0.57 in a P(LLA-*b*-CL) copolymer, the PLLA exhibited a melting point depression and an enhanced crystallinity.[29] These PLLA characteristics were observed in sample BN37, suggesting a copolymer formation. Conversely, the PCL exhibited a high crystallinity compared with PLLA in all cases regardless of the polymerization temperature. However, PCL in BU37 and BN37 samples presented the highest crystallinity with 69% and 73%, respectively. The high crystallinity of PCL at 37 ºC resulted from the ROP carried out below its melting point, as discussed by Pérez-García et al.[17] The semicrystalline character of all polyesters was further demonstrated by X-ray diffraction showing the PCL and PLLA characteristic peaks (XRD; Figure 2-B).

The PLLA/PCL ratio was determined by ^{1}H NMR spectroscopy by dividing the integral of the signal assigned to the repeating groups in the synthesized polyesters. In the case of PLLA, the methine group at δ= 5.19 ppm was used, while for PCL, the ε-methylene group at δ= 3.67 ppm. The differences in the composition between the original ratio (3:7 LLA/CL) and the final PLLA/PCL ratios (Table 1) were associated with the loss of PCL oligomers during the washing process with ethanol, which also reflects the polydispersity of PCL likely due to CL diffusion constrained at high conversion in the second step of ROP, as the whole reaction mixture solidifies into polymers in the case of low temperatures, and the high viscosity of the medium even at higher temperatures. The purification of sample BU37 was followed by ^{1}H NMR, including the analysis of the washing ethanol solution Figure 3. Peaks found at 3.1-3.6 and 2.0-2.3 ppm in the sample before the purification step and in the ethanol solution, are associated to the organocatalyst and residual unreacted monomers. The additional peaks in the ethanol solution at 4.1, 3.7, 2.3 and 1.4-1.7 ppm were associated to the PCL oligomers, see Figure 3-C.

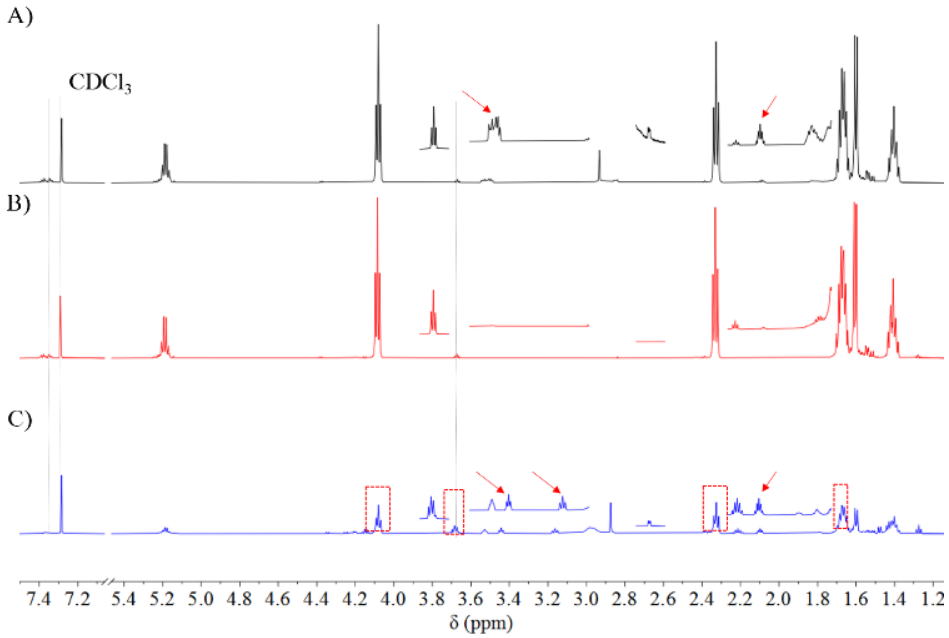

Figure 3. ^{1}H NMR spectra of synthesized polyesters of A) sample BU37 (black) without purification process, B) sample BU37 after were washing with ethanol (red), and C) Ethanol solution (blue) used in purification step for sample BU37.

To get deeper insights into the architecture of the final polyesters, selected samples were analyzed by ^{1}H NMR diffusion-ordered spectroscopy (DOSY). Polyesters BU37 and BN37 were selected owing to their high crystallinity and thermal properties. Samples BU60 and BN60 were also included for comparison. DOSY spectrum of polyester BU37 (Figure 4-A) shows two different diffusion coefficients (D_M), D_M BU37 = 9 .17 x10^{-9} m^2/s and $D_{M'}$ BU37 = 9.12 x10^{-9} m^2/s, consistent with the M_n of PCL and PLLA, respectively, calculated in Table 1. The signals of each species were compared with the upper axis representing the corresponding ^{1}H NMR spectra. It is confirmed that the sample contains a blend of homopolymers, the higher diffusion coefficient corresponding to heavier species, which was associated with PCL. In contrast, the low diffusion coefficient corresponds to PLLA. These results corroborated that M_n of PCL was higher than PLLA as determined by ^{1}H NMR and in accord with previous MALDI-TOF results reported by our group.[17]

In the case of sample BN37 (Figure 4-B), only one diffusion coefficient was observed, D_M BN37 = 8.83 x10^{-9} m^2/s, consistent with the presence of P(LLA-*b*-CL) copolymer, resulting from the sequential ROP of the DESm. The DOSY spectrum presented both signals in the upper axis associated with PLLA and PCL. These results revealed the successful formation of a block copolymer P(LLA-*b*-CL) from the ROP of LLA/CL DESm. As mentioned before, the polymerization rate of LLA using DBN is lower than DBU in solution.[28] In this scenario, it is possible that PLLA formed in the LLA/CL DESm presents available hydroxyl groups at the end chain, which then played the role of macroinitiator in the subsequent ROP of CL.

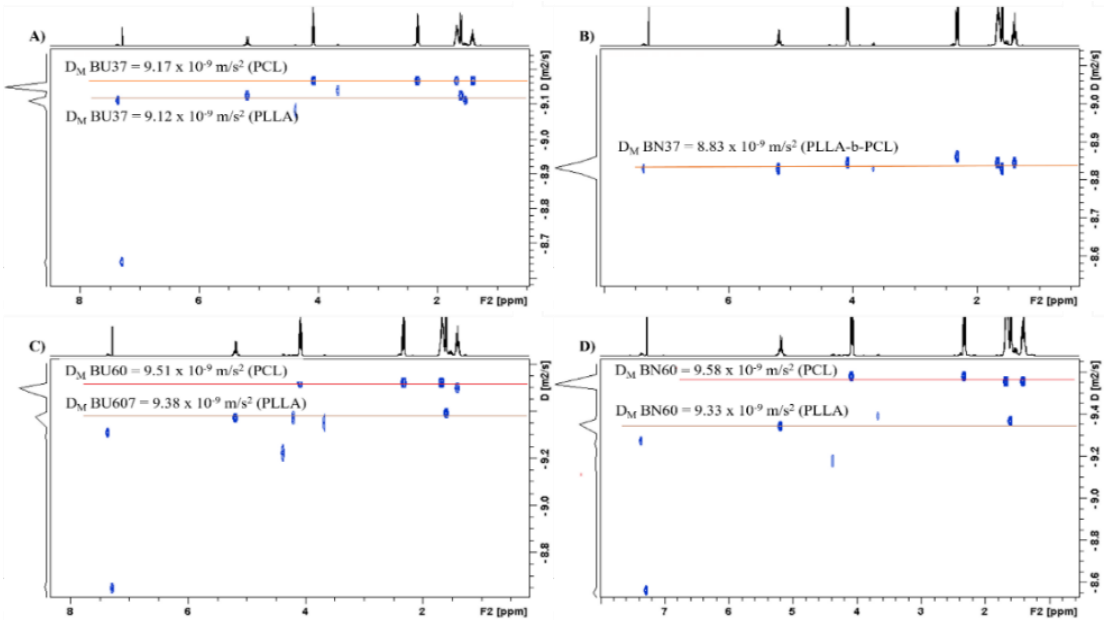

Figure 4. DOSY spectra in deuterated chloroform of **A)** BU37 and **B)** BN37; the ROPs were carried out at 37ºC; **C)** BU60 and **D)** BN60 the ROP was carried out at 60 ºC. The DOSY signals were associated with ^{1}H NMR spectra. The diffusion coefficient D_M (in m^2/s) is indicated for each component.

To determine the difference in the thermal stability of the polyesters after the purification step (all oligomers and organocatalyst, which are readily soluble in ethanol, were removed in this process, see Figure 3), their thermal decomposition was measured by TGA. PLLA has been reported to have low thermal stability compared to PCL.[30] Sample BN37 composed of P(LLA-*b*-CL) copolymer showed higher thermal stability, e.g., at 307.1 °C the weight loss was about 5%, while for sample BU37 that contained a blend of PLLA and PCL, the 5 % weight loss occurred at 212 °C.

In the case of the polymer blend, the degradation of PLLA at 320.6 °C corresponded to ca. 23.7% of weight loss, which is close to the PLLA content in the blend as observed in Figure 5-A.

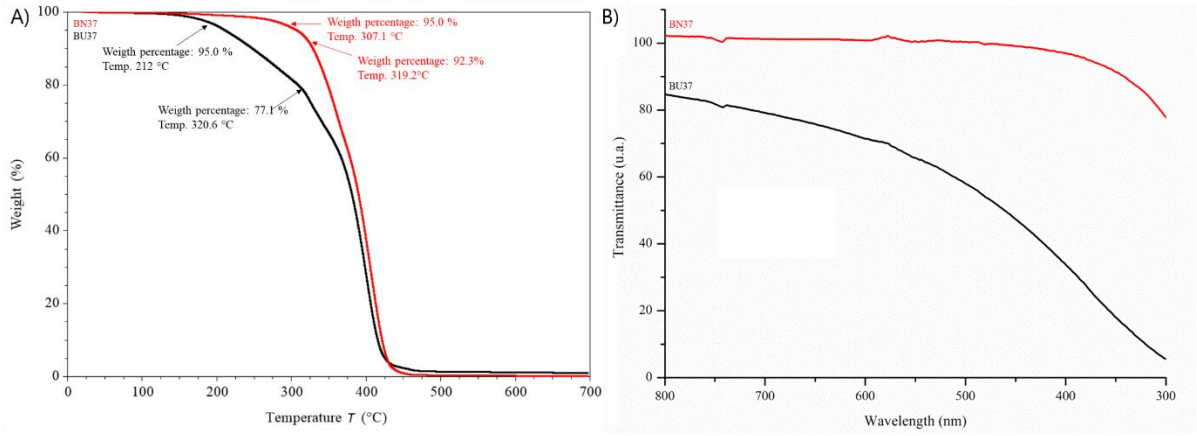

Figure 5. A) TGA thermograms of BU37 and BN37. B) Spectra of transmittance for samples BU37 and BN37 at 2.7 wt. % in toluene, the test was carried out in a wavelength from 300 to 800 nm.

In addition, a solubility test of both samples BU37 and BN37 was performed in toluene at RT. The insolubility of PLLA in toluene was greatly improved by the PCL counterpart presented in the copolymer as can be observed in Figure 6, in which turbidity was lower compared to the sample containing the blend of homopolymers (BU37). Differences in transmittance were observed when measured with a spectrometer in the range from 300 nm to 800 nm. The copolymer whose solution was less turbid showed a slight reduction in transmittance of about 20% in the whole range of the spectrum. Otherwise, turbidity was observed by the insolubility of PLLA in the blend solution, so the transmittance is reduced up to 80% in the same range. See Figure 5-B.

Figure 6. Photographs of BN37 (left) and BU37 (right) solutions in toluene.

The solubility test was performed by adding 40 mg of BU37 or BN37 in 1500 mL toluene. Sample BU37 (right) contains PLLA/PCL blend; PLLA in cold conditions tends to precipitate due to its low solubility. PCL present in copolymer BN37 (left) increased the solubility of PLLA.

BN37 and BU37 were further analyzed by the matrix-assisted laser desorption/ ionization time-of-flight (MALDI-TOF MS) and two main distributions were observed in both samples between 1000 and 8000 m/z, see Figure 7-A and 7-B, respectively. In BN37, the first population in the region between 1000 and 3000 m /z corresponded to the presence of PLLA with a separation of 72 units and initiated by BnOH. The most intense peaks were found at 1715-1900 m/z; this value matched the M_n determined by ^{1}H NMR spectroscopy. Some traces from another PLLA species were also found between 1481-2027 m/z, in which water played the role of initiator. In the region from 1600 to 3000 m/z the presence of a fraction of block copolymer was observed, constituted between 9-11 lactidyl units initiated by benzyl alcohol (BnOH), followed by caproyl units between 12 and 20; the same species were also reported by Pérez-García et al.[17], See Fig. 7-A. Finally, in 2200 to 3000 m/z region, signals from PCL initiated by residual water, and a P(LLA-*b*-CL) block copolymer appeared, which will be explained in more detail below.

In the second distribution between 3000 and 8000 m/z, PCL homopolymers were found between 4000 and 6500 m/z, where the mass of 114 between adjacent peaks corresponded to CL repeating units, and residual water controlled the polymerization. See Figure 8-B. From the second population, copolymers composed of PLLA and PCL were identified, corroborating previous results from ^{1}H NMR, DOSY, and thermal analyses. Lactidyl units initiated these copolymers, and water controlled the polymerization once the BnOH was consumed by LLA, followed by the ROP of CL monomers due to terminal hydroxyl groups in PLLA playing the role of macroinitiator.

It is important to mention that the PLLA block in sample BN37 previously identified by ^{1}H NMR, M_n = 1835 g/mol, was calculated considering that BnOH initiated the ROP. From MALDI-TOF it was observed that there exist copolymers initiated by both residual water (red star in Fig. 8A) and BnOH (orange arrow in Fig. 8A).

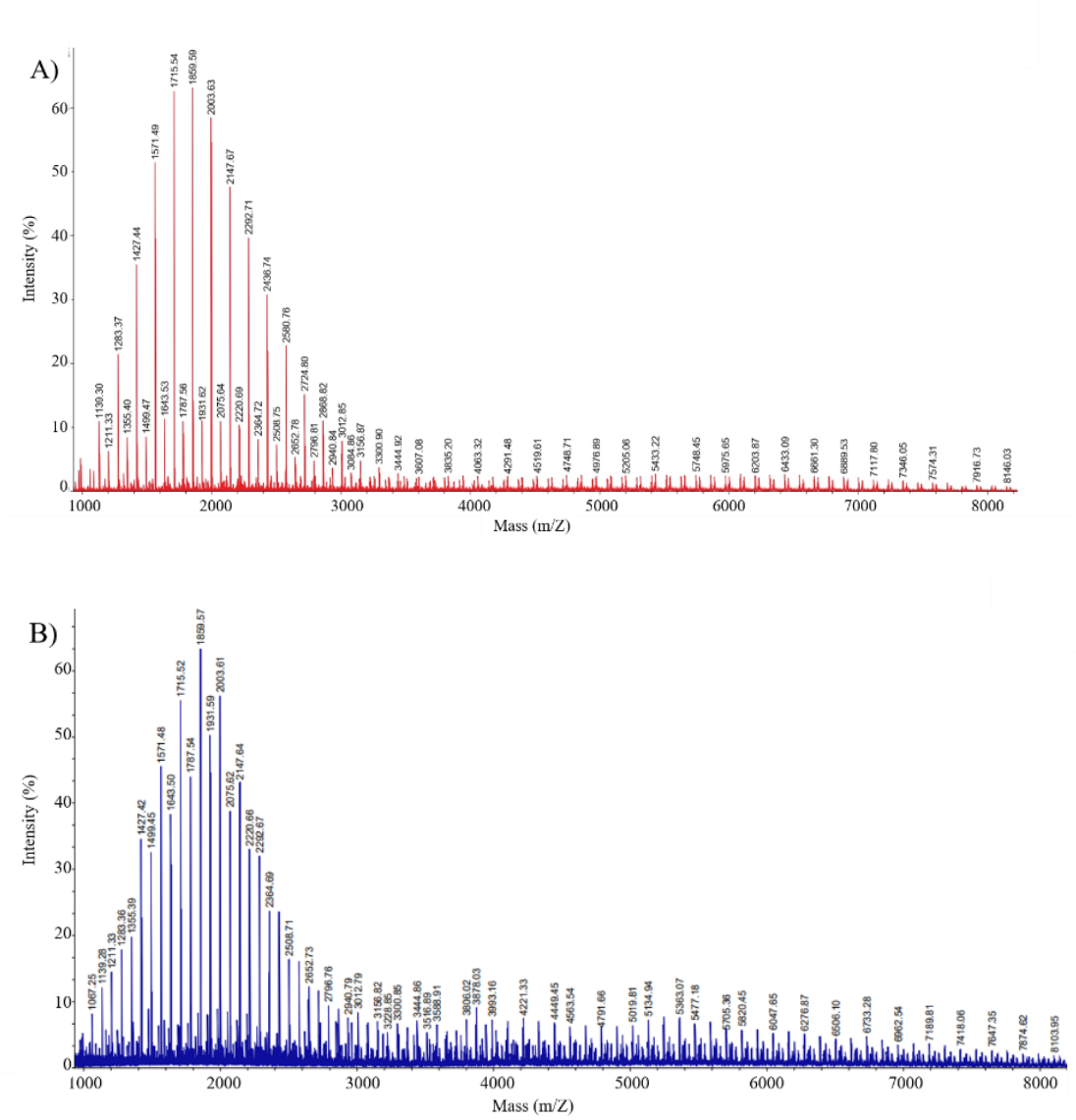

Figure 7. MALDI-ToF MS spectrum of the ROP of DES LLA/CL at 3:7 mol. ratio. The synthesis was carried out at 37°C, and BnOH as initiator. A) Sample BN37 in which DBN and MSA were used as organocatalysts; B) Sample BU37 which DBU and MSA were used as organocatalysts.

Thus, it is possible that the PLLA block determined by ^{1}H NMR corresponded to a PLLA homopolymer (ca. 1860 m/z, blue triangle in Fig. 8A). Overall, the copolymers identified between 3500 and 6500 m/z were composed of a small fraction of LLA units followed by 18 to 46 CL units (Figure 8-B). It is noteworthy that MALDI-TOF was able to identify homopolymers and copolymers in the sample, but not their ratio in the mixture.

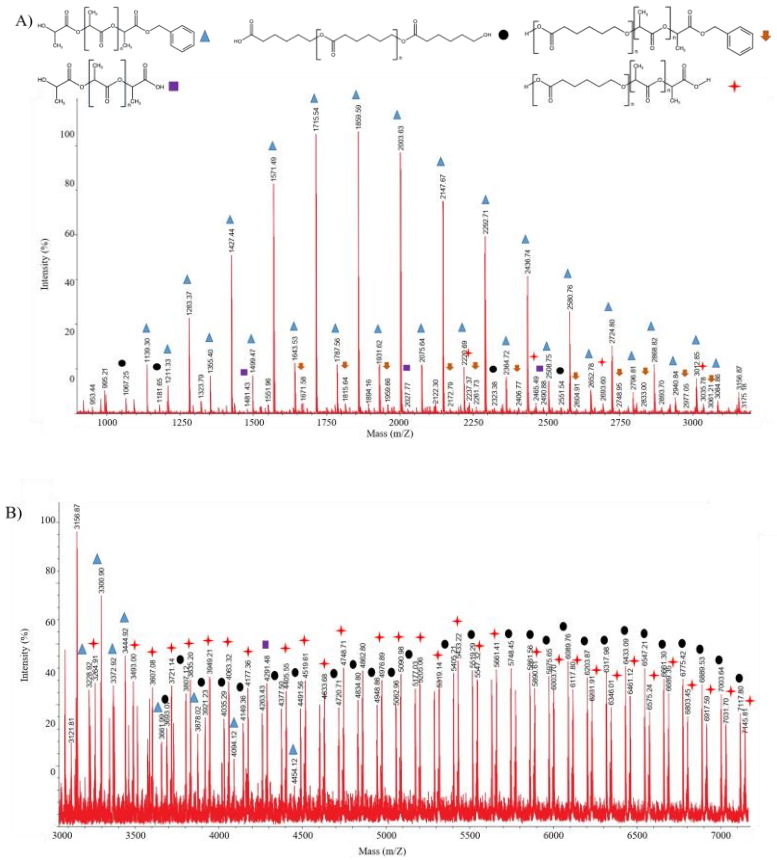

Figure 8. MALDI-TOF MS spectrum of BN37 A) from ranging 1000 to 3000 m/z B) from 3000 to 7000 m/z.

(⬇) Poly(L-lactide-*b*-ε-CL) copopolymer: Lactic acid$_{(n)}$ (M_w = 72 g/mol^{-1}) + ε-Caprolactone$_{(n)}$ (M_w = 114 g/mol^{-1}) + H (M_w = 1 g/mol^{-1}) + BnOH (M_w = 108 g/mol^{-1}) + Na^+ (M_w = 23 g/mol^{-1})

(✦) PCL copolymer: Lactic acid$_{(n)}$ (M_w = 72 g/mol^{-1}) + ε-Caprolactone$_{(m)}$ (M_w = 114 g/mol^{-1}) + H (M_w = 1 g/mol^{-1}) + OH (M_w = 17 g/mol^{-1}) + Na^+ (M_w = 23 g/mol^{-1})

(▲) PLLA homopolymer: Lactic acid$_{(n)}$ (M_w = 72 g/mol^{-1}) + BnOH (M_w = 108 g/mol^{-1}) + Na^+ (M_w = 23 g/mol^{-1})

(■) PLLA homopolymer: Lactic acid$_{(n)}$ (M_w = 72 g/ mol^{-1}) + H (M_w = 1 g/mol^{-1}) + OH (M_w = 17 g/mol^{-1}) + Na^+ (M_w = 23 g/mol^{-1})

(●) PCL homopolymer: ε-Caprolactone$_{(n)}$ (M_w = 114 g/mol^{-1}) + H (M_w = 1 g/mol^{-1}) + OH (M_w = 17 g/mol^{-1}) + Na^+ (M_w = 23 g/mol^{-1})

For example, in the first region that exhibited peaks associated with the presence of PLLA (Figure 7), its relatively high intensity in the mixture was not consistent with the molar ratio of LLA which was lower than CL (3:7 molar ratio LLA/CL, respectively), although it indicated that PLLA ionized better than the PCL.[31] On the contrary, with the original large molar ratio of CL in the DES, it was expected that the PCL homopolymer and the P(LLA-*b*-CL) copolymer peaks would have relatively higher intensities, but this was not observed in the spectra, meaning that their ionization capacity was lower for PLLA.

Thus, it is clear, that the single diffusion signal observed in the DOSY (Figure 4-B) can be ascribed mainly to the presence of copolymers in sample BN37 ultimately functioning as a compatibilizer of fractions of PCL and PLLA homopolymers, which gave rise to the enhanced thermal stability (Figure 5-A) and improved the toluene solvation capacity of the final products (Figure 6). A further opportunity for future work will be to find the conditions to increase the PLLA content in the copolymer beyond the 3:7 molar ratio of the eutectic composition of LLA/CL, respectively. For the samples BU60 (Figure 4-C) and BN60 (Figure 4-D), no changes were observed by using either DBU or DBN organocatalysts in the ROP of the PLLA/PCL DESm at 60 ºC; DOSY spectra for BU60 and BN60 resulted similarly. Their DOSY spectra were associated with the corresponding ^{1}H NMR spectra and two diffusion coefficients were observed for each sample, where both diffusion coefficients corresponded to a blend of homopolyesters (PCL/PLLA). BU60 exhibited the first diffusion coefficient D_M BU60 = 9.51 x10^{-9} m^2/s and the second one $D_{M'}$ BU60 = 9.38 x10^{-9} m^2/s, while BN60 showed the first diffusion coefficient D_M BN60 = 9.58 x10^{-9} m^2/s and the second one $D_{M'}$ BN60 = 9.33 x10^{-9} m^2/s.

The higher diffusion coefficient corresponds to the PCL, whereas the lower diffusion coefficient corresponds to PLLA. These results are in line with ^{1}H NMR, as the M_n of PLLA was slightly higher in the ROP catalyzed by DBU (Table 1).

Therefore, while the slower rate of LLA ROP at 37 ºC in the presence of DBN resulted in copolymer formation, increasing the temperature from 37 to 60 ºC counteracted this effect. This could be attributed to the higher polymerization rate at 60 ºC, leading to the formation of homopolymer blends regardless of whether DBN or BDU was used. Finally, size-exclusion chromatography (SEC) was performed on BU37, BU60, and BN37. SEC traces in samples BU37 and BU60 were similar due to the presence of homopolymers blend (PLLA/PCL). However, BN37 presented a different trace due to the copolymer presence P(LLA-*b*-CL) (Figure 9).

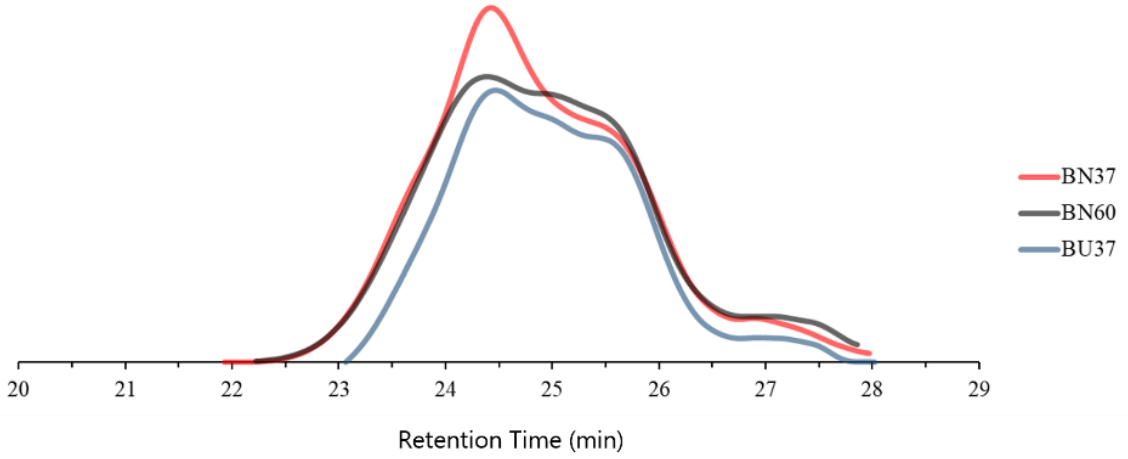

Figure 9. SEC traces for polyesters BU37 and BU60 that contain PLLA/PCL blend, and sample BN37 that was composed of copolymer P(LLA-*b*-CL).

2.3.3 Effect of benzyl alcohol (BnOH) as initiator on the molecular weight of PLLA

The average molecular weight of PCL in the ROP of the LLA/ CL eutectic mixture was modified in the range of ca. 4000-7000 g mol^{-1} by the appropriate selection of catalysts (DBU/DBN and MSA) and the temperature of polymerization (Table 1). However, as previously noted, the ROP is a sequential reaction where LLA polymerizes first within minutes,[17] and after the LLA monomer is depleted, it is not possible to increase the PLLA M_n despite raising the temperature of polymerization. Thus, lower concentrations of the initiator BnOH (2.0, 1.0, and 0.5 wt.%, with respect to the monomers) were employed to increase the molecular weight of PLLA homopolymer, keeping the same conditions described before for the ROP catalyzed by DBU at 37°C (Table 2).

Table 2. Properties of polyesters obtained by ROP of LLA/CL with different initiator (BnOH) concentration.

Sample	ROP Temp (ºC)	Initiator Conc. (wt. %)	Conv (%)[b]	PLLA/PCL[c]	$M_{n,\ NMR}$ $_{PLLA}$[d] (g mol^{-1})	$M_{n,\ NMR}$ $_{PCL}$[d] (g mol^{-1})	$X_{c,PLLA}$[e] (ºC)	$X_{c,PCL}$[e] (ºC)
BU37-2i	37	2.0	89	41 : 59	1746	4477	34	68
BU37-1i	37	1.0	87	40 : 60	3372	4730	31	64
BU37-0i	37	0.5	88	39 : 61	4048	4869	29	66

BU37-2i, BU37-1i and BU37-0i correspond to the polyesters obtained by the ROP of LLA/CL eutectic mixture, 3:7 mol ratio, respectively. 2.92 wt.% of DBU, varied concentrations of BnOH, 2.0, 1.0, and 0.5 wt.%, and 3 wt.% of MSA, all with respect to the eutectic mixture were used. [b] Experimental conversions were obtained by gravimetry. [c] Molar ratio and [d] number-average molecular weight were obtained by ^{1}H NMR. [e] Thermal properties were calculated by DSC.

The average molecular weight of PLLA increased from 1746 to 4048 mol g^{-1} as the initiator decreased from 2 wt.% to 0.5 wt.%, as expected, i.e., less initiator with a fixed concentration of monomer means more monomer available for the polymer chain growth. It was also observed a decrease of PLLA crystallinity from 34% to 29% as the average molecular weight increases (Table 2), pointing to unfavorable conditions to assemble larger chains into crystalline domains. Thus, the selectivity of the organocatalyst DBU for the ROP of LLA together with the different concentrations of BnOH effectively modified the molecular weight of PLLA. On the other hand, because the specific catalytic activity of MSA towards the ROP of CL and the role of water presented in the media as initiator in the second ROP, the molecular weight of PCL yielded similar values between 4477 and 4869 mol g^{-1}. The samples also were analyzed by SEC (Figure 10). Interestingly, the trace of sample BU37-0i showed a narrower peak due to the close elution time of PLLA and PCL (Fig. 10-C), meaning similar molecular weight, which is consistent with the closer value of their M_n calculated from ^{1}H NMR, 4048 and 4869 mol g^{-1}, respectively. In contrast, samples BU37-1i and BU37-2i showed similar bimodal peaks (Fig. 10 A and B) as the PLLA/PCL blend in sample BU37 (Fig. 9). Based on these results, it is easy to envisage the design of block copolymers with the PLLA block of tunable length.

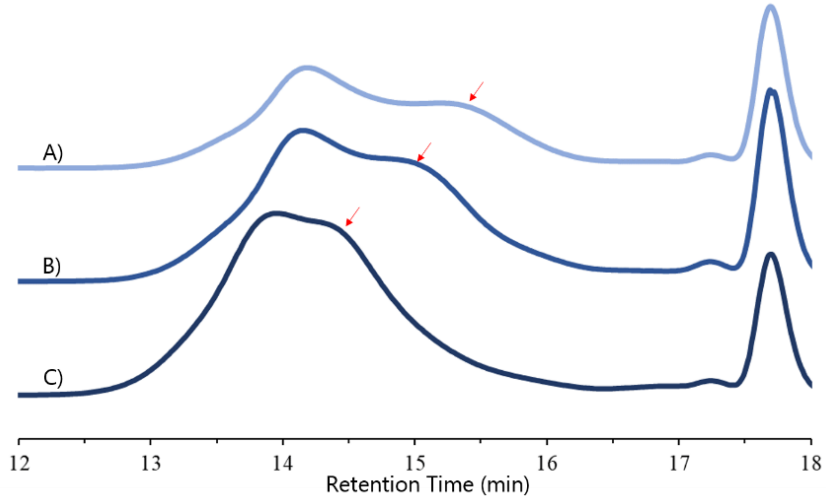

Figure 10. SEC traces for polyesters obtained by the ROP of LLA/CL at 37 mol. ratio, and at 37 ºC, DBU, and MSA were used as organocatalyst at 2.92 wt% and 3 wt.% respect with the eutectic mixture, respectively. The ratio of benzyl alcohol, which was used as initiator, was A) 2.0 wt.%, B) 1.0 wt.% and C) 0.5 wt.% all of them were respect to the mixture LLA/CL. Red arrows represented the low elution time in each sample which were associated to PLLA homopolymers.

2.3.4 Effect of water

The content of residual water in the LLA/CL in the molar ratio of 3:7 is a parameter that modified the conversion, the degree of crystallinity, and the molecular weight in the polymerization. Pérez-García et al. reported that residual water in the LLA/CL DESm plays the role of initiator in the sequential ROP of CL, at 37 ºC when the polymerization occurred in the presence of DBU and MSA organocatalysts and BnOH as initiator.[17] The ROP of CL is highly sensitive to water content. To study the role of water in the ROP of DESm of LLA and CL, the eutectic mixtures of LLA/CL were prepared, and 0.4 and 0.8 wt. % of water were added. Then, the ROP was carried out under the same conditions as mentioned before. The content of water in sample BU37, obtained by Karl Fisher titration, was 0.207 wt.% in LLA/CL DES. As water content increased in the eutectic mixture, the M_n of PCL and the crystallinity of PLLA, both decreased. The rapid ROP of LLA with DBU initiated by BnOH occurred in ca. 1 min, as reported by Perez-García.[17]

Residual water in the system served as initiator for remaining LLA monomer and mostly initiated the ROP of CL, aided by the second organocatalyst MSA, as MALDI TOF revealed that OH is found in some chain ends.

However, the molecular weight of PCL was more significantly affected than PLLA, despite water can react acid-base with the DBU organocatalysts for the LLA ROP and promote the presence of acid species that can deactivate the polymerization and hydrolyze the polyesters.[8,12] Either of these possible scenarios was conducted to a reduction of the final conversion, mainly due to water serving as initiator of CL producing PCL with lower molecular weight oligomers that were lost during the purification process (see Table 3 and Figure 3).

Table 3. Properties of polyesters obtained by ROP of LLA/CL and water.

Sample	ROP Temp (ºC)	H_2O Conc. (%)	Conv (%)[b]	PLLA/PCL[c]	$M_{n,\ NMR\ PLLA}$[d] (g mol^{-1})	$M_{n,\ NMR\ PCL}$[d] (g mol^{-1})	$X_{c,PLLA}$[e] (ºC)	$X_{c,PCL}$[e] (ºC)
BU 37	37	0	89	38 : 62	1964	4013	30	69
BU37-4	37	0.4	85	36 : 64	1651	3433	19	62
BU37-8	37	0.8	81	33 : 67	1765	3171	14	67

BU37, BU37-4 and BU37-8 correspond to polyesters obtained by ROP of LLA/CL with 0, 0.4 and 0.8 wt.% additional water, respectively.

[b] Experimental conversions obtained by gravimetry, [c] Molar ratio and [d] number-average molecular weight obtained by ^{1}H NMR. [e] Thermal properties calculated by DSC.

Thus, the water content in the DES plays a major role, and water above 0.2 % is a critical threshold for achieving high conversions. These results provide new insights into the ROP of L-lactide/ε-caprolactone eutectic mixture that are relevant for synthetic conditions translatable to polymerization of HIPEs and preparation of hierarchical 3D scaffolds with programmable degradability. [17,18] These includes unsophisticated atmospheres and the presence of remaining water from environmental conditions.

2.3.5 Effect of stereochemistry of lactide

Another parameter studied was the stereochemistry of lactide. In solution, a secondary reactions typically occur during the ROP of LLA and cause loss of stereoregularity or tacticity in PLLA chains.[6] A powerful method to identify these changes is ^{1}H NMR, where the typical signal for methine repeating groups in the PLLA is found from 5.17 ppm to 5.20 ppm as a well-defined quadruplet.[17] The appearance of asymmetrically substituted methyl groups in the polymer chains modifies the quadruple signal into a multiplet. [6] Figure 11 shows the ^{1}H NMR spectra of samples in the region from 5.17 to 5.20 ppm, where the quadruplet signal is well defined in all samples (e.g., black arrow in BU37). To study the effect of the stereochemistry of the lactide in the DESm, D isomer of lactide (DLA) was incorporated into the LLA/CL eutectic mixture as a racemic mixture. The new eutectic mixtures contained both isomers of lactide. As a result, the signal of the methine repeating group in polylactide was a multiplet instead of a well-defined quadruplet, identified in Figure 11, with red arrows. The final polyesters PLA/PCL, which contain polylactides (PLA) with disrupted stereoregularity, were atactic, completely amorphous, fragile, and presented a high rate of degradation. For instance, the samples crumble in less than 24 hours, at 37 ºC in phosphate-buffered saline PBS, pH = 7.4. Thus, the presence of D-lactide in a blend of PLLA/PCL prepared by the ROP of the eutectic mixture causes a reduction of the overall properties as reported to occur for traditional PLA synthesized in solution.[3]

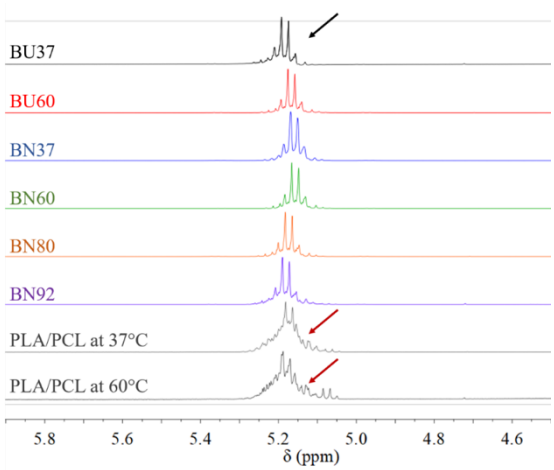

Figure 11. ^{1}H NMR spectra of methine group signals of A) PLLA in samples BU37 (black), BU60 (red), BN37 (blue), BN60 (green), BN80 (orange), and BN92 (purple). B) Polylactide (PLA), including the lactide isomer (DLA) in the polymerization obtained by the ROP of DES, contained isomer of lactide and CL at 37ºC and 60ºC.

2.3.6 Degradability test

Overall, the remarkable green features implemented in the present work, excluding organic solvents and metallic catalysts in the synthesis of PLLA and PCL polyesters open the possibility to apply these biodegradable polymers in tissue engineering and biodegradable materials fields. From this perspective, polymers were subjected to degradation profile assays. The samples were incubated at 37 ºC in phosphate-buffered saline (PBS, pH = 7.4) with orbital mixing (at 140 rpm for 14 days), then removed from the medium and rinsed with ethanol to remove any residue. Finally, samples were dried at room temperature. The final pH of the medium was measured, and the relative mass loss was calculated gravimetrically. It has been reported that the mass loss in polyesters is caused by the hydrolytic scission and surface erosion, which accelerates the hydrolysis by the autocatalytic effect of their acidic byproducts.[32,33]

Figure 12-A shows the mass loss profile degradation for the synthesized polyesters. The samples obtained above 60 ºC, showed larger degradations, with mass losses between 7.5 to 11.1 wt.% after 14 days. Conversely, when the ROP was carried out at 37 ºC the mass loss was ca. 4 wt.%. Furthermore, as degradation increased, the pH value of medium acidified with a pH value dropped to 5, as expected. The lower degradation profile caused the pH of the medium remaining close to neutral (ca. 6.4) (see Figure 12-B).

Samples BU37 and BN37 exhibited the highest crystallinity and, consequently, lower mass loss compared with the rest of the samples (Table 1, and Figure 12-A). These results indicate that the high crystallinity restricted the diffusion of the medium inside the matrix of the samples endowing the samples with a lower hydrolysis rate.[32,33] For the samples, the surface degradation or erosion was assessed by the reduction of the diameter after the degradation test, as observed in sample BU37 (Figure 13).

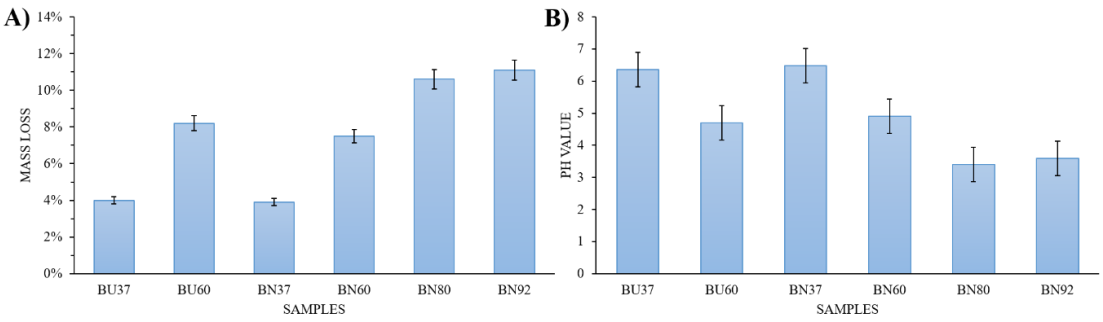

Figure 12. A) Mass loss (wt.%) profile degradation of the samples after 14 days at 37 ºC. B) pH values of final PBS solution (initial pH=7.4).

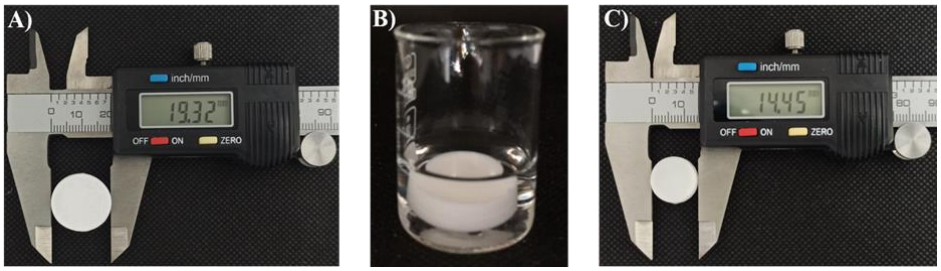

Figure 13. The degradation test was performed by exposing the samples for 14 days in PBS, pH = 7.4, at 37 ºC. This Figure represents the running test for BU37. A) Mass loss (wt. %) profile degradation of the samples after 14 days at 37 ºC. B) pH values of final PBS solution (initial pH=7.4).

2.4 Conclusions

In summary, we demonstrated the successful synthesis of a series of PLLA and PCL polyesters in the form of blends (PLLA/PCL) and copolymer P(LLA-*b*-CL) through a sustainable and alternative route, excluding the use of volatile organic solvents by taking advantage of using a non-ionic DES monomer, and substituting metallic catalyst by organocatalysts such as DBU and MSA that were readily extracted from the final polymers. Furthermore, it was demonstrated for the first time the use of DBN as a suitable organocatalyst for the ROP of LLA/CL DESm, whose reaction rate enabled the formation of a block copolymer. These green features, e.g., solventless conditions and mild temperatures of polymerization, open the possibility of applying the LLA/CL DESm ROP for the synthesis of biomaterials with tunable mechanical properties, programmable biodegradability, and enhanced biocompatibility for tissue engineering and drug delivery purposes.

2.5 References

1 A. He, C. C. Han and G. Yang, *Polymer.*, 2004, **45**, 8231–8237.

2 C. Jehanno, L. Mezzasalma, H. Sardon, F. Ruipérez, O. Coulembier and D. Taton, *Macromolecules*, 2019, **52**, 9238–9247.

3 A. Sanchez-Sanchez, I. Rivilla, M. Agirre, A. Basterretxea, A. Etxeberria, A. Veloso, H. Sardon, D. Mecerreyes and F. P. Cossío, *J. Am. Chem. Soc.*, 2017, **139**, 4805–4814.

4 A. Basterretxea, C. Jehanno, D. Mecerreyes and H. Sardon, *ACS Macro Lett.*, 2019, 1055–1062.

5 L. Mezzasalma, A. P. Dove and O. Coulembier, *Eur. Polym. J.*, 2017, **95**, 628–634.

6 A. Basterretxea, E. Gabirondo, C. Jehanno, H. Zhu, O. Coulembier, D. Mecerreyes and H. Sardon, *Macromolecules*, 2021, **54**, 6214–6225.

7 E. Castro-Aguirre, F. Iñiguez-Franco, H. Samsudin, X. Fang and R. Auras, *Adv. Drug Deliv. Rev.*, 2016, **107**, 333–366.

8 A. Dzienia, P. Maksym, B. Hachuła, M. Tarnacka, T. Biela, S. Golba, A. Zięba, M. Chorążewski, K. Kaminski and M. Paluch, *Polym. Chem.*, 2019, **10**, 6047–6061.

9 B. Lee Tin Sin, Lee and Soo Tueen, in *Polylactic Acid*, ed. B. S. T. Lee Tin Sin, William Andrew Publishing, Oxford, United Kingdom, Second Ed., 2019, pp. 53–95.

10 N. E. Kamber, W. Jeong, R. M. Waymouth, R. C. Pratt, B. G. G. Lohmeijer and J. L. Hedrick, *Chem. Rev.*, 2007, **107**, 5813–5840.

11 S. Gazeau-Bureau, D. Delcroix, B. Martín-Vaca, D. Bourissou, C. Navarro and S. Magnet, *Macromolecules*, 2008, **41**, 3782–3784.

12 N. J. Sherck, H. C. Kim and Y. Y. Won, *Macromolecules*, 2016, **49**, 4699–4713.

13 J. D. Mota-Morales, Deep Eutectic Solvents, Shyntesis, properties, and applications, ed. Diego J. Ramon and Gabriela Guillena, Wiley-VCH, Weinheim, Germany, 2020, Polymerizations, 187–21611.

14 A. P. Abbott, G. Capper, D. L. Davies, R. K. Rasheed and V. Tambyrajah, *Chem. Commun.*, 2003, **9**, 70–71.

15 J. D. Mota-Morales, R. J. Sánchez-Leija, A. Carranza, J. A. Pojman, F. del Monte and G. Luna-Bárcenas, *Prog. Polym. Sci.*, 2018, **78**, 139–153.

16 O. Coulembier, V. Lemaur, T. Josse, A. Minoia, J. Cornil and P. Dubois, *Chem. Sci.*, 2012, **3**, 723–726.

17 M. G. Pérez-García, M. C. Gutiérrez, J. D. Mota-Morales, G. Luna-Bárcenas and F. Del Monte, *ACS Appl. Mater. Interfaces*, 2016, **8**, 16939–16949.

18 S. A. García-Landeros, J. M. Cervantes-Díaz, A. Gutiérrez-Becerra, J. B. Pelayo-Vázquez, G. Landazuri-Gomez, J. Herrera-Ordonez, J. F. A. Soltero-Martínez, J. D. Mota-Morales and M. G. Pérez-García, *Chem. Commun.*, 2019, **55**, 12292–12295.

19 M. S. Zaky, A. L. Wirotius, O. Coulembier, G. Guichard and D. Taton, *Chem. Commun.*, 2021, **57**, 3777–3780.

20 J. K. Muiruri, S. Liu, W. S. Teo, J. Kong and C. He, *ACS Sustain. Chem. Eng.*, 2017, **5**, 3929–3937.

21 S. Maria, R. Oliva, M. Montesi, S. Panseri, G. Bassi, A. Mazzaglia, A. Piperno, O. Coulembier and A. Scala, *Biomater. Adv.*, 2022, **140**, 213043.

22 Y. Chen, J. Zhang, W. Xiao, A. Chen, Z. Dong, J. Xu, W. Xu and C. Lei, *Eur. Polym. J.*, 2021, **161**, 110861.

23 Z. Zhao, Y. Sun, L. Wang, X. Chen, Y. Sun, L. Lin, Y. Tang, F. Li and D. Chen, *Tetrahedron Lett.*, 2019, **60**, 800–804.

24 H. R. Kricheldorf, S. M. Weidner and A. Meyer, *Mater. Adv.*, 2022, **3**, 1007–1016.

25 E. Blázquez-Blázquez, E. Pérez, V. Lorenzo, M.L. Cerrada, *Polymers*., 2019, 11, 1874.

26 M. E. Broz, D. L. VanderHart and N. R. Washburn, *Biomaterials*, 2003, **24**, 4181–4190.

27 Q. Lv, D. Wu, H. Xie, S. Peng, Y. Chen and C. Xu, *RSC Adv.*, 2016, **6**, 37721–37730.

28 O. Coulembier, in *RSC Polymer Chemistry Series*, 2019, vol. 2019-Janua, pp. 1–36.

29 W. Han, X. Liao, Q. Yang, G. Li, B. He, W. Zhu and Z. Hao, *RSC Adv.*, 2017, **7**, 22515–22523.

30 K. Nalampang, R. Molloy and W. Punyodom, *Polym. Adv. Technol.*, 2007, **18**, 240–248.

31 G. Montaudo, F. Samperi and M. S. Montaudo, *Prog. Polym. Sci.*, 2006, **31**, 277–357.

32 L. N. Woodard and M. A. Grunlan, *ACS Macro Lett.*, 2018, **7**, 976–982.

33 W. J. Choi, K. S. Hwang, Y. Kim, C. Lee, S. H. Ju, H. J. Kwon, W.G. Koh and J.-Y. Lee, *ACS Appl. Polym. Mater.*, 2022, **4**, 1570–1575.

CHAPTER 3

Low-temperature and solventless ring-opening polymerization of eutectic mixtures of L-lactide and lactones for the production of biodegradable polyesters

Biodegradability is one of the key features for reducing the negative environmental impact of plastic waste disposal, which becomes critical in designing biocompatible polymeric biomaterials with programmable lifecycles. Herein, deep eutectic solvent monomers (DESm) composed of L-lactide and various lactones of different molecular weights were formulated to obtain polyesters at low temperatures with the aid of organocatalysts and in solventless conditions. The introduced DESm expand the eutectic mixtures capable of undergoing ring-opening polymerization (ROP) to mixtures of L-lactide (LLA) with δ-valerolactone (VAL) and δ-hexalactone (HEXL). Extending the toolbox for DESm preparation will allow for the design of polyesters with tailored molecular weight and crystallinity, which are conducive to programmable degradability. ROP of DESm carried out at low temperatures and in solventless conditions holds promise for a sustainable framework in preparing biodegradable polymers for biomedical applications.

This Chapter was accepted in *ACS Appl. Polym. Mater*., **2023**, 5, 5110-5125. https://doi.org/10.1021/acsapm.3c00591

3.1 Introduction

Poly(L-lactide) (PLLA) has been extensively studied in recent years due to its wide range of applications as the main component of polymeric materials in packing, pharmaceutical, and medical fields.[1] PLLA can be produced from renewable resources and stands out as a greener alternative to replace conventional petroleum-based polymers because of its biocompatibility and biodegradability. However, one of its main drawbacks is its brittleness, which limits its applications in areas where further processing and flexibility are needed. One strategy to improve its mechanical properties is to blend or copolymerize it with polyesters such as polylactones.[2–4]

Polylactones are biodegradable and biocompatible polyesters used in biomedicine and are usually obtained from monomers such as ε-caprolactone (CL), δ-valerolactone (VAL), δ-decalactone (DCL) and dodecalactone (DOCL).[2–4] Strategies for coupling the properties of PLLA with polycaprolactone (PCL) are currently the subject of intense research.[5,6] For instance, blending or copolymerizing PCL with PLLA to improve the strength and elongation properties of the resulting polymers without losing biodegradability has been previously reported.[7]

PLLA and polylactones are predominantly synthesized through ring-opening polymerization (ROP) of lactide and lactones, respectively. Compared to other methods of polymerization, ROP allows higher molecular weights and lower dispersity of the polymers, which are essential characteristics that define their performance for specific applications. In addition to controlling its molecular weight, the degradation of PLLA can be tuned by modifying the aggregate structure, crystallinity, and external factors in the media, such as the pH or the use of enzymes.[8] PLLA and polylactones are industrially produced at high temperatures,[9–11] and organic solvents are used occasionally,[1] although polymerization in bulk is preferred for its economy and sustainability.[11] The use of organic solvents has aroused deep concern about their toxicity and negative environmental effects due to the volatility of many of them.[1,12]

Similarly, tin metal catalysts approved by the FDA are typically used in PLLA and polylactone polymerization at high temperatures (above 120 °C),[10] offering an excellent control in designing complex architectures. However, recent regulations are limiting the use of metal-based catalysts, and because the purification of polymers can be arduous and can compromise the polymer performance in some areas, the use of organocatalysts stands as a viable alternative.[9,12,13]

In 2003, Abbott *et al.* reported a new family of solvents called deep eutectic solvents (DESs), comprised of mixtures of organic molecules and salts with hydrogen bond-forming capabilities at eutectic compositions, *e.g.*, choline chloride and urea in a 1:2 molar ratio.[14] DESs have also attracted attention in polymer chemistry. For instance, taking advantage of their compositional plasticity, they can be used as solvents for polymerization as well as monomers that are part of the DES.[15] The term DES monomer (DESm) was introduced for systems where the eutectic mixture contains monomers that can undergo polymerization reactions and form polymers.[16] Thus, DESm are a new type of eutectic mixtures with polymerizable units.[5,17] In a pioneering work, Coulembier *et al.* reported the ROP of DESm based on mixtures of LLA and trimethylene carbonate (TMC) rendering poly(PLLA-*g*-TMC) gradient copolymers.[17] Similarly, a DESm based on LLA and CL was employed for producing blends of PLLA and PCL homopolymers.[5] The ROP in these two studies was carried out in the absence of organic solvents and using amidine-based organocatalysts.[5,12]

Utilizing a DESm as an all-in-one system (solvent and monomers) has proven to be a versatile and greener approach for polyester production at low temperature and in solventless conditions, either as homopolymer blends or copolymers. In this work, we studied the thermal behavior of three novel eutectic mixtures composed of LLA and different lactones such as δ-valerolactone (VAL), δ-hexalactone (HEXL), and δ-decalactone (DCL) at different molar ratios. The sequential ROP of the resulting DESm was studied using various organocatalysts such as 1,8-diazabicyclo [5.4.0] undec-7-ene (DBU), 5-diazabicyclo (4.3.0) non-5-ene (DBN), and methanesulfonic acid (MSA), and also benzyl alcohol (BnOH) as the initiator. Of the three DESm, only that formed by LLA-VAL yielded polyesters with high molecular weights.

The obtained final product was PLLA and poly(δ-valerolactone) (PVAL) polymer blends, whose properties depended on the selection of the organocatalyst for LLA and the polymerization temperatures, including the controlled degradability under physiological conditions.

3.2 Experimental section

3.2.1 Materials

δ-Valerolactone (VAL, ≥ 97.5%), L-lactide (LLA, 98%), 1,8-diazabicyclo [5.4.0] undec-7-ene (DBU, 98%), 1,5-diazabicyclo (4.3.0) non-5-ene (DBN, 99%), methanesulfonic acid (MSA, 99.5%), benzyl alcohol (BnOH, 99%), *δ*-decalactone (DCL, ≥ 99%), and deuterated chloroform ($CDCl_3$, 99.8 atom%) were obtained from Sigma–Aldrich. *ε*-Caprolactone (CL, 97%) was obtained from Thermo Fisher Scientific. *δ*-hexalactone (HEXL, > 99.0%) was acquired from TCI Europe N.V. Absolute ethanol (EtOH, AR), methanol (MeOH, AR), and chloroform ($CHCl_3$, > 98%) were purchased from Biosolve Chemicals. All materials were used without further purification.

3.2.2 Eutectic mixture synthesis

The eutectic mixtures (DESm) were prepared by mixing LLA with CL, VAL, HEXL, or DCL at different molar ratios (*i.e.*, 20:80, 30:70, 40:60, and 50:50, LLA-lactone, respectively). The mixtures were heated at 90 °C until a clear homogeneous liquid was obtained. To refer to LLA-lactone molar ratios, a subscript in each of the systems under study will be used, *e.g.*, LLA_{30}-CL_{70} for a DESm composed of 30 mol ratio LLA and 70 mol ratio CL.

The LLA_{30}-CL_{70} eutectic mixture was subjected to ^1H nuclear magnetic resonance (NMR) spectroscopy analysis Varian VXR Spectrometer at RT spectrometer, using a capillary tube with deuterium chloroform serving as an external reference, in order to characterize its properties.

3.2.3 Ring-Opening Polymerizations (ROP) of Eutectic Mixture

The synthesis of polyesters was carried out by sequential ROP at 37 °C in bulk of DESm composed of LLA-CL, LLA-VAL and LLA-HEXL at a 30:70 molar ratio.

A solution of DBU or DBN (organocatalyst, [CAT] = 2.9 wt%) and BnOH (initiator, [In] = 2.1 wt with respect to DESm, in a proportion [CAT:In] = [1:1] mol%), both liquids at room temperature, was added to the DESm mixture with constant stirring. Subsequently, 3 wt% of MSA (co-organocatalyst) was added one minute after starting the reaction.

The obtained polyesters were named $PLLA_{CAT}$-P*Y*, where CAT = U for DBU or N for DBN was assigned to the organocatalyst used for the LLA ROP, and *Y* corresponded to CL or VAL, (see **Table 1)**. Once the polymerization reached high conversions after 24 h, the polyesters obtained were purified by adding an ethanol excess at room temperature and washing 6 to 8 times for each sample to completely remove the residual monomers and oligomers. The recovered solids were dried at room temperature (RT) for 24 h. The overall conversion ($X_{overall}$) was determined by gravimetry and ^{1}H NMR. For the kinetics studies of DESm based on LLA-CL and LLA-VAL, the samples were prepared in individual vials and were terminated at different times, and the X_{overal} was calculated by gravimetry. The general procedure was the same as described above. The final products were dissolved in chloroform and subsequently precipitated in cold methanol (-4 °C). The solution was then centrifuged at 4 500 rpm for 10 min. Finally, the precipitated product was separated by decantation.

3.2.4 Characterization of DESm and polyesters

^{1}H NMR spectra were recorded at 600 MHz with a Varian VXR Spectrometer at RT using deuterium chloroform ($CDCl_3$).

Attenuated total reflection Fourier (ATR-FTIR) spectra were recorded on a Bruker VERTEX 70 spectrometer equipped with a platinum-ATR diamond single reflection accessory. The measurement resolution was 1 $cm^{-1,}$ and spectra were collected in the range of 4 000 - 400 cm^{-1}.

Differential scanning calorimetry (DSC) measurements were carried out on a TA Instruments Q1000 DSC. The analysis method for DESm and polyesters obtained was performed on dry samples and with heating-cooling cycles.

Scans for any DESm consisted of initial cooling from RT to -70 °C at a scan rate of 10 ºC min^{-1}, keeping it at that temperature for 5 min, afterwards the temperature was increased to 90 °C, and finally decreased again to RT at the same scan rate. The data was collected during the heating run and the first scan. For the thermal properties of the polyesters, the analysis consisted of a similar initial cooling from RT to -70 °C, again at a scan rate of 10 ºC min^{-1}, holding them at that temperature for 5 min, then increasing the temperature to 220 °C, and finally cooling to RT at the same scan rate.

The thermal stability and degradation behavior of the different samples were studied using thermogravimetric analysis (TGA) on a TA Instruments Discovery TGA 5500 by using an aluminum pan. Thermograms were recorded in the temperature range of 30 °C to 700 °C at a heating rate of 10 °C min^{-1} under a nitrogen atmosphere.

The X-ray diffraction patterns (XRD) of powdered samples was carried out in a Bruker D8 Advance diffractometer with Cu Kα radiation (λ = 0.1542 nm) in the angular range of 5 – 40° (2θ) at RT.

The molecular weight distributions (M_w/M_n) were determined by size exclusion chromatography (SEC) equipped with a triple detector: Viscotek Ralls detector, Viscotek Viscosimeter model H502 and Schambeck RI2912 refractive index detector. The separation was carried out by two PLgel 5μm MIXED-C and 300 mm columns from Agilent Technologies at 35 °C in THF (99% extra pure) stabilized with BHT as the eluent at a flow rate of 1.0 mL min^{-1}. The data acquisition was processed by using Viscotek Omnisec software version 5.0.

DOSY (Diffusion Order Spectroscopy) data were acquired using the pulse program *ledbpgp2s* installed in the topspin 3.6.2 software from Bruker with 95 gradient levels with a linear increase from 2% to 95% using a gradient of strengths up to 54 G/cm and 8 transients. The diffusion delay (Δ) was 150 ms, and the length of the square diffusion encoding gradient pulse (δ) was 0.6 ms. Laplace transformations for generating the diffusion dimensions were obtained with the Bruker Biospin Dynamics Center using a least-squares fitting routine with Monte Carlo error estimation analysis.

The contact angle was recorded by OCA20 (Data physics). The measurements were performed on films prepared by solvent casting. The obtained polyesters were dispersed in $CHCl_3$ and poured onto a glass plate, allowing the solvent to evaporate.

3.3 Results and discussions

3.3.1 DESm Synthesis and characterization of LLA-lactone DESm

Polymerizable eutectic mixtures (DESm) composed of mixtures of LLA and lactones, namely, VAL, HEXL, DCL and CL (**Figure 1**), were prepared in different molar ratios, 20:80, 30:70, 40:60, and 50:50 LLA-lactone, respectively, by heating the mixtures to 90 °C until transparent and homogeneous mixtures were obtained. The mixtures LLA_{30}-VAL_{70}, LLA_{30}-$HEXL_{70}$ and LLA_{30}-CL_{70} remained liquid upon cooling to RT. The rest of the samples with different molar ratios presented crystallization or were not homogeneous (**Figure 1 (a-c)**). The thermal properties of the mixtures that remained stable and liquid at RT were further studied by differential scanning calorimetry (DSC). It is worth highlighting that the stability of these mixtures played a crucial role in obtaining the thermograms.

DSC scans of DESm composed of LLA and VAL (**Figure 2a**) show T_m = -28.6 °C and T_m = -29.1 °C for LLA_{30}-VAL_{70} and LLA_{20}-VAL_{80}, respectively. The observed melting points were lower than those of their pure constituents (T_m = -13 °C and T_m = 98 °C for VAL and LLA, respectively). However, in the 20:80 molar ratio, an additional melting point at T =-25.7 °C was observed, which indicates a different component or phase out of the eutectic composition, as reported for other mixtures near the eutectic point.[5,18]

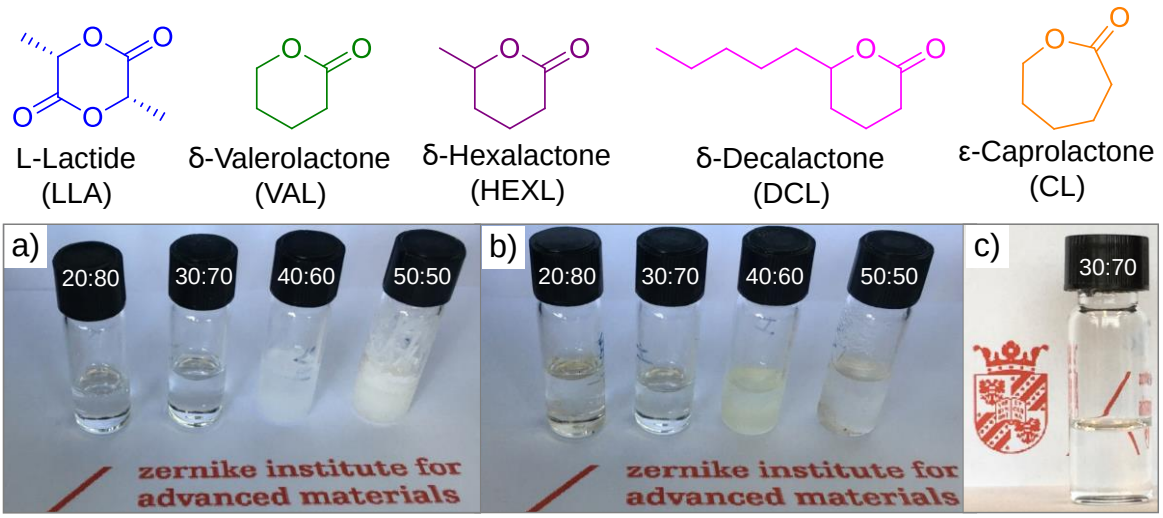

Figure 1. Chemical structures of LLA and lactones (upper panel) and their mixtures (DESm) used in this study: (a) LLA-VAL, (b) LLA-HEXL, and (c) LLA-DCL at different molar ratios.

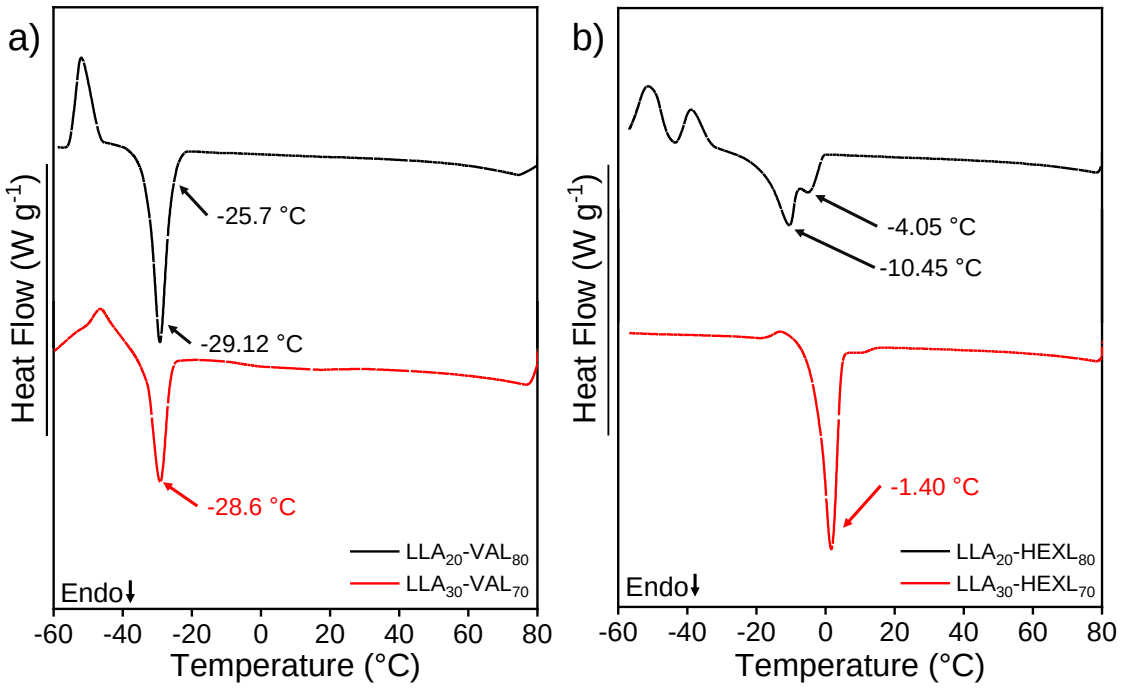

Figure 2. DSC scans for mixtures of a) LLA-VAL and b) LLA-HEXL at 20:80 and 30:70 molar ratios, respectively.

DSC results of LLA-HEXL mixtures are shown in **Figure 2b**, where a decrease in the melting point was observed for the LLA-HEXL DESm compared to the pure components. For the LLA_{30}-$HEXL_{70}$ mixture, only one melting point at T_m = -1.4 °C was detected, while for LLA_{20}-$HEXL_{80}$, two endothermic peaks appeared at T = -10.45 and -4.05 °C. These melting points are below the ones of their original constituents (HEXL T_m = 31 °C, and LLA T_m = 98.3 °C), which again indicates the DESm formation. However, the presence of two thermal events in the 20:80 mixture suggests that this mixture is not completely homogeneous and that other phases or components are present in excess.[5,18]

From the DSC scan of the LLA and DCL mixture, no thermal transition could be observed due to the absence of any melting point under the conditions assayed (**Figure 3)**. This can be explained by the steric hindrance and branching effects presented in the aliphatic moieties of DCL.

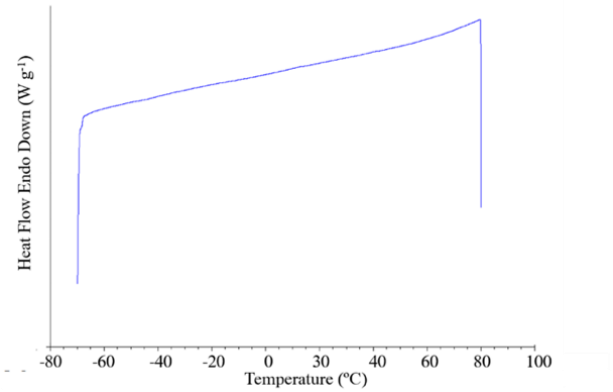

Figure 3. DSC scans for mixtures of LLA_{30}-DCL_{70} DESm

The LLA_{30}-VAL_{70} DESm was also analyzed by ^{1}H NMR spectroscopy once the presence of a single melting point was verified by DSC. The spectrum in **Figure 4a**, revealed that the peaks assigned to H_a (δ = 5.05 ppm) and H_b (δ = 1.70 ppm) corresponding to the methine proton [–C**H**–] and methyl group [–C**H$_3$**] of pure LLA shifted to 5.11 and 1.55 ppm, respectively, in the formed eutectic mixture of LLA_{30}-VAL_{70}. Similarly, shifts in the signals were observed in the mixture LLA_{30}- $HEXL_{70}$ (**Figure 4e**). These shifts confirm the formation of the desired eutectic mixtures, as previously reported by Pérez-García *et al*., where similar peak shifts behavior of LLA_{30}-CL_{70} DESm were observed.[5]

For instance, the methylene proton [–C**H**$_2$–] (H_c) of pure VAL shifted from 4.36 to 4.27 ppm (**Figure 4b**), the methine proton [–C**H**–] (H_l) and methyl group [–C**H**$_2$–] (H_i) of pure HEXL shifted from 4.46 to 4.36 ppm and 2.58 to 2.48 ppm, respectively (**Figure 4d**).

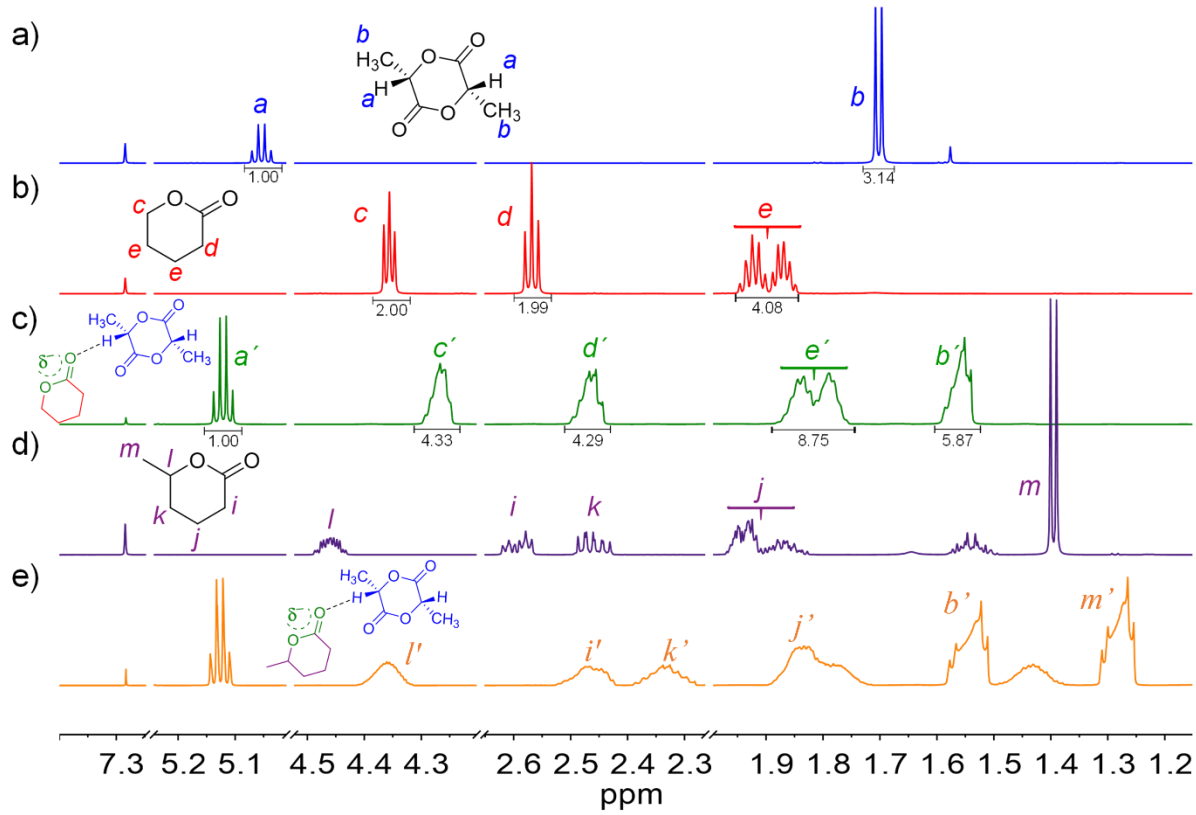

Figure 4. ^{1}H NMR spectra of pure components (a) LLA, (b)VAL, (d) HEXL and (c) LLA_{30}-VAL_{70} and (e) LLA_{30}-$HEXL_{70}$ DESm.

The LLA_{30}-VAL_{70} and LLA_{20}-VAL_{80} mixtures were also compared and studied by ^{1}H NMR analysis (**Figure 5a**). A larger shift in the signals of groups [–C**H**–] (H_a) and [–C**H**$_3$] (H_b) of LLA was observed in the ^{1}H NMR spectra of the mixture at a 30:70 molar ratio because it establishes stronger interactions with VAL in comparison to the 20:80 molar composition. This is further supported by the DSC results, where a single melting point was observed for the mixture with 30:70 molar ratio, corresponding to the formation of the eutectic mixture (**Figure 2a**). However, for the corresponding LLA-DCL mixture, only the LLA methine at approximately 5.05 ppm slightly shifted (see **Figure 5b**).

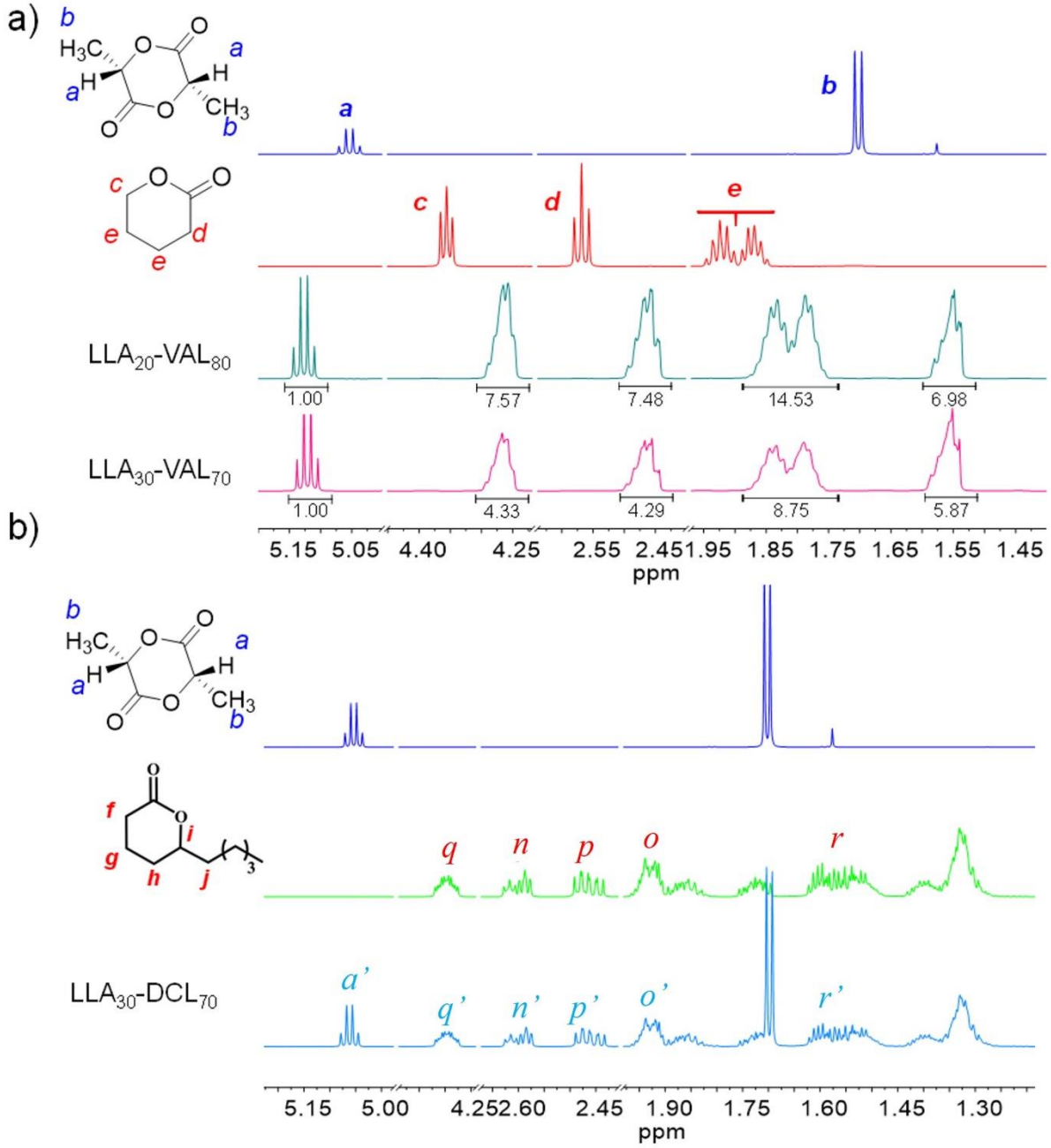

Figure 5. (a) ^{1}H NMR spectra of pure LLA, VAL, and LLA_{20}-VAL_{80} and LLA_{30}-VAL_{70} DESm. (b) ^{1}H NMR spectra of pure LLA, DCL, and LLA_{30}-DCL_{70} DESm.

To gain more understanding of the interactions between LLA and lactones, mixtures at a 30:70 molar ratio that presented a single melting point by DSC were studied by ATR-FTIR.

These included mixtures of LLA-VAL, LLA-HEXL and the mixture of LLA-CL for comparison. In **Figure 6**, the ATR-FTIR spectrum of LLA_{30}-VAL_{70} shows that the ester group peak of LLA shifted from 1756 to 1764 cm^{-1}, and for VAL, it shifted from 1722 to 1724 cm^{-1} and the relative intensity of the carboxylic group [**–COO–**] increased in the DESm form. This behavior suggests the establishment of hydrogen bond interactions between the [–**COO**–] group of VAL and the protons of [–C**H**– and –C**H**$_3$] groups from LLA, which also support the shifts observed by ^{1}H NMR.

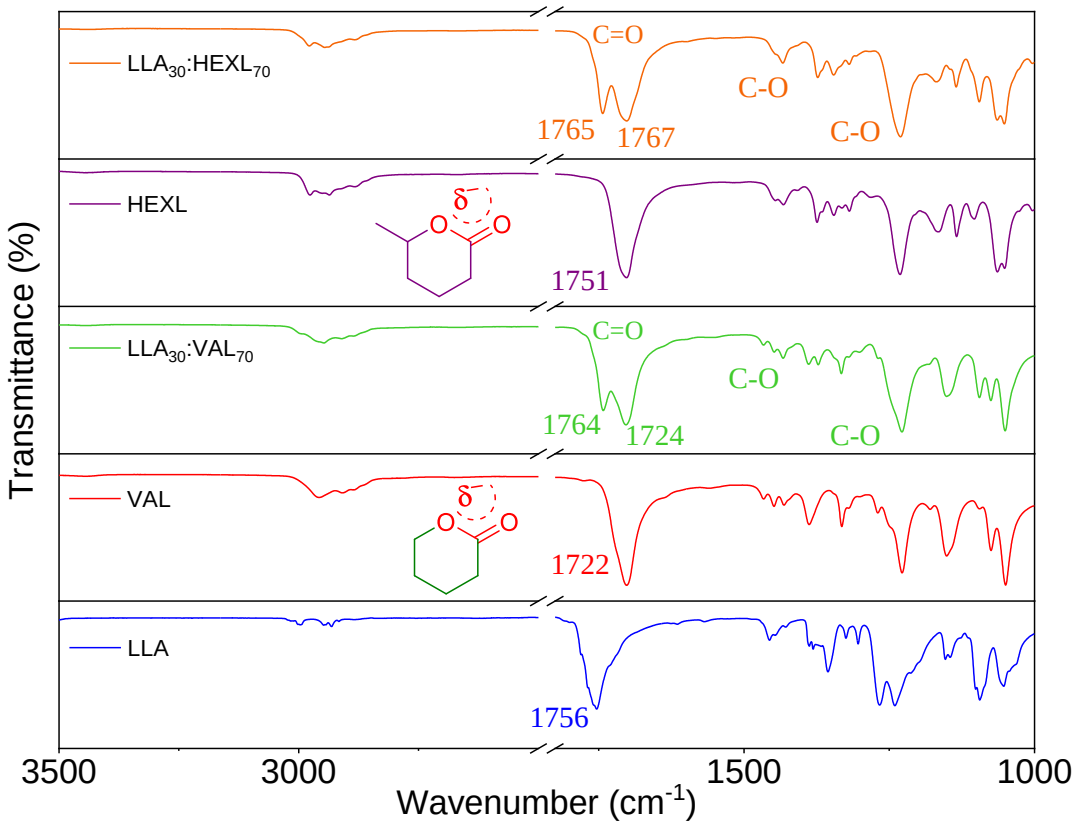

Figure 6. Normalized ATR-FTIR spectra for LLA_{30}-VAL_{70} and LLA_{30}-$HEXL_{70}$ DESm

The ATR-FTIR spectroscopy results of the other eutectic mixtures LLA_{30}- $HEXL_{70}$ and LLA_{30}-DCL_{70} were also studied. In **Figure 6**, it is observed that the [–**COO**–] group of LLA shifted from 1756 cm^{-1} to 1765 cm^{-1} when mixed with HEXL, and from 1751 cm^{-1} to 1767 cm^{-1} when mixed with DCL (**Figure 7a)**.

However, the [–**COO**–] groups of HEXL and DCL at 1723 and 1728 cm^{-1}, respectively, did not show any shift in the mixtures, which points to weaker interactions with LLA in these mixtures. On the other hand, by comparing the relative intensity of the carbonyl group in HEXL and VAL when mixed with LLA in a 30:70 molar ratio, the increasing intensity when forming DESm was higher in VAL (**Figure 7b**).

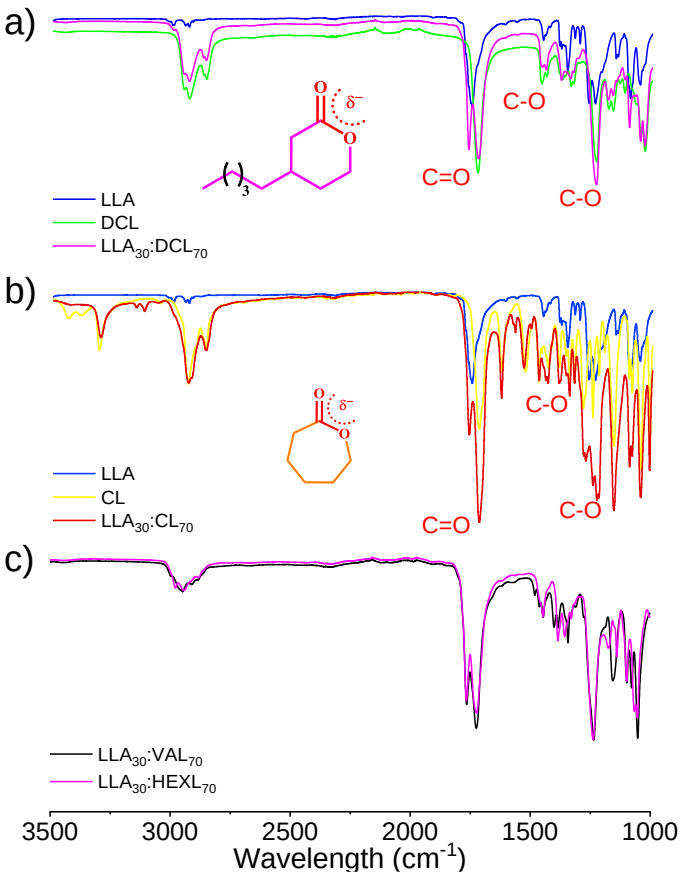

Figure 7. ATR-FTIR spectra from pure LLA (blue), (a) pure DCL (green), and LLA_{30}-DCL_{70} DESm (pink). (b) Pure CL (yellow) and LLA_{30}-CL_{70} DESm (red) (c) Relative intensity observed by ATR-FTIR spectra of LLA_{30}-VAL_{70} and LLA_{30}-$HEXL_{70}$ DESm.

The change in the carbonyl vibrations of the DESm constituents confirms hydrogen bonding as the origin of the interactions that formed them, which in turn caused the depression in the melting points of DESm compared with the melting temperature of their individual components.[5]

3.3.2 Ring opening polymerization of LLA- DESm

LLA_{30}-VAL_{70} and LLA_{30}-$HEXL_{70}$ eutectic mixtures were selected as DESm for polymerization. We followed the methodology described in our previous work with the DESm of LLA-CL at the same molar ratio.[6] The overall reaction is depicted in **Scheme 1**. To ensure high conversions, the reaction was carried out for 24 h. Once the polymerization was completed, the purified products were studied by ^{1}H NMR spectroscopy.

The $X_{overall}$ was determined gravimetrically by dividing the final mass of polymers by the theoretical mass expected from the complete polymerization of the corresponding monomers. For LLA-VAL DESm, the conversion was approximately 84%, and for LLA-HEXL mixture, the conversion obtained was ca. 30%. See **Table 1.**

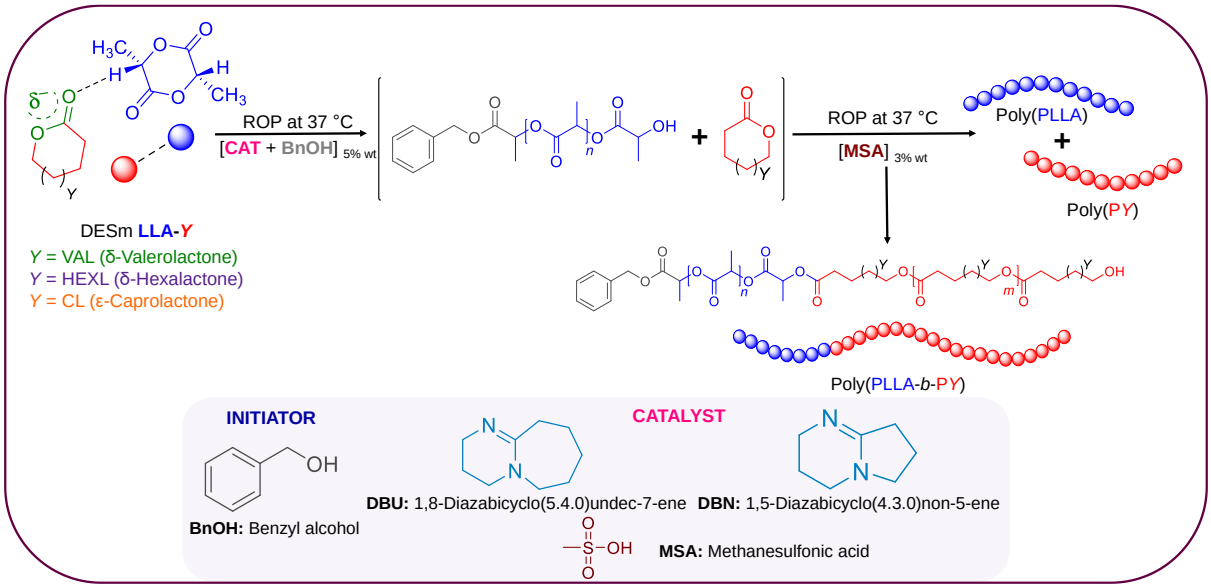

Scheme 1. Sequential Ring-Opening Polymerization of the DESm composed of LLA and lactones (*i.e.*, LLA_{30}-VAL_{70} and LLA_{30}-CL_{70}) at 37 °C.

The ROP of LLA in LLA-VAL DESm is selectively carried out when using DBU or DBN as the catalysts through a possible activation of both the alcohol and the monomer. Consequently, at the end of this stage, the PLLA chains were dispersed in the lactone, *i.e.*, VAL was released from the liquid DESm as the LLA was consumed during ROP. Subsequently, MSA, as the second organocatalyst, was added to the reaction mixture and catalyzed the ROP of the remaining VAL.

In this second step, the hydroxyl groups of the previously formed lactidyl or residual water acted as initiators. Finally, PLLA-PVAL was obtained as the product. The rate of polymerization depended on the first catalyst used: DBU or DBN, as will be explained later. **Figure 8** shows a comparative ^{1}H NMR spectra of the LLA_{30}-VAL_{70} DESm and the polymers resulting from their ROP at 37 °C. The signals H_a (δ = 5.11 ppm) and H_b (δ = 1.55 ppm) corresponding to the methine [–C**H**–] and methyl group [–C**H**$_3$] of the LLA monomer in the DESm shifted in the ^{1}H NMR spectra of PLLA-PVAL (*i.e.*, $\delta_{Ha'}$= 5.2 ppm and $\delta_{Hb'}$= 1.60 ppm), and H_h and H_f denote the terminal aromatic group of BnOH (δ = 7.34 ppm) and the terminal methine (δ = 4.37 ppm), respectively, of PLLA. This confirms that the catalysts (DBU and DBN) selectively polymerized LLA in the DESm (**Figure 8a and b)**.

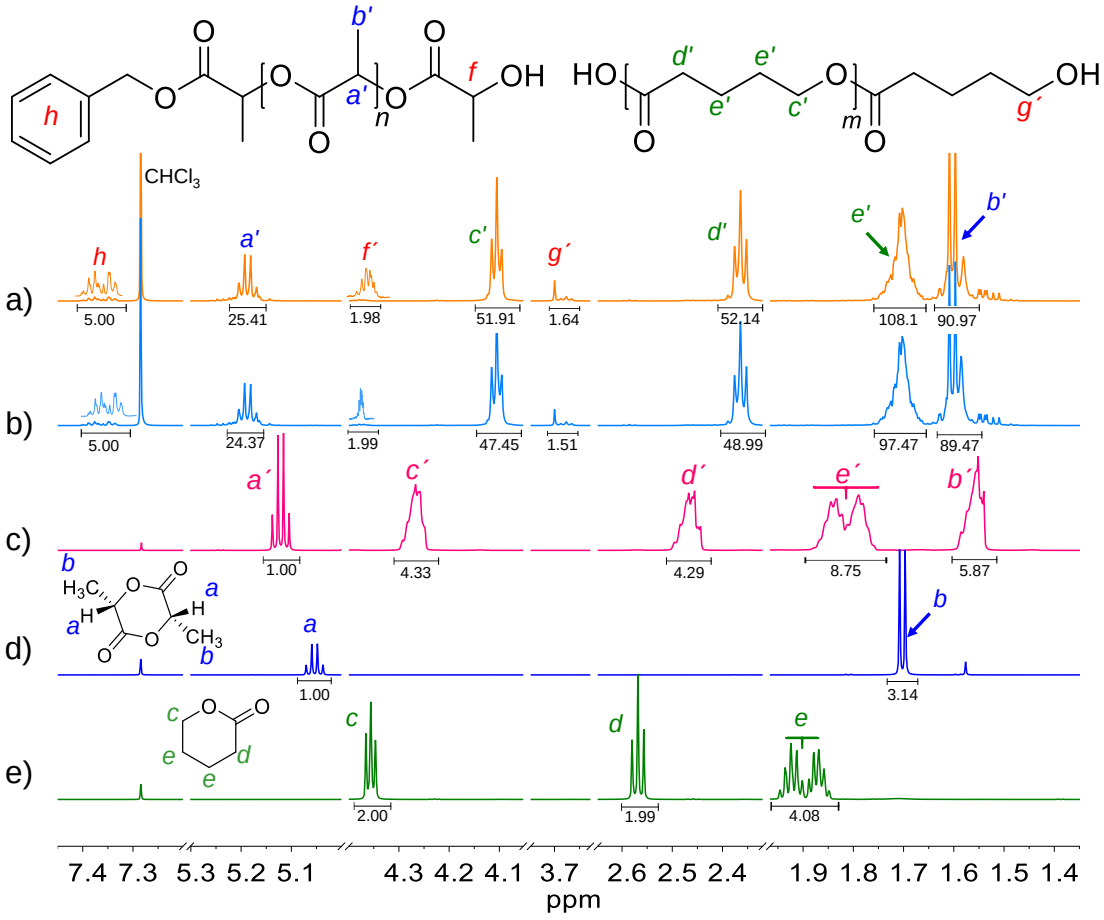

Figure 8. ^{1}H NMR spectra of the final product of the ROP of LLA_{30}-VAL_{70} at 37 °C using (a) DBU and (b) DBN as the organocatalysts of PLLA, (c) LLA_{30}-VAL_{70} DES mixture and the monomers (d) LLA, (e) VAL.

As shown in **Figure 8(a-b)**, the ROP of LLA_{30}-VAL_{70} using DBU and DBN as catalysts of PLLA was confirmed by ^1H NMR analysis. However, different molecular weights calculated by NMR resulted from varying the initiator, being comparable to those reported in the literature.[19] Additionally, in accordance with Perez-García,[19] their molecular weights (M_n) of PLLA and PVAL were calculated as reported by Perez-García, using **Equations (1)** and **(2)**, where MW_{LLA} and MW_{VAL} are the molecular weights of LLA and VAL, respectively. M_n and $X_{overall}$ are listed in **Table 1**.

$$M_n(\text{gmol}^{-1}) = \frac{\int H_{a'}}{\int H_f}(MW_{LLA}) \quad (1)$$

$$M_n(\text{gmol}^{-1}) = \frac{\int H_{d'}}{\int H_g}(MW_{VAL}) \quad (2)$$

Table 1. The overall conversion ($X_{overall}$) of PLLA-P*Y* (*Y* = CL or VAL) and molecular weight (M_n) of the polyester obtained from ROP of LLA_{30}-CL_{70} and LLA_{30}-VAL_{70}.

Sample[a]	CAT	Temp. (°C)	[CAT:In] (mol. ratio)	$X_{overall}$ [b] (%)[c]	$M_{n,\,PLLA}$[c] (g mol^{-1})	$M_{n,\,PY}$[c] (g mol^{-1})
$PLLA_U$-PCL	DBU	37	1:1	91	2 001	3 402
$PLLA_N$-PCL	DBN	37	1:1	90	1 879	3 332
$PLLA_U$-PVAL-60	DBU	60	1:1	91	2 257	5 810
$PLLA_U$-PVAL	DBU	37	1:1	85	1 850	3 181
$PLLA_U$-PVAL-1	DBU	37	1:0.5	91	3 848	4 788
$PLLA_U$-PVAL-0	DBU	37	1:0.25	91	4 951	4 152
$PLLA_N$-PVAL	DBN	37	1:1	84	1 757	3 242

[a] ROP of LLA_{30}-VAL_{70} or LLA_{30}-CL_{70} DESm was carried out using MSA as the second organocatalyst and BnOH as the initiator (In). The molar ratio of [CAT:In] and [MSA] represented 5 and 3 wt% to DESm, respectively. In all the entries ROP was performed at 37 ºC except for sample $PLLA_U$-PVAL-60.

[b] Overall conversion was obtained by gravimetry. [c] M_n obtained by ^1H NMR.

Furthermore, as a result of MSA catalyzing the second ROP of VAL, the peaks of H_c (δ = 4.26 ppm), H_d (δ = 2.56 ppm) and H_e (δ = 1.89 ppm) assigned to the [–C**H**$_2$–] groups in the ^{1}H NMR spectrum of VAL in the DESm also shifted in the ^{1}H NMR spectra of the final product (*i.e.*, $\delta_{Hc'}$= 4.10 ppm, $\delta_{Hd'}$= 2.36 ppm and $\delta_{He'}$= 1.70 ppm). This confirms that MSA is a suitable organocatalyst for VAL ROP in the DESm (**Figure 8)**. On the other hand, LLA-HEXL polymerization was carried out under the same conditions, but the signals corresponding to polymers were of very low intensity, corresponding to the low conversion obtained by gravimetry. Therefore, it was decided not to continue with the study of LLA-HEXL ROP (**Figure 9**). This indicates that the ROP of HEXL is not efficiently catalyzed by MSA and could be explained by the steric effects of the methyl moiety in the HEXL structure compared with VAL. Hence, we will focus on the ROP of the LLA_{30}-VAL_{70} system, and a comparative study will be made with the previously reported LLA_{30}-CL_{70} system.[6]

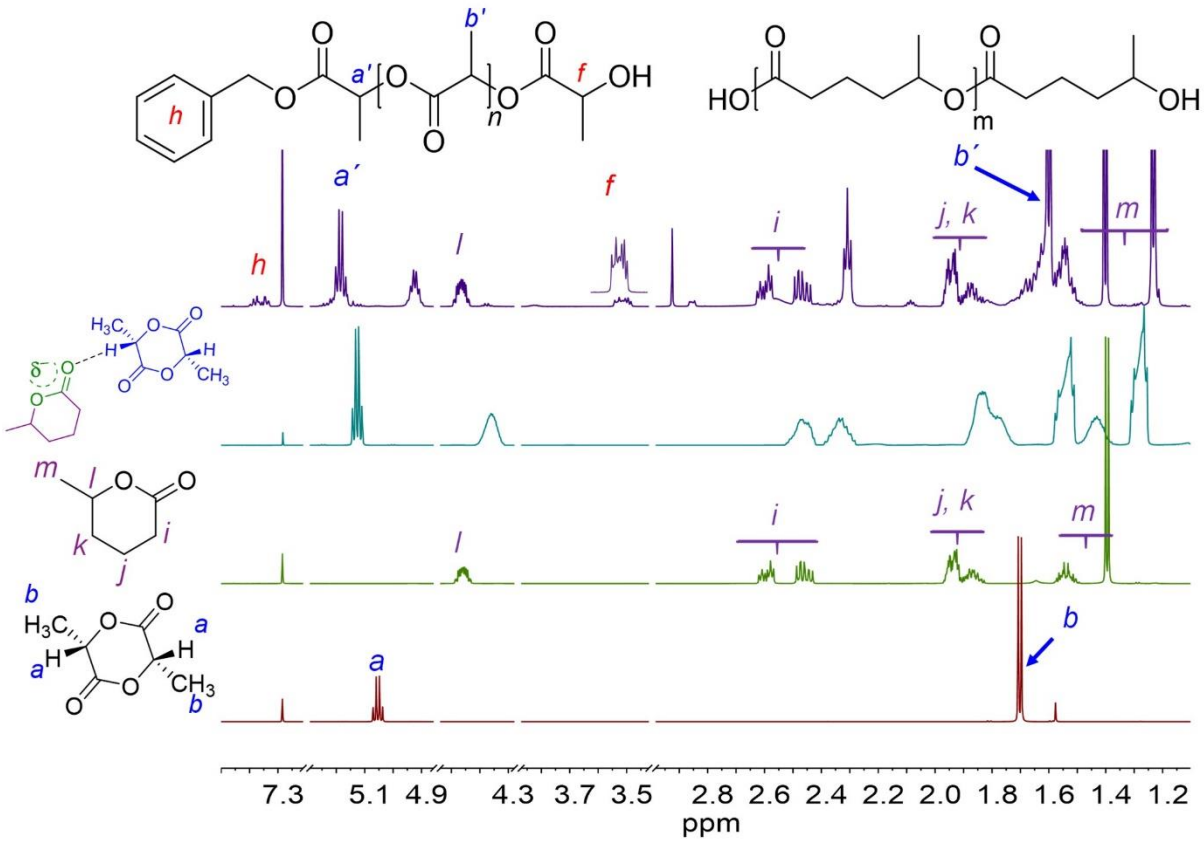

Figure 9. ^{1}H NMR spectra of LLA, HEXL, DESm and the ROP of LLA_{30}-$HEXL_{70}$ DESm at 37 °C using DBU/MSA as the catalyst and BnOH as the initiator.

3.3.3 Kinetics studies of LLA-CL and LLA-VAL by ROP at 37 °C varying the catalyst.

To better understand the sequential ROP of the LLA-forming DESm with VAL and CL, the ROP kinetics of LLA_{30}-VAL_{70} and LLA_{30}-CL_{70} were comparatively studied. The M_n and $X_{overall}$ of PLLA and PCL were calculated as described above.[6] The relationship between the conversion of LLA_{30}-CL_{70} DESm and the polymerization time is shown in **Figure 10a**, where it is observed that $X_{overall}$ is close to 90%, being slightly higher when DBU is used as a catalyst.

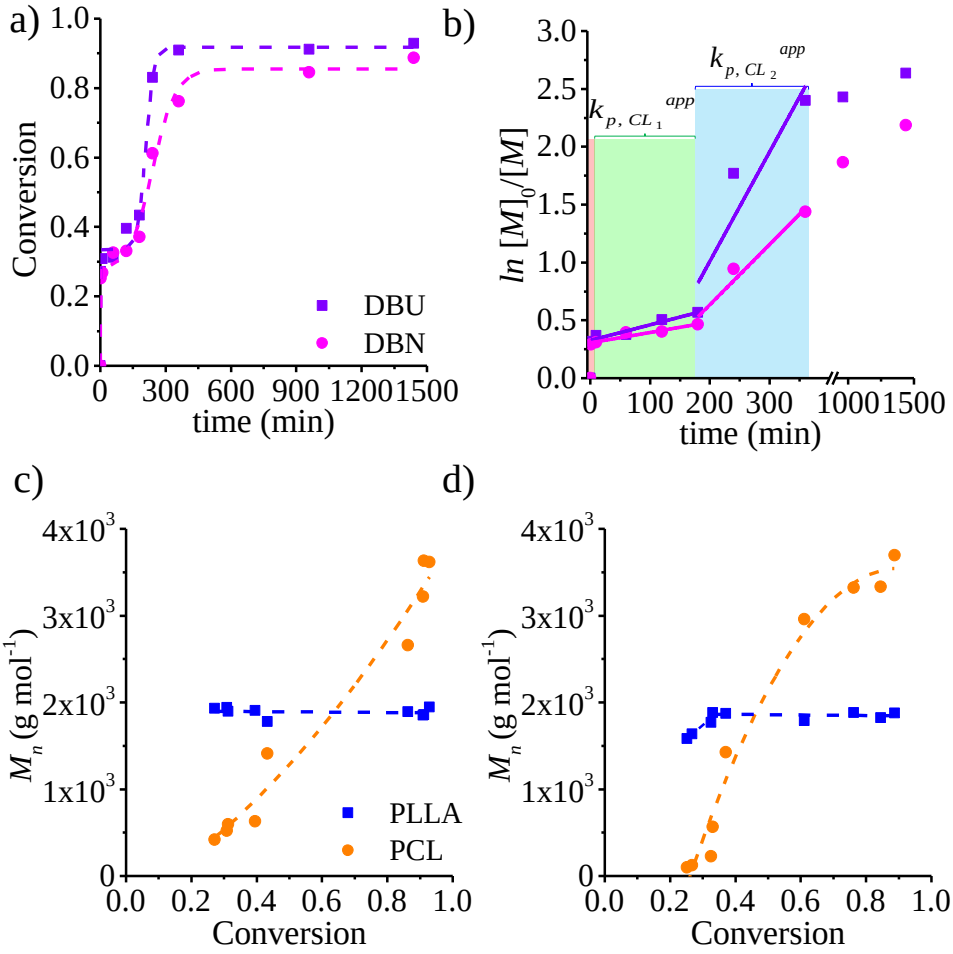

Figure 10. (a) Evolution of the conversion profiles, (b) linear fitting of **Equation (3)** and dependence of M_n versus $X_{overall}$ using (c) DBU and (d) DBN as organocatalysts of PLLA for the sequential ROP of LLA_{30}-CL_{70} DESm at 37 °C**.** (Dashed lines denote tendencies, and solid lines are the linear regressions).

Figure 10b exhibits the semilogarithmic plot, $\ln([M]_0/[M])$ *versus* time, where $[M]_0$ and $[M]$ are the concentration of monomers at the initial time (t = 0) and at any time, respectively, showing that the polymerization of LLA_{30}-CL_{70} follows three-stage kinetics, accounting for sequential polymerization. The first stage is observed almost instantaneously, reaching an $X_{overall}$ up to 25% in just one minute of reaction, which is attributed to the rapid and complete polymerization of PLLA (30% molar ratio of the LLA-CL DESm) catalyzed by DBU or DBN, as previously reported.[20,21]

The second stage encompassing the ROP of CL becomes slower, following *first-order* kinetics in an interval of 10 to 200 min, associated with the slope of the curve corresponding to the initiation rate constant ($k_{p,CL1}^{app}$). This stage can be considered an induction period, representing the existence of structural rearrangement processes due to the initiator forming the active sites in a system having PLLA chains in the media after the addition of MSA, suggesting that rearrangement of the reacting species is required (*e.g.*, CL and MSA catalysts) before polymerization begins. Here, monomer molecules can access the active species without competition, which increases the rate of polymerization.[22]

In the third stage, the increase in viscosity in the reaction medium induces an abrupt increase in $X_{overall}$ in the system, where the propagation and termination steps become diffusion controlled. This scenario is consistent with what has already been reported in the literature and results in a change in the slope of the last stage corresponding to the propagation velocity constant ($k_{p,CL2}^{app}$) of the PCL.[23,24]

The values $k_{p,CL1}^{app}$ and $k_{p,CL2}^{app}$ can be determined with the other parameters associated with **Equation (3),** where $k_{p,Yi}^{app}$ (Y = CL or VAL, i = 1 or 2) corresponds to the term $k_p[I]_0$. Notably, no segregation of the final polymers is observed. The results are shown in **Table 2**. In the third stage, the increase in viscosity in the reaction medium induces an abrupt increase.

$$\ln \frac{[M]_0}{[M]} = k_{p,Y_i}^{app} \times t \qquad (3)$$

Table 2. Estimation of $k_{p,Y1}^{app}$ and $k_{p,Y2}^{app}$ for DESm of LLA_{30}-CL_{70} and LLA_{30}-VAL_{70} by ROP at 37 °C in bulk with a molar ratio $[CAT]_0$:$[In]_0$ = [1:1] and MSA as co-catalyst.[a]

	LLA_{30}-CL_{70}		LLA_{30}-VAL_{70}	
[CAT]	$k_{p,\,CL1}^{app}$ (s^{-1})	$k_{p,\,CL2}^{app}$ (s^{-1})	$k_{p,\,VAL1}^{app}$ (s^{-1})	$k_{p,\,VAL2}^{app}$ (s^{-1})
DBU	2.23×10^{-5}	1.58×10^{-4}	1.82×10^{-4}	1.62×10^{-6}
DBN	1.50×10^{-5}	8.70×10^{-5}	2.12×10^{-4}	9.30×10^{-7}

[a] The weight of MSA was 3 wt% with respect to the DESm.

In the induction period of the second stage, it is evident that there is no significant difference in the value of $k_{p,CL1}^{app}$ using either DBU or DBN, as these catalysts affect only the ROP of LLA, which formed rapidly during the first stage. However, the difference becomes present in the final stage of the CL propagation, since the value $k_{p,CL2}^{app}$ increases up to 4.5 times for the ROP where the previous LLA polymerization is catalyzed by DBU compared with the reaction catalyzed by DBN. However, it is worth mentioning that these polymerizations were carried out under the same conditions of $[DESm]_0$:$[CAT]_{0:}[In]_0$, only changing the nature of the catalyst for LLA (DBU or DBN) and adding to both MSA as the catalyst for the ROP of CL. Therefore, the increase in $k_{p,CL2}^{app}$ when DBU is used with respect to DBN is likely due to the type of polymers obtained at the end, a blend of homopolymers or a block copolymer, as follows.

It was reported that the choice of organocatalyst for the ROP of the LLA_{30}-CL_{70} DESm at 37 °C is decisive to obtain a blend of PLLA and PCL homopolymers in the case of DBU or a PLLA-PCL block copolymer in the case of DBN.[6] In the former case, PCL chains initiate with residual water and propagate independently of PLLA already formed, producing a blend of PLLA and PCL homopolymers. Conversely, in the latter case, PLLA chains serve as the macroinitiator of CL, yielding block copolymers with slower kinetics. **Figure 10 (c-d)** depicts the evolution of M_n *versus* $X_{overall}$ in LLA_{30}-CL_{70} polymerization. As mentioned above, it is evident that the polymerization of PLLA in the first reaction times is faster, almost immediately reaching $M_n \approx 2\ 000$ g mol^{-1} with an $X_{overall}$ = 25% and remaining constant throughout the reaction when DBU is used as catalyst.

When using DBN, the $X_{overall}$ of PLLA increases discreetly linearly between 20 and 25% of M_n until reaching 2 000 g mol^{-1}, remaining constant throughout the conversion profile (**Figure 10d**). The M_n of PCL increases with respect to $X_{overall}$ of the system, indicating the growth of the polymer chain, continuously forming PCL and reaching a $M_n \approx 3\ 000$ g mol^{-1}, irrespective of the organocatalyst employed for the ROP of LLA. However, some kinetics differences are noticed in both cases, attributed to the formation of blends of homopolymers or block copolymers, as discussed above. Kinetic studies of the ROP of LLA_{30}-VAL_{70} were also carried out under the same conditions as LLA_{30}-CL_{70}. The $X_{overall}$ of monomers was monitored by gravimetry, and **Figure 11a** shows that the conversion reached approximately 80%, however, showing no significant difference in their behavior when using DBU or DBN as the catalyst.

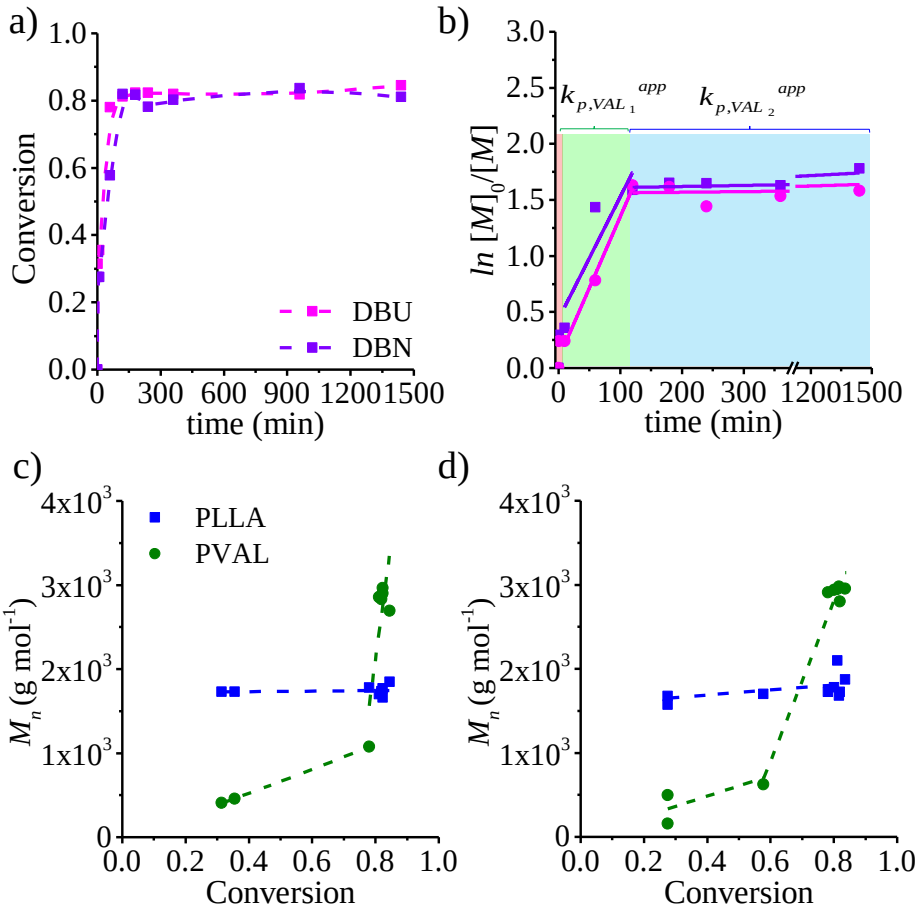

Figure 11. (a) Evolution of the conversion profiles, (b) linear fitting of **Equation (3)** and dependence of M_n *versus* $X_{overall}$ using (c) DBU and (d) DBN as organocatalysts of PLLA for the sequential ROP of LLA_{30}-VAL_{70} DESm at 37 °C. (Dashed lines denote tendencies, and solid lines are the linear regressions).

Table 2 shows the values of $k_{p,VAL1}^{app}$ and $k_{p,VAL2}^{app}$ during the sequential ROP of LLA_{30}-VAL_{70}. These were obtained by adjusting the *first-order* kinetic data according to **Equation (3)** in an interval of 10 to 150 min ($k_{p,VAL1}^{app}$) , *i.e.*, after the first ROP of LLA is completed. **Figure 11a** shows that the polymerization is inhibited during the rest of the reaction after 150 min, since the evolution of the polymerization rate presents a constant behavior and the estimated values for $k_{p,VAL2}^{app}$ are extremely small, irrespective of using DBU or DBN as the catalyst (on the order of 10^{-6} s^{-1}); the opposite behavior is observed when performing the ROP of LLA_{30}-CL_{70} under the same conditions. In addition, the comparative of **Figures 11b** and **10b** confirms that the polymerization of LLA_{30}-VAL_{70} is much faster than that of LLA_{30}-CL_{70}. This is in agreement with results reported in the literature about these ROP in solution.[13,25–27]

In **Figures 11 (c-d),** the evolution of M_n in the LLA_{30}-VAL_{70} conversion was followed, varying the type of catalyst for the ROP of LLA, observing that in both systems, LLA reached $X_{overall}$ = 30%, generating initial PLLA chains embedded in liquid VAL. However, VAL, unlike CL, begins to add in low proportions under a linear behavior in conversions from 30 to 80%, when DBU is used as the catalyst, and up to 60% when DBN is used. At conversions higher than 60%, the viscosity of the medium increases, thus favoring the polymerization of VAL, reaching Mn ≈ 3 000 g mol^{-1}.

3.3.4 Thermal properties and crystallinity of PLLA-PCL and PLLA-PVAL

The mole fraction of monomers (F_{PLLA}:F_Y, Y = CL or VAL) in the polymers resulting from the ROP of LLA_{30}-CL_{70} and LLA_{30}-VAL_{70} was determined from ^{1}H NMR spectra after removal of oligomers and residual monomers by the purification step. The mole fraction (F_{PLLA}:F_Y) of homopolymer composition of PLLA-PCL and PLLA-PVAL at the end of the polymerization, 47:53 and 45:55, respectively, differed with respect to the initial molar composition (f_{LLA}:f_Y), 30:70 LLA-lactone. This means that oligomers of PVAL or PCL and residual monomers of VAL and CL were removed from the final product during the purification process. **Figure 12** shows the SEC results and the elution of the $PLLA_U$-PCL sample before and after the purification step.

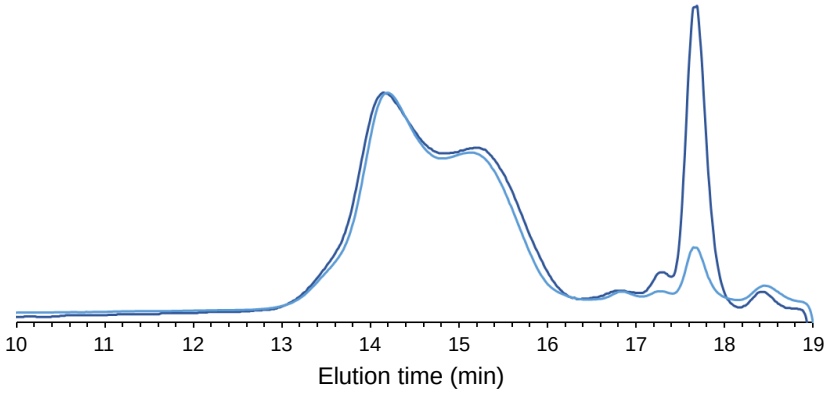

Figure 12. SEC traces of the sample PLLA$_U$-PCL before (dark blue) and after (light blue) the purification step.

The first bimodal peak at low retention volume corresponds to the PCL and PLLA blend, while the peak at higher retention volume corresponded to PCL oligomers. The decreased intensity of the oligomer peak after purification indicates the successful removal of oligomers. The thermal properties of the obtained polyesters were studied by DSC. **Figure 13** shows the thermograms for the samples listed in **Table 3**. The first endothermic peaks at 61 °C and 57 °C correspond to the melting point (T_m) of PCL (T_m = 62 °C)[28] and PVAL (T_m = 58 °C),[29] and the second endothermal peaks corresponded to the T_m of PLLA, which was found between 122.2 and 133.5 °C. The crystallinity (X_c) of the final polyester was calculated by **Equation (4)**.

$$X_c = \frac{100}{x^a}\left(\frac{\Delta H_m^a}{\Delta H_0}\right) \quad (4)$$

where X_c and x^a denote the degree of crystallinity and mass fraction of component *a*, respectively, in the eutectic mixture. ΔH_m^a and ΔH_0 correspond to the experimental melting enthalpy of component *a* (obtained by DSC) and the theoretical value with 100% crystallinity ($\Delta H_{0,PVAL}$=182 g mol^{-1}, $\Delta H_{0,PCL}$=135.44 g mol^{-1}, $\Delta H_{0,PLLA}$=106 g mol^{-1},respectively).[5,30]

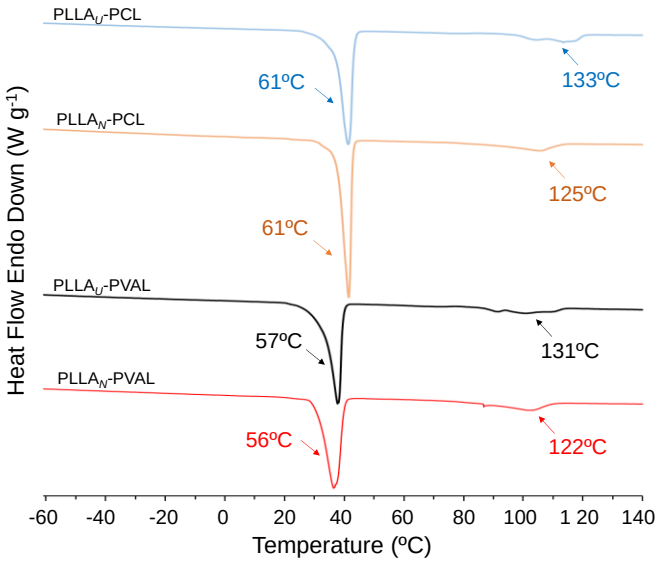

Figure 13. DSC scans of the final product of the ROP of LLA_{30}-CL_{70} and LLA_{30}-VAL_{70} at 37 °C using DBN (for PLLA$_N$-PCL and PLLA$_N$-PVAL) and DBU (for PLLA$_U$-PCL and PLLA$_U$-PVAL) as the organocatalysts of PLLA.

Table 3. Mole fraction of polymers (F_i, *i* = PLLA, PCL or PVAL and thermal properties of the polyester obtained from the ROP of LLA_{30}-CL_{70} and LLA_{30}-VAL_{70}.

Sample[a]	[CAT:In] (mol ratio)	F_{PLLA}:F_Y [b] (mol %)	$T_{m,\,PLLA}$ [c] (ºC)	$T_{m,\,Y}$ [c] (ºC)	$X_{c,\,PLLA}$ [c] (%)	$X_{c,\,Y}$ [c] (%)
PLLA$_U$-PCL	1:1	45:55	133	61	35	73
PLLA$_N$-PCL	1:1	45:55	125	61	38	73
PLLA$_U$-PVAL-60	1:1	46:54	127	56	36	35
PLLA$_U$-PVAL	1:1	47:53	131	57	34	69
PLLA$_U$-PVAL-1	1:0.5	47:53	121	56	39	47
PLLA$_U$-PVAL-0	1:0.25	47:53	128	60	36	50
PLLA$_N$-PVAL	1:1	47:53	122	56	44	70

[a] ROP of LLA_{30}-VAL_{70} or LLA_{30}-CL_{70} DESm was carried out using MSA as the second organocatalyst and BnOH as the initiator. The molar ratio of [CAT:In] and [MSA represented 5 and 3 wt% to the DESm, respectively. In all the entries ROP was performed at 37 ºC except for sample PLLA$_U$-PVAL-60. [b] The mole fraction of monomers (F_{PLLA};F_Y) was obtained by ^{1}H NMR. [c] Thermal properties calculated by DSC.

The T_m and X_c of the PLLA-PVAL and PLLA-PCL in the polymer varying the DBU or DBN as catalyst are shown in **Figure 14**. **Figure 14a** shows that the crystallinity of the resulting PLLA is slightly favored when using DBN for the ROP of LLA_{30}-CL_{70}, being greater for the ROP of LLA_{30}-VAL_{70}.

It is important to mention that regardless of the type of catalyst used, DBU or DBN, there is no significant difference when comparing the T_m values for the final polyesters (**Figure 14** blue and purple solid and dotted bars).

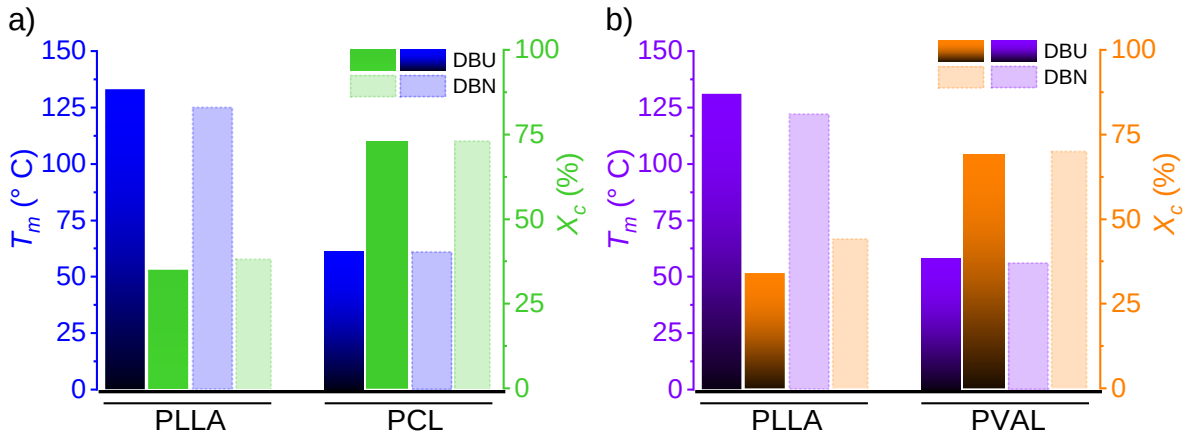

Figure 14. Melting point (T_m, blue and purple bars) and crystallinity (X_c, green and orange bars) of (a) PLLA-PCL and (b) PLLA-PVAL in the polymer blends varying the use of DBU (solid line bars) or DBN (dashed lines bars) as the catalyst.

As discussed previously, although the polymerization of LLA in both systems ($PLLA_U$-PCL and $PLLA_N$-PCL) reached complete conversions within minutes, slightly lower kinetics in the case of DBN may have allowed the rearrangement of PLLA chains and thus increased its crystallinity (see **Figure 10d**). PCL and PVAL exhibit higher crystallinity than PLLA. Furthermore, the lower rate of polymerization of CL compared to VAL in the mixtures with LLA did not significantly affect the crystallinity of the corresponding PCL and PVAL ($X_c \approx$ 73% and X_c = 70%, respectively).

The T_m of PLLA of all samples are significantly lower than the T_m of PLLA synthesized via conventional methods ($T_m \approx 176$ °C);[32] this could be associated with a diluent effect of PVAL or PCL embedded in the crystalline regions of PLLA, either as blends or forming block copolymers, thus resulting in materials with lower T_m. In general, PVAL has a lower melting point than PCL, and as expected, PVAL polymerized in the presence of PLLA also exhibits a lower T_m than PCL polymerized under similar conditions.[33] Similarly, PLLA synthesized using DBN as the organocatalyst and PLLA$_N$-PCL or PLLA$_N$-PVAL possess a lower T_m compared with those obtained with DBU.

These obtained polyesters presented semicrystalline behavior by X-ray diffraction, showing the characteristic peaks of PLLA at 2θ values of 16 and 19°, PCL at 21.4 and 23.8°, and PVAL at 21.7 and 24.11° (**Figure 15**).[31]

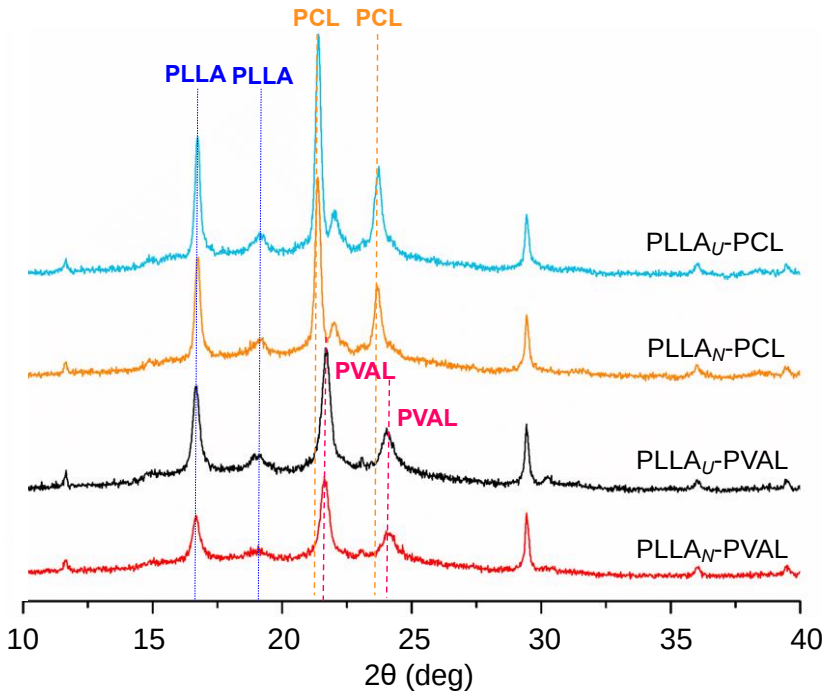

Figure 15. XRD scans of the final product of the ROP of LLA$_{30}$-CL$_{70}$ and LLA$_{30}$-VAL$_{70}$ at 37 °C using (c) DBN and (d) DBU as the organocatalysts of PLLA.

The effect of the variation in the molar ratio of BnOH and the reaction temperature on thermal properties and crystallinity of final products, are shown in **Figure 16**. The T_m of PLLA$_U$ and PVAL remained nearly unchanged when decreasing the molar ratio of initiator (1 to 0.25) (**Figure 16a**), being ca. 130 and 57 °C, respectively. However, the molar ratio of BnOH with respect to DBU has a direct impact on the X_c of PVAL, for instance, reaching a maximum of 69% at higher concentrations. This corresponds to the fact that M_n of PLLA is ca. of 1 850 g mol^{-1} with a higher proportion of initiator, which allows the polymeric chains with low M_n to form crystalline domains more easily.

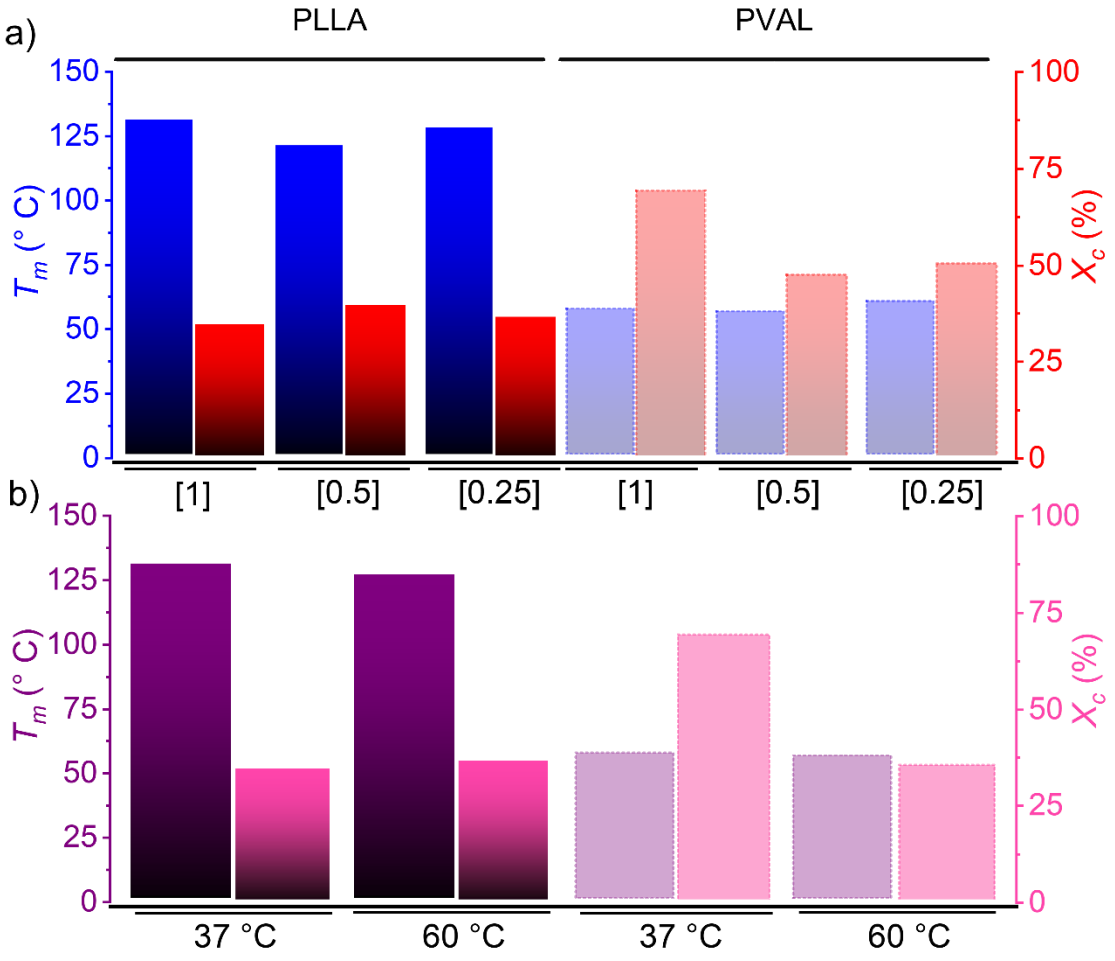

Figure 16. Thermal properties of PLLA$_U$-PVAL in the polymer blend varying (a) molar ratio of BnOH in [DBU:BnOH]=[1: BnOH] and (b) temperature. (T_m, blue and purple bars) and crystallinity (X_c, red and pink bars).

On the other hand, **Figure 16b**, shows that the increasing of the reaction temperature from 37 to 60 °C, do not have a noticeable effect on the T_m and X_c of PLLA$_U$ remaining both unchanged (T_m = 128 °C and X_c = 35), while for PVAL, the X_c is higher when the ROP is carried out at 37 °C. These results agree with the M_n values of polyesters obtained at the same temperatures (**Figure 17)**, being lower at 60 ºC than at 37 ºC, since lower temperature allows the polymeric chains to better reorganize into highly crystalline domains.

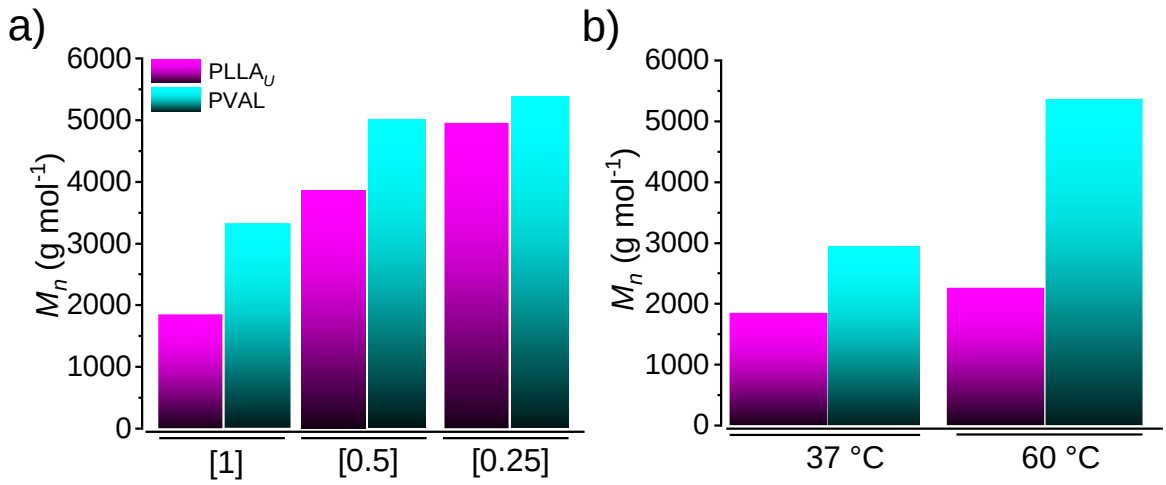

Figure 17. M_n of PLLA$_U$-PVAL in the polymer blends varying (a) molar ratio of BnOH in [DBU:BnOH]=[1: BnOH] and (b) temperature of the ROP.

3.3.5 Polymers architecture

To obtain deeper insights into the final product composition, PLLA$_U$-PVAL and PLLA$_N$-PVAL were analyzed by ^{1}H NMR diffusion-ordered spectroscopy (DOSY). **Figure 18a** shows a broad distribution of coefficients in the DOSY spectrum of polyester PLLA$_U$-PVAL. The higher diffusion coefficient corresponded to heavier species, consistent with PVAL, and the lower diffusion coefficient corresponded to PLLA.

The signals of each species were compared with the upper axis representing the corresponding ^{1}H NMR spectrum. These results show that the M_n of PVAL was higher than that of PLLA, as observed by the M_n calculation obtained from ^{1}H NMR (see **Table 1** and **Figure 18**). Additionally, the signals of terminal OH-containing groups [–C**H**–] (H_f) and [–C**H**$_2$–] (H_g) identified in the ^{1}H NMR spectra of PLLA$_{CAT}$-PVAL, do not show any changes in their chemical shift neither their intensity along the ROP (**Figure 8**), which confirmed that both PLLA and PVAL exist as independent homopolymers in a polymer blend.

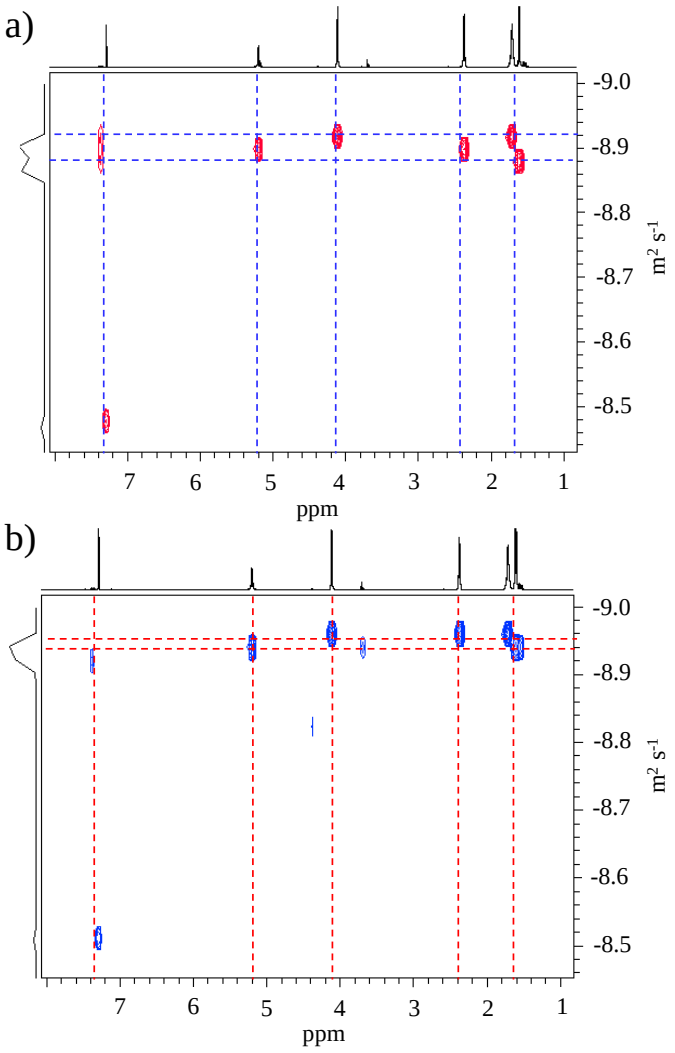

Figure 18. DOSY spectra of (a) PLLA$_U$-PVAL and (b) PLLA$_N$-PVAL in $CDCl_3$. The diffusion coefficient D_M (m^2/s) is indicated for each component.

Conversely, in the case of sample PLLA$_N$-PVAL (**Figure 18b**), a narrower set of diffusion coefficients were observed, which can be mainly attributed to the presence of a block copolymer of poly(PLLA$_N$-*b*-PVAL), but other species cannot be ruled out. These results suggest the successful synthesis of poly(PLLA-*b*-PVAL) from the ROP of VAL based DESm, where the initial hydroxyl-terminated PLLA homopolymer acts as the macroinitiator for the subsequent ROP of VAL catalyzed by MSA. Nevertheless, compared with the results of poly(PLLA-*b*-PCL)[6], here, the distribution of the diffusion coefficients in **Figure 18b** is broad and presents a small shoulder. This is consistent with a polymer mixture of block copolymers and homopolymers, as the presence of the terminal H_f in the ^{1}H NMR of PLLA suggests in **Figure 8**.

Size-exclusion chromatography (SEC) measurements were conducted to analyze the polyesters listed in **Table 1**. **Figure 19** shows bimodal peaks at low elution times (13-16 min) corresponding to PCL with higher molecular weight, and PLLA with lower molecular weight, in PLLA$_U$-PCL and PLLA$_N$-PCL. Similarly, peaks of PVAL and PLLA are observed in PLLA$_U$-PVAL and PLLA$_N$-PVAL. These results are in line with the M_n obtained by ^{1}H NMR spectroscopy (**Table 1**). It is important to mention that the distribution of peaks is independent of the polymer architecture (homopolymers and block copolymers), and the differences between M_n and M_w were attributed to the change in the hydrodynamic volume.

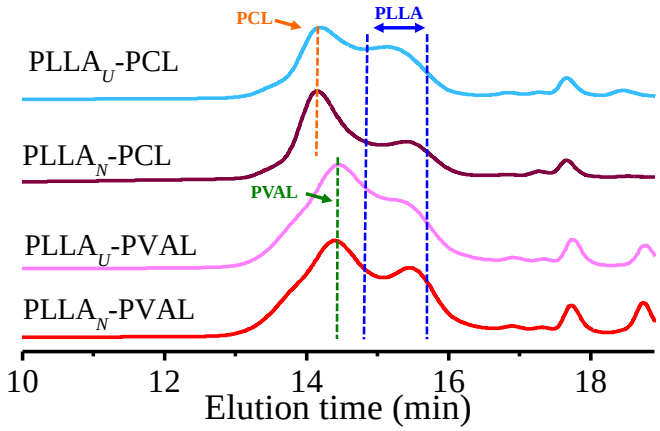

Figure 19. SEC scans of final product of the ROP of LLA$_{30}$-CL$_{70}$ and LLA$_{30}$-VAL$_{70}$ at 37 °C using DBN and DBU as the organocatalysts of PLLA.

To demonstrate differences in samples mainly composed of homopolymers or block copolymers, a solubility test of the polyesters PLLA$_U$-PVAL and PLLA$_N$-PVAL was performed in THF at -4 °C, with a concentration of the polyesters of 0.55 g mL^{-1}. The insolubility of PLLA in THF under cold conditions was considerably improved with the PVAL counterpart presented in sample PLLA$_N$-PVAL, which contains block-copolymers. Therefore, a stable and clear solution was observed. Conversely, the scant solubility of PLLA$_U$ in PLLA$_U$-PVAL led to gelled solutions in THF at -4 °C (see **Figure 20**), as direct consequence of the presence of individual homopolymers (*i.e.*, PLLA and PVAL) in the polyester, forming a heterogeneous mixture.

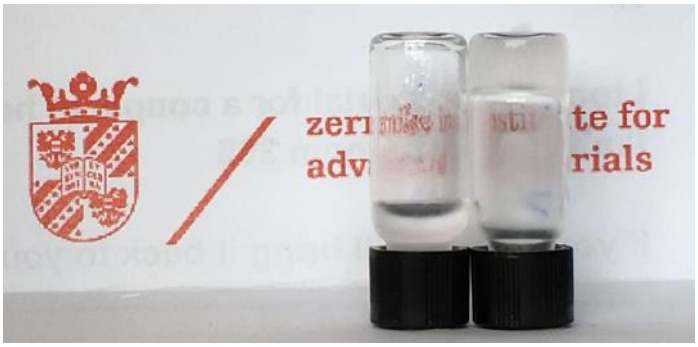

Figure 20. Photographs of PLLA$_N$-PVAL (left) and PLLA$_U$-PVAL (right) solutions in tetrahydrofuran at -4 °C.

3.3.6 Thermal stability

The thermal stability and thermal degradation of the polyesters were studied by TGA. The PLLA$_U$-PCL and PLLA$_U$-PVAL samples, mainly composed of homopolymer blends, showed two thermal degradation (T_d) steps. The first degradation occurred at $T_d \approx 327$ °C and $T_d \approx 307$ °C with mass losses of approximately ca. 22% and 37%, for the polymers containing PCL and PVAL, respectively. They were attributed to PLLA degradation (with a previously reported T_d of about 365 °C),[34] being PLLA approximately 30 mol% of the final composition of the polymer blend), The second step of degradation occurred between $T_d \approx 395$ - 425 °C, temperatures at which decomposition of PVAL and PCL occur in accordance with the values reported, $T_d \approx 410$ and 520 °C, respectively [29,34].

This evidence indicates that PLLA$_U$-PVAL and PLLA$_U$-PCL were composed of blends of homopolymers. Conversely, the samples polymerized with DBN (PLLA$_N$-PCL and PLLA$_N$-PVAL) showed one main step of degradation denoting higher thermostability. At temperatures of approximately 330 °C, mass losses of 7 and 10% occurred in PLLA$_N$-PCL and PLLA$_N$-PVAL, respectively, which are lower than those in the PLLA$_U$-PCL and PLLA$_U$-PVAL samples due to the presence of block copolymers (**Figure 21)**.

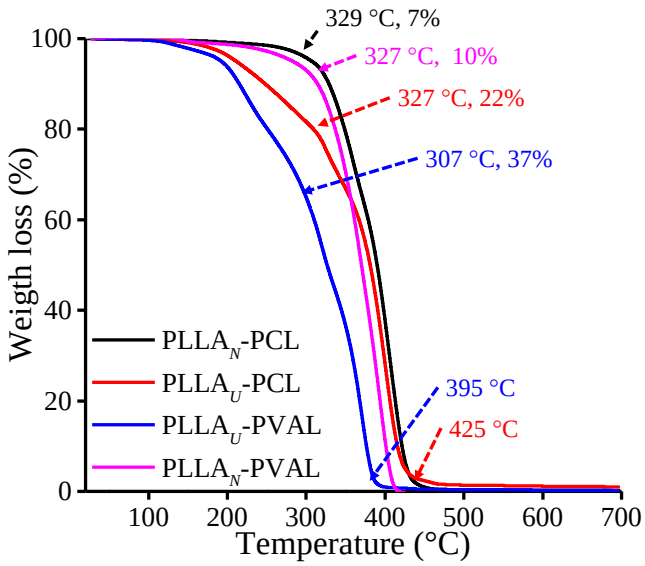

Figure 21. TGA curves of final product of the ROP of LLA$_{30}$-CL$_{70}$ and LLA$_{30}$-VAL$_{70}$ at 37 °C using DBN and DBU as the organocatalysts of PLLA.

3.3.7 Degradability test and contact angle.

The design of polyesters with rapid and controllable degradation can benefit from polyesters with low M_n, between 2 000 and 3 000 g mol^{-1}, such as those in this work obtained from the ROP of DESm at 37 °C. These polymerizations were carried out at a low temperature, excluding metal catalysts and organic solvents, which opens the possibility for applications in biomedical areas exploiting the green credential of the synthesis. Degradation of polyesters such as PLLA and PVAL occurs through two stages by surface or bulk degradation mechanisms and is autocatalyzed by acidic byproducts that are produced by chain hydrolytic incision.[35]

Parameters such as crystallinity, molecular weight and molecular architecture all play important roles in the degradation performance, where water diffusion is restricted in highly crystalline polyesters, thus decreasing the degradation rate.[35] **Figure 22a** shows the mass loss degradation profile for PLLA$_U$-PVAL and PLLA$_N$-PVAL in phosphate buffer solution (PBS) solution with pH = 7.4 at 37 °C, being the mass losses after 28 days of ca. 50 and 55%, respectively. The higher crystallinity of PLLA$_U$-PVAL resulted in a lower mass loss.

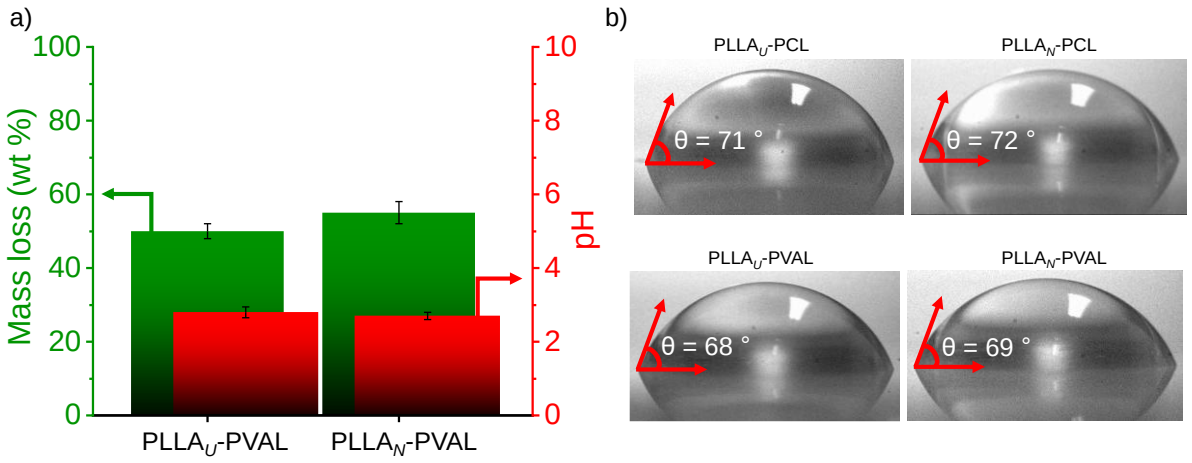

Figure 22. (a) Mass loss (wt%) profile degradation of the samples after 28 days at 37 °C and (b) water contact angle of final product of the ROP of LLA$_{30}$-CL$_{70}$ and LLA$_{30}$-VAL$_{70}$ at 37 °C using DBN and DBU as the organocatalysts of PLLA.

Early degradation was reported to take place on the surface,[35] as could be observed in the PLLA$_N$-PVAL sample in **Figure 23**, where after 28 days, the diameter decreased as well as the pH of the solution from 7.4 to 2.8 due to the acidic nature of the released byproducts of degradation. The degradation characteristics of polyesters could be applied in areas that require short-term degradation profiles in acidic media, such as drug delivery systems or the release of special cargos in the agroindustry.[31,33,36–39]

Figure 22b shows the water contact angle of the polyesters obtained from ROP of LLA$_{30}$-VAL$_{70}$ at 37 °C using DBN and DBU compared with their counterparts having PCL (LLA$_{30}$-CL$_{70}$). The contact angle was approximately 70° in all the samples, *i.e.*, slightly hydrophobic, as expected.[38,40–42] The water contact angle obtained for the PLLA$_U$-PCL sample was 71°, and for PLLA$_U$-PVAL, it was 68°.

A slightly decreased contact angle indicates reduced hydrophobicity, in agreement with data reported for PVAL, being comparatively less hydrophobic than PLLA-PCL.[37] In general, hydrophobicity decreases the water permeability in both polycaprolactone and polyvalerolactone, which reduces degradation by erosion.

Figure 23. Profile degradation of PLLA$_N$-PVAL and PLLA$_U$-PVAL after 28 days at 37 ºC (a) sample before and (b) after degradation test. At pH values (2.8) of final PBS solution (initial pH=7.4).

3.4 Conclusions

In this work, we successfully obtained binary DESm composed of LLA with lactones, such as δ-valerolactone and δ-hexalactone, at a 30:70 molar ratio. Sequential ROP of the DESm at low temperatures in solventless conditions involved two steps. In the first step, the organocatalys (DBU or DBN) allowed the ROP of LLA contained in the DESm, with BnOH as the initiator. In the second step, lactone ROP (VAL or HEXL) was carried out by adding a second organocatalyst (MSA). Notably, a high conversion (ca. 80%) was only reached in the ROP of the LLA and VAL mixture, resulting in homopolymers and copolymer blends composed of PLLA and PVAL with high crystallinity.

The kinetics of the ROP of the LLA_{30}-VAL_{70} DESm comprise three stages; the first stage is attributed to the almost instantaneous polymerization of LLA, while the second and third stages include the induction and propagation periods of VAL. Contrary to the polymerization rate of LLA in CL, different amidine organocatalysts (DBU or DBN) did not affect the VAL rate in the LLA_{30}-VAL_{70} DESm, and both reached similar rates M_n. Nevertheless, properties such as thermal stability, diffusion coefficients of the polymeric species (by DOSY NMR) or solubility differed in the final polyesters, which reflects the different architectures achieved, *e.g.*, mainly block copolymers in the case of $PLLA_N$-PVAL or homopolymer blends in $PLLA_U$-PVAL. These results point to a major effect of the organocatalyst employed for LLA polymerization, proving decisive for the final architecture of subsequent ROP of VAL, either PLLA functioning as a macroinitiator for PVAL blocks or as a mere spectator of the VAL ROP.

Thermal properties and crystallinity of the $PLLA_N$-PVAL and $PLLA_U$-PVAL are in accord with their overall architecture, being the $PLLA_N$ T_m higher than $PLLA_U$, and in the case of PVAL, the M_n and X_c remain constant, either when there is $PLLA_N$ or $PLLA_U$ in the second stage of polymerization. The effect of the initiator concentration on the M_n of PLLA was as expected in the LLA_{30}-VAL_{70} DESm, *i.e.*, the lower the initiator the higher the M_n. On the other hand, the increase of the ROP temperature led to lower crystallinity on PVAL and higher M_n in both PLLA and PVAL.

In summary, the ROP of DESm composed of LLA and VAL was carried out excluding metal catalysts and organic solvents under mild temperature conditions and unsophisticated atmospheres, thereby underscoring the green credentials of the processes. These findings pave the way for the design of polyesters with rapid and controllable degradation, potentially applicable to biomedical devices.

3.5 References

(1) Castro-Aguirre, E., Iñiguez-Franco, F.; Samsudin, H., Fang, X., Auras, R. *Adv. Drug Deliv. Rev.* 2016, **107**, 333–366.

(2) Hamad, K., Kaseem, M., Yang, H. W., Deri, F., Ko, Y. G. *Express Polym. Lett.* 2015, **9**, 435–455.

(3) Li, F. J., Zhang, S. D., Liang, J. Z., Wang, J. Z. *Polym. Adv. Technol.* 2015, **26**, 465–475.

(4) Sangroniz, A., Sangroniz, L., Hamzehlou, S., Aranburu, N., Sardon, H., Sarasua, J. R., Iriarte, M., Leiza, J. R., Etxeberria, A., *Polymers.* 2022, **14**, 1–14.

(5) Pérez-García, M. G., Gutiérrez, M. C., Mota-Morales, J. D., Luna-Bárcenas, G., Del Monte, F. *ACS Appl. Mater. Interfaces,* 2016, ***8***, 16939–16949.

(6) Castillo-Santillan, M., Torres-Lubian, J. R., Martínez-Richa, A., Huerta-Marcial, S. T., Gutierrez, M. C., Loos, K., Peréz-García, M. G., Mota-Morales, J. D. *Polymer.* 2022, **262**, 125432.

(7) Yang, X., Liu, S., Yu, E., Wei, Z. *ACS Omega* 2020, **5**, 29284–29291.

(8) Sherck, N. J., Kim, H. C., Won, Y. Y. *Macromolecules*, 2016, **49**, 4699–4713.

(9) Basterretxea, A., Gabirondo, E., Jehanno, C., Zhu, H., Coulembier, O., Mecerreyes, D., Sardon, H. *Macromolecules*, 2021, **54**, 6214–6225.

(10) Basterretxea, A., Jehanno, C., Mecerreyes, D., Sardon, H. *ACS Macro Lett.,* 2019, **8** 1055–1062.

(11) Chen, Y., Zhang, J., Xiao, W., Chen, A., Dong, Z., Xu, J., Xu, W., Lei, C. *Eur. Polym. J.*, 2021, **161**, 110861.

(12) Mezzasalma, L., Dove, A. P., Coulembier, O. *Eur. Polym. J.*, 2017, **95**, 628–634.

(13) Makiguchi, K., Satoh, T., Kakuchi, T. *Macromolecules*, 2011, **44**, 1999–2005.

(14) Abbott, A. P., Capper, G., Davies, D. L., Rasheed, R. K., Tambyrajah, V. *Chem. Commun.*, 2003, **9**, 70–71.

(15) Mota-Morales, J. D., Sánchez-Leija, R. J., Carranza, A., Pojman, J. A., del Monte, F., Luna-Bárcenas, G. *Prog. Polym. Sci.*, 2018, **78**, 139–153.

(16) Mota-Morales, J. D., Gutiérrez, M. C., Sanchez, I. C., Luna-Bárcenas, G., Del Monte, F. *Chem. Commun.*, 2011**, 47**, 5328–5330.

(17) Coulembier, O., Lemaur, V., Josse, T., Minoia, A., Cornil, J., Dubois, P. *Chem. Sci.*, 2012, **3**, 723–726.

(18) García-Argüelles, S., García, C., Serrano, M. C., Gutiérrez, M. C., Ferrer, M. L., Del Monte, F. *Green Chem.*, 2015, **17**, 3632–3643.

(19) Chen, S., Wang, H., Li, Z., Wei, F., Zhu, H., Xu, S., Xu, J., Liu, J., Gebru, H., Guo, K.. *Polym. Chem.*, 2018, ***9***, 732–742.

(20) Mosnáček, J., Duda, A., Libiszowski, J., Penczek, S. *Macromolecules*, 2005, **38**, 2027–2029.

(21) Basterretxea, A., Gabirondo, E., Jehanno, C., Zhu, H., Coulembier, O., Mecerreyes, D., Sardon, H. *Macromolecules*, 2021, **54**, 6214–6225.

(22) Wang, B., Pan, L., Ma, Z., Li, Y. *Macromolecules*, 2018, **51**, 836–845.

(23) Wu, D., Lv, Y., Guo, R., Li, J.; Habadati, A., Lu, B., Wang, H., Wei, Z. *Macromol. Res.*, 2017, **25**, 1070–1075.

(24) Rudin, A., Choi, P. In *Polymer Science and Engineering*; Academic Press, Elsevier: Boston, MA, USA, 2013; pp 275–304.

(25) Lohmeijer, B. G. G., Pratt, R. C., Leibfarth, F., Logan, J. W., Long, D. A., Dove, A. P., Nederberg, F., Choi, J., Wade, C., Waymouth, R. M., Hedrick, J. L. *Macromolecules,* 2006, **39**, 8574–8583.

(26) Wang, X., Liu, J., Xu, S., Xu, J., Pan, X., Liu, J., Cui, S., Li, Z., Guo, K. *Polym. Chem.*, 2016, **7**, 6297–6308.

(27) Gagliardi, M., Bifone, A. *PLoS One*, 2018, **13**, 1–15.

(28) Broz, M. E., VanderHart, D. L., Washburn, N. R. *Biomaterials*, 2003, 4, 4181–4190.

(29) Saeed, W., Al-Odayni, A.B., Alghamdi, A., Alrahlah, A., Aouak, T. *Crystals*, 2018, **8**, 452.

(30) Zhang, D., Dashtimoghadam, E., Fahimipour, F., Hu, X., Li, Q., Bersenev, E. A., Ivanov, D. A., Vatankhah-Varnoosfaderani, M., Sheiko, S. S. *Adv. Mater.*, 2020, ***32***, 1–11.

(31) Alghamdi, A. A., Saeed, W. S., Al-Odayni, A. B., Alharthi, F. A., Semlali, A., Aouak, T. *Polymers.*, 2019, **11**, 1–24.

(32) He, A., Han, C. C., Yang, G. *Polymer.*, 2004, **45**, 8231–8237.

(33) Han, W., Liao, X., Yang, Q., Li, G., He, B., Zhu, W., Hao, Z. *RSC Adv.*, 2017, **7**, 22515–22523.

(34) Mofokeng, J. P., Luyt, A. S. *Polym. Test.*, 2015, **45**, 93–100.

(35) Yin, G., Zhao, D., Wang, X., Ren, Y., Zhang, L., Wu, X., Nie, S., Li, Q. *RSC Adv.*, 2015, **5**, 79070–79080.

(36) Huang, W., Wen, X., Zhou, J., Zhang, X. *Int. J. Biol. Macromol.*, 2022, **222**, 961–971.

(37) Mishra, G. P., Kinser, R., Wierzbicki, I. H., Alany, R. G., Alani, A. W. G. *Eur. J. Pharm. Biopharm.*, 2014, *88*, 397–405.

(38) Fernández, J., Etxeberria, A., Sarasua, J. R. *Polym. Degrad. Stab.*, 2015, ***112***, 104–116.

(39) Saeed, W. S., Al-Odayni, A. B., Alrahlah, A., Alghamdi, A. A., Aouak, T. *Materials.*, 2019, **46**. *12*.

(40) Athanasoulia, I. G., Tarantili, P. A. *Pure Appl. Chem.*, 2017, *89*, 141–152.

(41) Viral Tamboli, Mishra, G. P., Mitra, A. K. *Colloid Polym Sci*,. 2013, **291**, 1235–1245.

(42) Doshi, B., Sillanpää, M., Kalliola, S. *Water Res.*, 2018, **135**, 262–277.

CHAPTER 4

Ring-opening polymerization of emulsion-templated deep-eutectic system monomers for macroporous polyesters with controlled degradability as crude oils sorbents

Macroporous, interconnected, and biodegradable polyesters, such as poly(L-lactide) (PLLA) and poly(ε-caprolactone) (PCL) have become central materials in tissue engineering and separation fields. This study introduces functional macroinitiators, namely polycaprolactone triol (PCL_T) and polyethylene glycol (PEG), in the ring-opening polymerization (ROP) of a deep eutectic system monomer (DESm) composed of LLA and CL at a 30:70 molar ratio. The macroinitiators selectively initiate the ROP of LLA in the first step of polymerization and modify the PLLA architecture, resulting in branched PCL_T-*b*-PLLA or a linear copolymer depending on the macroinitiator PCL_T and PEG, respectively. Subsequently, the CL counterpart in the DESm undergoes polymerization to produce PCL, which is then blended with the previously obtained products from the first step. The insights gained into the PLLA architecture during the first stage of the DESm ROP, along with the overall molecular weight and hydrophobicity of the resulting PLLA and PCL blends in bulk, were used advantageously to design polymerizable high internal phase emulsions (HIPEs) oil-in-DESm. The liquid nature of the DESm and macroinitiators (PCL_T or PEG) enabled the formulation of stable HIPEs that sustained the efficient organocatalyzed ROP of the continuous phase at 37 °C with high conversions. The resulting macroporous and interconnected polymer replicas of the HIPEs were subjected to a degradation assay in PBS at pH 7.4 and 37 °C and remained mechanically stable for at least 30 days. Interestingly, they demonstrate the ability to sorb crude oil in an adsorption proof-of concept, with a rate of 2 g g^{-1}. The interconnected and macroporous structures of the polyHIPEs, combined with their inherent degradation properties, render them suitable degradable polymeric sorbents for the efficient separation of hydrophobic fluids from water.

This Chapter was submitted.

4.1 Introduction

Crude oil spills have detrimental effects on numerous ecosystems.[1–3] When an oil spill occurs in the ocean, wind and currents cause it to spread, resulting in an expanded affected area. The damage includes accumulation and sedimentation of the oil, leading to severe environmental and health consequences.[4–6]. Removing the crude oil from the water poses a significant challenge, prompting the proposal of various physical, mechanical, chemical, and microbiological methods to address the problem.[6–10]

The complexity of oil spills means complete elimination unachievable through a single method or technology, as each approach has inherent limitations in terms of its effectiveness. Often, a combination of several methods is employed to tackle the overall issues of oil spills.[6,10] The development of non-toxic and biodegradable materials with advantageous shape-size and mechanical properties is crucial for effective oil spill treatment. These materials serve as alternatives for environmentally sustainable oil disposal, addressing the key challenge of finding suitable solutions.[6]

Recently, materials such as aerogels, permeable foams, or bio-based fibrous materials have been proposed as effective sorbent for removing oil from water.[6,11] While some of these materials are biodegradable and non-toxic, there are still limitations regarding their production cost and scalability. In most cases, functionalization of their large surface area is necessary to achieve satisfactory performance.[6,12] Therefore, research efforts have focused on engineering the large surface area and interconnected pores in these materials, as oil molecules are absorbed through capillarity, diffuse into the pores, and accumulate and attach to the sorbent surface. This sorption phenomenon is attributed to non-covalent and van der Waals interactions.[11,13] Porous polymers with a high surface represent a suitable option for separation processes, particularly if they are biodegradable.[6,14] In the broader context of oil spills, biodegradable porous polymers offer a solution to the issue of secondary contamination caused by sorbents. The surface area, interconnections, morphologies, and pore sizes of these materials can be modified depending on the chosen preparation methods.[15,16]

One such method for producing porous polymer materials is emulsion templating, which offer the advantage of designing specific surface areas and controlling the interconnectivity of the pores.[15] Common approaches to producing these materials involve designing high internal phase emulsion (HIPEs), which are subsequently polymerized. HIPEs consist of densely packed droplets of an internal phase that act as a template, stabilized by surfactants, and separated by a thin layer of continuous phase containing monomers.[14,16,17] Polyesters, such as polycaprolactone (PCL) and poly(L-lactide) (PLLA), are widely recognized as important polymers due to their cleavable bonds through hydrolysis.[18,19] However, synthesizing biodegradable porous polyesters in the form of polyHIPEs through ring opening polymerization (ROP) under mild conditions presents challenges. The conventional synthesis methods for these polyesters typically require high temperatures and low pressures.[18] To address this, recent studies have focused on introducing deep eutectic systems monomers (DESm) composed of L-lactide and ε-caprolactone as the polymerizable continuous phase of non-aqueous HIPEs. The main challenge lies in controlling the properties of the polyesters to achieve polyHIPEs with tunable biodegradability, morphology, and mechanical properties.

In this study, we investigate the incorporation of macroinitiators in the ROP of a DESm composed of L-lactide and ε-caprolactone to improve the properties of the resulting polyesters, which can be translated into the preparation of polyHIPEs. The macroinitiators selectively initiate the ROP of LLA in the first polymerization stage, yielding branched PCL_T-*b*-PLLA or a linear PEG-*b*-PLLA copolymers, depending on the macroinitiator used (PCL_T and PEG, respectively). Blending the PCL, which were produced in the second stage of the ROP, with the branched PCL_T-*b*-PLLA or linear PEG-*b*-PLLA copolymers, allows for the fine tuning of hydrophobicity and thermal properties both in bulk and in polyHIPE, thereby improving the overall performance of PLLA/PCL polyHIPEs as crude oil sorbent. The resulting polyesters, which contain branched PCL_T-*b*-PLLA or linear PEG-*b*-PLLA copolymers and PCL, exhibit structural stability in PBS solution at pH 7.4 and 37 °C for 30 days and effectively sorb crude oil without collapsing. Due to their high macroporosity, interconnected morphology, compostability, absence of metal-based catalyst, and low polymerization temperature during their preparation, polyester-based polyHIPEs represent a promising class of biodegradable macroporous materials for separation processes in crude oil spill treatments.[6]

4.2 Experimental section

4.2.1 Materials

L-lactide (LLA, 98%), 1,8-diazabicyclo [5.4.0] undec-7-ene (DBU, 98%), Polyethylene Glycol Diol (PEG, M_n = 6 000 g mol^{-1}), methanesulfonic acid (MSA, 99.5%), Polycaprolactone triol (PCL_T, $M_n \approx$ 900 g mol^{-1}) and Pluronic® F-127 [poly(ethylene oxide)-*b*-poly(propylene oxide)-*b*-polyethylene oxide) triblock copolymer, $M_n \approx$ 12 600 g mol^{-1}] were obtained from Sigma-Aldrich. ε-Caprolactone (CL, 97%) was obtained from Thermo Fisher Scientific. Tetradecane (> 99.0 %) was acquired from TCI Europe N.V. Absolute ethanol (EtOH, AR), Methanol (MeOH, AR), and Chloroform ($CHCl_3$, > 98%) were purchased from Biosolve Chemicals. *n*-Hexane (> 99.0 %) was obtained from Macron Fine Chemicals. All materials were used without further purification. Sweet crude oil (< 0,5% sulfur) of the Rotterdam field was provided by Nederlandse Aardolie Maatschappij (NAM).

4.2.2 Methods

4.2.2.1 Deep eutectic system monomer (DESm) synthesis

The deep eutectic system monomer (DESm) was prepared by mixing LLA with CL at 30:70 molar ratio at 90 °C to obtain a clear and homogeneous liquid, following the methodology reported in literature.[18] To refer to DESm composed of 30:70 mol% LLA-CL, respectively, will be use the nomenclature LLA_{30}-CL_{70}.

4.2.2.2 Synthesis of PLLA and PCL polymers blend

PLLA and PCL blends were obtained by the sequential ROP at 37 °C in bulk of the DESm LLA_{30}-CL_{70}, using DBU and MSA as organocatalysts and benzyl alcohol (BnOH) as initiator.[18] The final polyesters were named PLLA/PCL. The same method was used to obtain PLLA homopolymer by terminating the reaction at one minute.[19] After that, the samples were dissolved in chloroform and immediately precipitated in cold methanol. In the next step, the sample was centrifuged at 4 500 rpm for 10 min, and the precipitate was dried. Finally, the resulting product was labeled as PLLA, with an approximate molecular weight of 1 800 g mol^{-1}.

4.2.2.3 Synthesis of polyesters of PLLA and PCL varying the macroinitiator

The synthesis of polyesters was carried out by sequential ROP at 37 °C in bulk of LLA_{30}-CL_{70} DESm using two macroinitiators: polycaprolactone triol (PCL_T) and polyethylene glycol (PEG). Then following the methodology reported in literature,[18] LLA_{30}-CL_{70} DEsm was heated at 60 °C with constant stirring by mixing for 10 min, which contained the macroinitiator, then the first organocatalyst (DBU) was added (1.0 wt% and 2.92 wt% with respect to the DESm, respectively). Subsequently, after 1 min, MSA (second organocatalyst, 3 wt% with respect to the DESm) was added to start the ROP of PCL. When PCL_T was used as the macroinitiator, the resulting polyesters were designated as branched PCL_T-*b*-PLLA/PCL, whereas the use of PEG as the macroinitiator led to the formation of linear PEG-*b*-PLLA/PCL polyesters.

After 24 h. of polymerization, the polyesters obtained were purified with an excess of ethanol 3 to 5 times for each sample to remove all residual monomers and oligomers. The solid polyesters were dried at room temperature (RT) for 24 h. The experimental conversion (X_{exp}) was determined by gravimetry, that is, the ratio between the final mass of the polymer and the initial mass of monomers.

Kinetics studies of branched PCL_T-*b*-PLLA/PCL and linear PEG-*b*-PLLA/PCL were prepared in individual vials and were terminated at different times to analyze the time-dependent polymerization.

4.2.2.4 Preparation of High-Internal-Phase-Emulsions (HIPEs)

The continuous phase of HIPEs was prepared by adding PCL_T or PEG at 1 wt% with respect to LLA_{30}-CL_{70} DESm and heated to 60 °C for 10 min and cooled down to RT. Afterwards, the surfactant Pluronic F-127 was added at 10 wt% with respect to HIPEs.

The HIPEs were prepared by gradually adding tetradecane dropwise to the dispersed phase with stirring, which accounted for 80 vol% of the solution consisting of a mixture of DESm-initiator-Pluronic® F-127, (the continuous phase was 20 %vol) in a 10 ml glass vial at 25 °C with constant agitation at 2 500 rpm until a white homogeneous emulsion was obtained.

4.2.2.5 Production of macroporous polyesters (polyHIPES)

The monoliths were synthesized by the ROP of the HIPE continuous phase with DBU (2.92 wt% respect to the DESm) as organocatalyst. The solution was kept under constant stirring for one minute, and the second catalyst MSA (3 wt% with respect to the DESm) was added. HIPEs were homogenized by vortexing for 2 min. ROP was carried out for 24 hours at 37 °C. After polymerization, polyHIPEs (pHIPES) were purified with an excess of *n*-hexane, for 12 h to remove the oil phase (tetradecane), and with ethanol for another 3 days by orbital mixing to remove oligomers, residual monomers, and surfactant. The purification process was performed following the procedure reported by Perez-García.[19] Finally, monoliths were dried at RT until constant weight was reached.

4.2.2.6 Production of self-assembly particles

To produce the self-assembled particles of linear PEG-*b*-PLLA/PCL, 30 mg of the sample was added to 200 ml of THF, and then water (ca. 2 ml) was added dropwise to the clear solution while stirring until a steady change to white was observed. THF was removed by evaporation while the medium was stirred for 24 h. Finally, a milky solution was obtained. It is noteworthy that the same methodology was followed for the PCL_T-*b*-PLLA/PCL sample, however, the polymer precipitated in water due to the absence of hydrophilic segments.

4.2.2.7 Degradation test

Porous polyesters were subjected to degradation profile assays. The samples were incubated at 37 °C in phosphate-buffered saline (PBS) pH=7.4, and the degradation test was conducted for 14 and 30 days. Then, the polyesters were removed from the medium and rinsed with ethanol to remove any PBS residues. Finally, the samples were dried at RT. The pH of the medium was measured, and the remaining mass of the samples was calculated by gravimetry.

4.2.2.8 Crude oil sorption test

The absorption capacities of monoliths (*Q*) were carried out in crude oil at RT. The monoliths were immersed in excess of crude oil until the equilibrium mass of crude oil was taken up.

The Q was determined by the equation $Q = (W\text{-}W_0)/W_0$, where W_0 and W are the weight of the monoliths before and after the absorption, respectively, and it was expressed in terms of the mass of crude oil per gram of dry monolith, and from now on, it will be represented as (g g^{-1}). The experiment was realized three times for each sample.

4.2.3 Polyesters Characterizations

The final polyesters were analyzed by ^{1}H and ^{13}C NMR (600 MHz) spectra were recorded on a Bruker Advance NEO 600 at 64 scans, and samples were prepared by dissolving in deuterium chloroform ($CDCl_3$) as an internal reference.

Equations. The mole fraction of monomers (F_i, were i = PLLA or PCL) was obtained by ^{1}H NMR.

$$F_{PLLA} = \frac{\int H_e}{\int H_e + \left[z \int \frac{H_a}{2} - \left(\frac{\int H_g}{3} * \omega\right)\right]} \quad (1)$$

$$F_{PLLA} = \frac{\int H_e}{\int H_e + \int \frac{H_a}{2}} \quad (2)$$

$$F_{PCL} = 1 - F_{PLLA} \quad (3)$$

Where ω is the number of hydrogens assigned to (-C**H**$_2$-) group (H_b) corresponding at the three arms units of PCL_T with $M_n \approx 900$ g mol^{-1}, $\omega = 48$. The **Equation (1)** was used only when the macroinitiator was PCL_T.

$$M_{n,PLLA}(gmol^{-1}) = \frac{\int H_e}{\int H_f}\left(MW_{LLA}\right) \quad (4)$$

$$M_{n,PCL}(gmol^{-1}) = \frac{\int \frac{H_b}{2} - \left(\int \frac{H_g}{3} * \omega\right)}{\int \frac{H_c}{2}}(MW_{CL}) \quad (5)$$

$$M_{n,PCL}(gmol^{-1}) = \frac{\int H_b}{\int H_c}(MW_{CL}) \quad (6)$$

Where ω is the number of hydrogens assigned to (-C**H**$_2$-) group (H_b) corresponding at the three arms units of PCL_T with $M_n \approx 900$ g mol^{-1}, $\omega = 48$. The **Equation (5)** was used only when the macroinitiator was PCL_T.

DOSY (Diffusion Order Spectroscopy) data were acquired using the pulse program *ledbpgp2s* installed in the topspin 3.6.2 software from Bruker with 95 gradient levels with a linear increase from 2 to 95% using a gradient of strengths up to 54 G/cm and 8 transients. The diffusion delay (Δ) was 150 ms, and the length of the square diffusion encoding gradient pulse (δ) was 0.6 ms. Laplace transformations for generating the diffusion dimensions were obtained with the Bruker Biospin Dynamics Center using a least-squares fitting routine with Monte Carlo error estimation analysis.

Attenuated total reflection Fourier (ATR-FTIR) spectra were recorded on a Bruker VERTEX 70 spectrometer equipped with a platinum-ATR diamond single reflection accessory. The measurement resolution was 1 cm^{-1}, and spectra were collected in the range of 4 000 - 400 cm^{-1}.

Differential scanning calorimetry (DSC) measurements were carried out on a TA Instruments Q1000 DSC. The analysis method for polyesters was performed on dry samples and with heating-cooling cycles. The analysis consisted of an initial cooling from RT to -70 °C, at a scan rate of 10 ºC min^{-1}, keeping it at that temperature for 5 min, then increasing the temperature to 220 °C, and finally cooling to RT at the same scan rate.

The thermal stability and degradation behavior of the different samples were studied using thermogravimetric analysis (TGA) on a TA Instruments Discovery TGA 5 500 using an aluminum pan. Thermograms were recorded in the temperature range of 30 °C to 700 °C at heating rate of 10 °C min^{-1} under a nitrogen atmosphere.

The X-ray diffraction patterns (XRD) of powdered samples was carried out in a Bruker D8 Advance diffractometer with Cu Kα radiation (λ = 0.1542 nm) in the angular range of 5–40° (2θ) at RT.

The molecular weight distributions ($Đ$) were determined by size exclusion chromatography (SEC) equipped with a triple detector: Viscotek Ralls detector, Viscotek Viscosimeter model H502 and Schambeck RI2912 refractive index detector. The separation was carried out by two PLgel 5μm MIXED-C and 300 mm columns from Agilent Technologies at 35 °C in THF (99% extra pure) stabilized with BHT as the eluent at a flow rate of 1.0 ml min^{-1}. The data acquisition was processed by using Viscotek Omnisec software version 5.0.

The contact angle was recorded by OCA20 (Data physics). The measurements were performed on films prepared by solvent casting. The obtained polyesters were dispersed in $CHCl_3$ and poured onto a glass plate, allowing the solvent to evaporate.

The surface morphology was examined by scanning electron microscopy (SEM, Hitachi S-4700). The macroporous structure of the monoliths was observed by scanning electron microscopy (SEM, Fei NovaNanoSEM 650) at an accelerating voltage of 5 kV. All samples were gold coated at 20 nanometers. The diameters of the pores were calculated by ImageJ analysis software as the average of 100 image readings. These values were used to estimate the degree of openness of porous polyesters by the application of the equation proposed by Pulko and Krajnc.[20]

Equations. PolyHIPE openness were estimated using by equation proposed by Pulko and Krajnc.[20]

$$O = \frac{Open\ surface\ of\ pores}{Surface\ of\ pore} = \frac{S_O}{S_C} \quad (7)$$

$$S_O = N\pi\left(\frac{d^2}{2}\right) \quad (8)$$

$$S_C = \pi D^2 \quad (9)$$

$$N = \frac{4\,n}{\sqrt{3}} \quad (10)$$

Where:

O = polyHIPES openness

N = number of interconnecting pores

n = average number of visible pores

d = average interconnecting pore diameter

D = average pore diameter

Dynamic light scattering (DLS) measurements were conducted on a Malvern Panalytical Zetasizer Ultra system equipped with a helium-neon laser (λ = 633 nm) and an avalanche photodiode detector.

TEM imaging was performed on a Philips CM120 transmission electron microscope equipped with a lanthanum hexaboride filament and operated at an accelerating voltage of 120 kV. Images were acquired using a Gatan slow-scan 4K CCD camera.

AFM imaging was conducted in standard tapping mode in air using a Bruker Dimension 3100 system equipped with VTESPA-300 tapping mode cantilevers from Bruker.

The polyHIPEs density (δ_B) was estimated by measuring the volume of monoliths with regular shapes. The total pore volume (V_T) was estimated at $1/\delta_B – 1/\delta_W$, where δ_W is the wall density that corresponded to the bulk polyesters, PCL_T-*b*-PLLA/PCL and linear PEG-*b*-PLLA/PCL blend density, ca. 0.9253 and 1.032 g ml^{-1}, respectively.

4.3 Results and discussion

4.3.1 Ring opening polymerization of LLA_{30}-CL_{70} DESm

The sequential ROP of the LLA_{30}-CL_{70} DESm at 37 °C in bulk yielded two polyesters blends, branched PCL_T-*b*-PLLA/PCL and linear PEG-*b*-PLLA/PCL, depending on the macroinitiator used (PCL_T or PEG, respectively). The macroinitiators accounted for 1 wt% with respect to DESm. The overall reaction is described in **Scheme 1**.

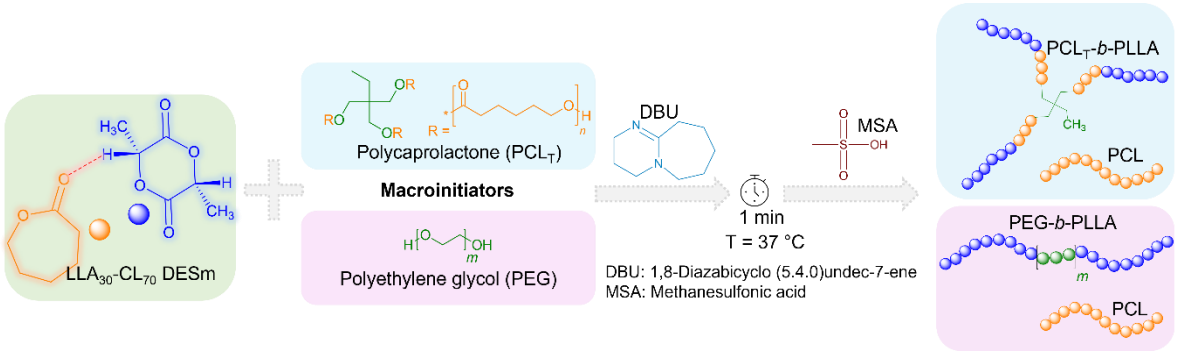

Scheme 1. Sequential Ring-Opening Polymerization of the LLA_{30}-CL_{70} DESm at 37 °C, varying the type of macroinitiator, PCL_T or PEG.

In the first step, DBU organocatalyst (2.92 wt% with respect to the DESm), was added to the reaction mixture. DBU selectively rapidly polymerized LLA in the DESm through the activation of both the alcohol and the monomer,[21] where either PCL_T or PEG served as macroinitiators via the -OH moieties. As reported in literature, DBU, has shown specificity in polymerizing LLA when it forms a DESm with CL. It is worth highlighting that the ROP of LLA can be successfully accomplished within a minute.[18,19] At this stage of the ROP, the average composition comprised PLLA blocks initiated by PCL_T or PEG, *i.e.*, branched PCL_T-*b*-PLLA or linear PEG-*b*-PLLA dispersed in liquid CL, which was released from the liquid eutectic composition as the LLA ROP proceeded. Additionally, as reported by Castillo-Santillan et. al., the occurrence of residual water-initiated the ROP of LLA or CL in the presence of DBU is highly limited or present in negligible concentrations.[18]

It is noteworthy that PCL_T has a M_n = 900 g mol^{-1} whereas PEG has a M_n = 6 000 g mol^{-1}, and both generated liquid solutions in DES at the polymerization temperature, thus, the whole reaction mixture is liquid at RT making all components readily available to polymerize. In the second step, MSA (second organocatalyst) was added to the reaction mixture promoting the ROP of CL, where residual water played the role of initiator as has been demonstrated in previous works.[18,19] Thus, blends of PCL whit branched PCL_T-*b*-PLLA or linear PEG-*b*-PLLA were obtained depending upon the initiator used in the ROP, yielding polyesters with interesting properties as it will be discussed in the next sections. Branched PCL_T-*b*-PLLA/PCL and linear PEG-*b*-PLLA/PCL polyesters were first studied in bulk. The presence of PLLA blocks in branched PCL_T-*b*-PLLA and linear PEG-*b*-PLLA were confirmed by ^{1}H NMR. Repeated group signals were identified as H followed by a letter assigned in the Figure 1, where the peaks at H_e= 5.17 and H_d= 1.66 ppm were assigned to the methine (-OC**H**CH_3-)$_n$ and methyl (-CHC**H$_3$**)$_n$.[22] Similarly, the presence of peaks at H_b= 4.09 ppm and H_a= 2.33 ppm were identified as the typical repeating methylene groups of PCL blocks (**Figure 1)**.[19]

Additionally, the PLLA block in the sample branched PCL_T-*b*-PLLA/PCL and linear PEG-*b*-PLLA/PCL was confirmed by the terminal peaks assigned H_f= 4.38 ppm to the methine group (–C**H**(CH_3)–OH), **Figure 1**.[19] Similarly, terminal peaks in PCL blocks presented in samples PCL_T-*b*-PLLA/PCL were confirmed by the peak H_c= 3.67 ppm (**Figure 1b**) and linear PEG-*b*-PLLA/PCL with the peak H_c= 3.77 ppm (**Figure 1d**), which is displaced to low field by the abundant presence of methylene groups corresponding to the repetitive units of ethylene glycol present in the polymer blend.

The formation of PLLA and PCL in the polyesters were corroborated by ^{13}C NMR spectroscopy. **Figure 2a**, shows the carbon peak at C_8 = 169 and C_7 = 64 ppm corresponding to the carbonyl (**C**OO-) and the repeated groups of methine (–**C**H(CH_3))$_n$ of PLLA, respectively, and the carbonyl (**C**OO-) of PCL at C_1 = 173 ppm were identified.[19]

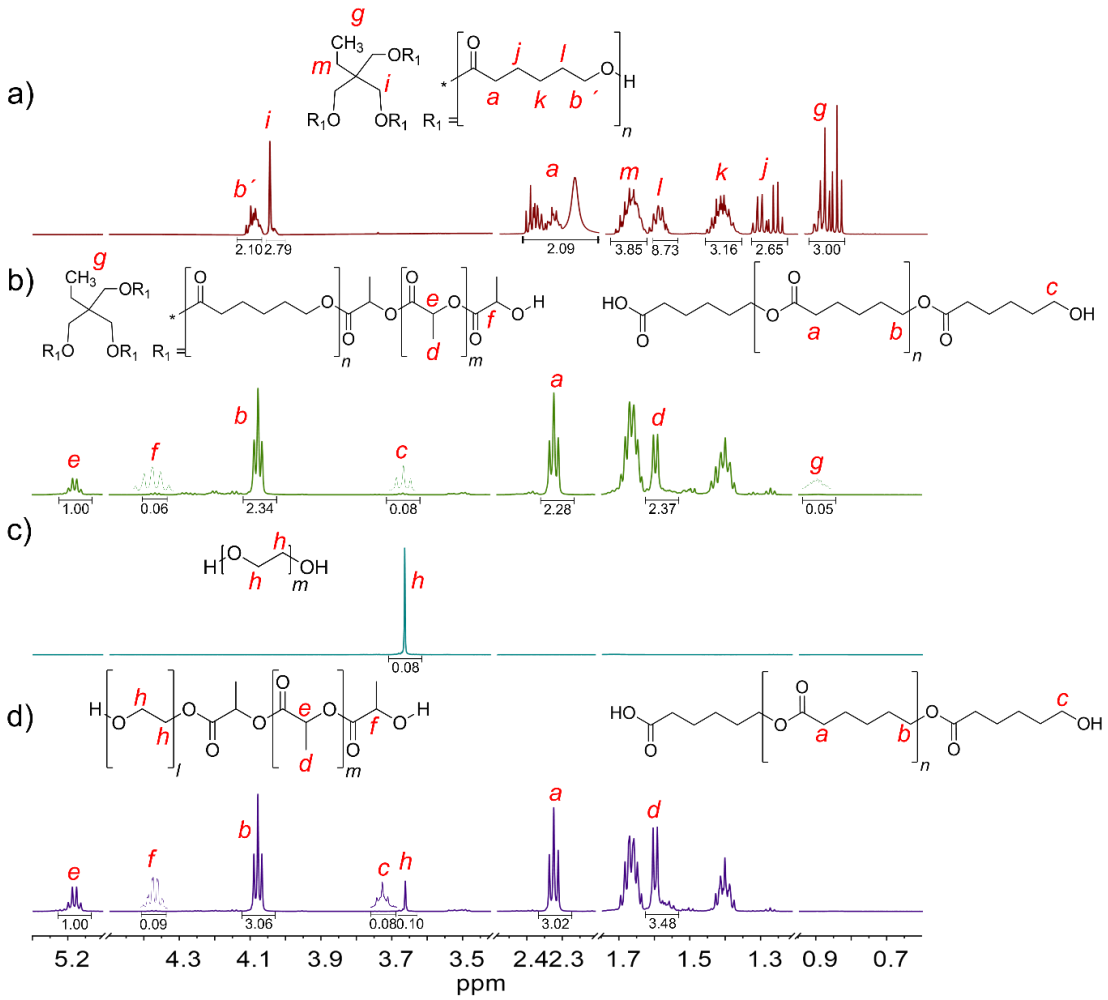

Figure 1. ^{1}H NMR spectra of the final product of the ROP of LLA_{30}-CL_{70} DESm at 37 °C varying (a) PCL_T or (c) PEG as the macroinitiator of polyesters: (b) branched PCL_T-*b*-PLLA/PCL, and (d) linear PEG-*b*-PLLA/PCL.

Furthermore, the presence of initiators, PCL_T and PEG, in branched PCL_T-*b*-PLLA/PCL and linear PEG-*b*-PLLA/PCL polyesters was confirmed by ^{1}H NMR. Specifically, PCL_T was identified by the signal H_g = 0.90 ppm attributed to the methyl terminal group (C**H**$_3$CH$_2$-), **Figure 1b**,[23] and the signal H_h = 3.66 ppm was assigned to the methylene groups (–C**H**$_2$C**H**$_2$O-)$_n$ of PEG.[24] **Figure 2b** shows the ^{13}C NMR spectra of linear PEG-*b*-PLLA/PCL, where the carbon peaks at C_7 = 64 ppm and C_2 = 69 corresponding to repeated groups of methine (–C**H**(CH$_3$))$_n$ and methylene (-C**H**$_2$O-)$_n$, from PLLA and PCL, respectively, are observed.[19] The presence of PEG in the polyesters was identified by the peak at 70 ppm which corresponds to the methylene group (–C**H**$_2$O–)$_n$.[25]

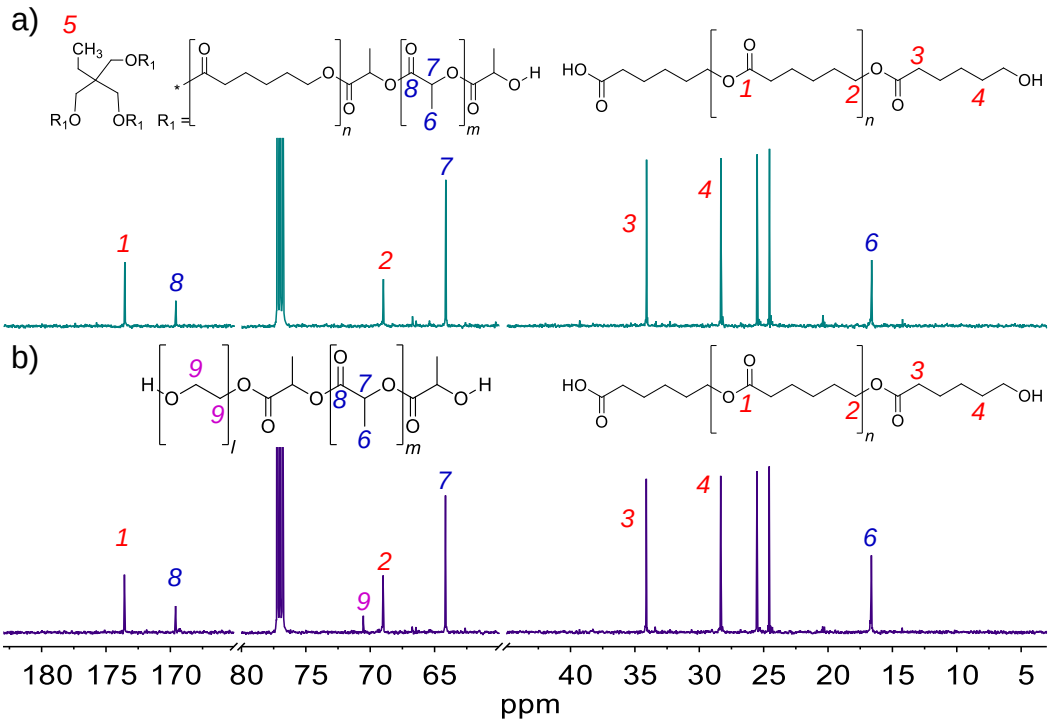

Figure 2. ^{13}C NMR spectra of the final product of the ROP of LLA_{30}-CL_{70} DESm at 37 °C varying PCL_T or PEG as the macroinitiators in the synthesis of polyesters: (a) branched PCL_T-*b*-PLLA/PCL, and (b) linear PEG-*b*-PLLA/PCL.

Altogether, the ^{1}H NMR and ^{13}C NMR spectra of branched PCL_T-*b*-PLLA/PCL and linear PEG-*b*-PLLA/PCL polyesters confirmed the role of PCL_T and PEG as macroinitiators in the ROP of LLA_{30}-CL_{70}. DESm experimental conversion (X_{exp}) were determined gravimetrically. The experimental conversion of branched PCL_T-*b*-PLLA/PCL was ca. 95% in 24 h, and for linear PEG-*b*-PLLA/PCL it was ca. 90% in 12 h.

Due to the presence of PLLA blocks in branched PCL_T-*b*-PLLA and linear PEG-*b*-PLLA, it was possible to determine the molecular weight (M_n) of PLLA blocks by following the method reported in the literature.[19,22] Similarly, the PCL homopolymer in the polyesters blends resulted from the ROP of the CL in the DESm, and the Mn was obtained using the same methodology for the PCL homopolymers. The molecular weights of PLLA and PCL in the polyesters were determined by SEC and ^{1}H NMR (**Table 1**). **Equations 4 and 5** are directly associated with using PCL_T as an initiator, while **Equations 4 and 6** should be directly associated with using PEG as an initiator.

Table 1. Chemical, thermal properties and contact angle of the polyesters obtained by the ROP of LLA_{30}-CL_{70} DESm at 37 °C in bulk, varying using PCL_T or PEG as macroinitiator.

Sample[a]	F_{PLLA}:F_{PCL}[b]	$M_{n,\ PLLA}$[c] (g mol^{-1})	$M_{n,\ PCL}$[c] (g mol^{-1})	M_n[d] (g mol^{-1})	$Đ$[d]	$T_{m,\ PLLA}$[e] (ºC)	$T_{m,\ PCL}$[e] (ºC)	Contact Angle (°)
Branched PCL_T-*b*-PLLA/PCL	40:60	2 402	4 394	9 585	1.69	133	58.7	71
Linear PEG-*b*-PLLA/PCL	40:60	1 601	8 732	6 220	4.09	122	60.2	56

[a] The ROP LLA_{30}-CL_{70} DESm, was carried out using DBU and MSA as organocatalysts. The molar ratio of catalyst DBU and the initiator was 2.92 and 1 wt%, respectively, and the MSA was 3 wt% all of them were respect to the DESm.

[b] The mole fraction of monomers (F_i, were i = PLLA or PCL) was obtained by ^{1}H NMR using the **Equation (1-3)**.

[c] M_n obtained by ^{1}H NMR using the **Equation (4-6)**.[d] M_n for the blend of polymers were obtained by SEC in THF.

[e] Thermal properties measured by DSC.

The estimation of the mole fraction of monomers (F_i, were i = PLLA or PCL) was obtained by ^{1}H NMR in the samples of branched PCL_T-*b*-PLLA/PCL and linear PEG-*b*-PLLA/PCL. The data give differences in the composition between the expected molar ratio of LLA_{30}-CL_{70} DESm and the final polyesters (**Table 1**), due to loss of PCL oligomers during the purification process with ethanol as it has been observed in the ROP of DESm initiated with BnOH.[26]

Size exclusion chromatography (SEC) was performed on the polyesters, and the traces are presented in **Figure 3**, and the M_n of the branched PCL_T-*b*-PLLA/PCL and linear PEG-*b*-PLLA/PCL samples are summarized in **Table 1**. Assuming that the result of the synthesis is a blend, the Mn taken from a blend is the combination of two separate molecular weight distributions, and M_n of PCL and PLLA values obtained by ^{1}H NMR spectroscopy were lower than those obtained by SEC. The differences arise from samples having different hydrodynamic volumes due to their different architectures, and the additional interactions with the PCL homopolymers in the blends.

Thus, the final polyesters blends eluted as broad distributions thanks to the high compatibility between the polymers composing the blends. This result was compared with a blend of homopolymers of PLLA and PCL and was discussed later in **Figure 10**. This behavior also observed in the peak distributions of branched PCL_T-*b*-PLLA/PCL and linear PEG-*b*-PLLA/PCL analyzed by ^{1}H NMR diffusion-ordered spectroscopy (DOSY). **Figure 4** shows the DOSY spectra of the polyester blends.

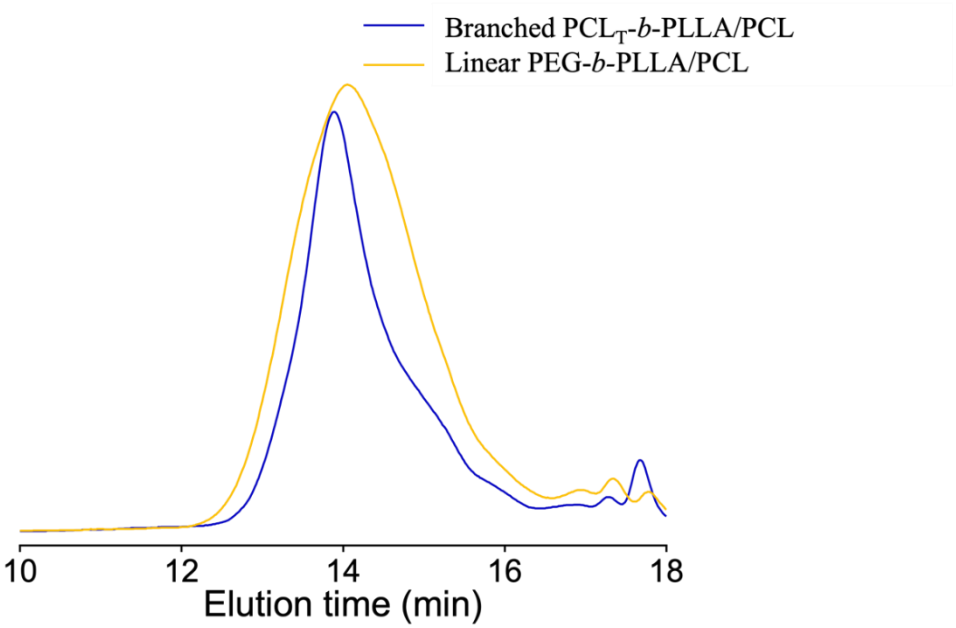

Figure 3. SEC profile of the branched PCL_T -*b*-PLLA/PCL and linear PEG-*b*-PLLA/PCL polyesters for analysis of the molar mass distribution.

The branched PCL_T-b-PLLA/PCL and linear PLLA-*b*-PEG/PCL polyesters were analyzed by DOSY spectroscopy. **Figure 4a** shows the DOSY spectra of the branched polyester blends PCL_T-*b*-PLLA/PCL. The diffusion coefficient distributions of the polymer species were made with the upper axis representing the corresponding ^{1}H NMR spectra. A narrower diffusion coefficient was observed for PCL_T-*b*-PLLA/PCL than linear PEG-*b*-PLLA/PCL, indicating a significant influence of the polymer architecture attributed to the PCL_T macroinitiator played the role as compatibility in the blend. The presence of blocks of PLLA with smaller Mn attached to the PCL_T macroinitiator led to the larger coefficient distribution in the same figure. These findings provide additional support to the discussion on thermal analysis.

The shoulder in the diffusion coefficient distribution of linear PEG-*b*-PLLA/PCL can be considered an effect of PCL homopolymer being less compatible with the more hydrophilic linear PEG-*b*-PLLA/PCL block compared with the branched PCL_T-*b*-PLLA/PCL. Although PEG has been reported to have better compatibility with PLLA than PCL,[27] the incorporation of a PEG block could still acted as a plasticizer[28] that enhances the overall compatibility between the PLLA and PCL blends, as no polymer segregation occurred. These findings point to PLLA copolymers polymerized in the first ROP and entangled with the PCL homopolymer from the second ROP.

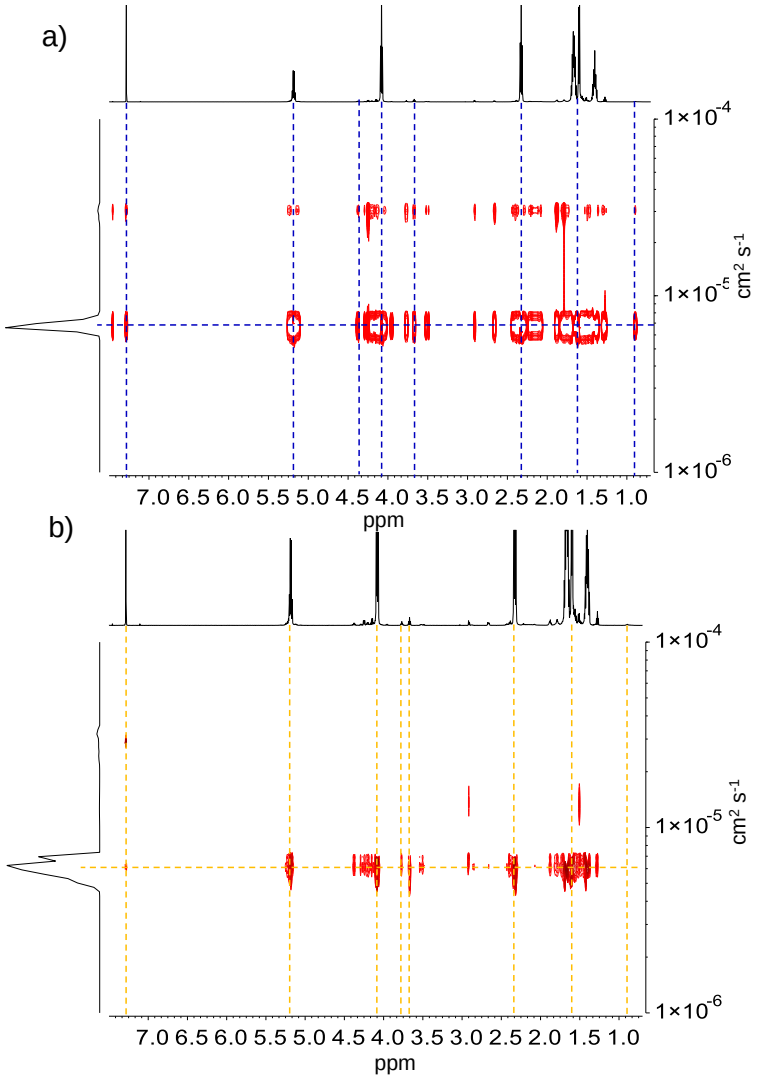

Figure 4. DOSY spectra of (a) branched PCL_T-*b*-PLLA/PCL and (b) linear PEG-*b*-PLLA/PCL in $CDCl_3$. The diffusion coefficient D_M ($cm^2\ s^{-1}$) is indicated for each component.

Ultimately, blending of PCL with branched PCL_T-*b*-PLLA or linear PEG-*b*-PLLA copolymers can be used to tune the hydrophobicity of the final materials. The blend that contained linear PEG-*b*-PLLA copolymer and PCL homopolymer had two different molecular weights, which resulted in different diffusion coefficients. This difference was confirmed by the broad M_n distribution obtained from SEC analysis, which has a dispersity index ($Đ$) of 4.09 (**Table 1**). As mentioned earlier, the PEG block in the copolymer played a critical role as a compatibilizer, determining the interactions between PLLA and PCL.

The thermal properties of the obtained polyesters were studied by DSC during the first heating run, listed in **Table 1**. **Figure 5a** shows the DSC thermograms during the first heating cycle of branched PCL_T-*b*-PLLA/PCL and linear PEG-*b*-PLLA/PCL. The first peak at around 60 °C corresponds to the melting point (T_m) of PCL (reported at around 62 °C),[29] and the second peak corresponds to the T_m of PLLA (122-133 °C) embedded in PCL.[30] Two endothermic peaks of PLLA in sample PCL_T-*b*-PLLA/PCL were observed at 128 °C and 133 °C, suggesting the presence of PLLA chains of different M_n in a single PCL_T, or different M_n amongst other PCL_T molecules.[31] Alternatively, it is possible that hydroxyl groups of PCL_T were not able to initiate the ROP of LLA; although hydroxyl groups in both PCL_T-*b*-PLLA/PCL and linear PEG-*b*-PLLA/PCL by ATR-FTIR (**Figure 6)** are negligible meaning remaining hydroxyl from PCL_T is not detected.

On the other hand, in the case of linear PEG-*b*-PLLA/PCL, it was observed that the melting point of PLLA was at around 122 °C (**Figure 5a)**. This can be attributed to PEG presented in the copolymer, whose segments were trapped in the crystalline regions of PLLA domains and acted as a diluent, ultimately depressing its T_m. This is in line with the findings of Weiqiang, H. *et al.*,[32] regarding the effect of the PCL block in copolymers with PLLA. The melting point of PCL was not affected by the presence of PEG block (T_m = 60 °C)[23] due to its higher affinity for PLLA,[28] nor was it affected by the presence of PCL_T. The glass transition temperature (T_g) of PLLA was observed both in PCL_T-*b*-PLLA/PCL and linear PEG-*b*-PLLA/PCL as a small shoulder at around 55 °C (**Figure 5a**), which corresponded to the PLLA amorphous phase.[33]

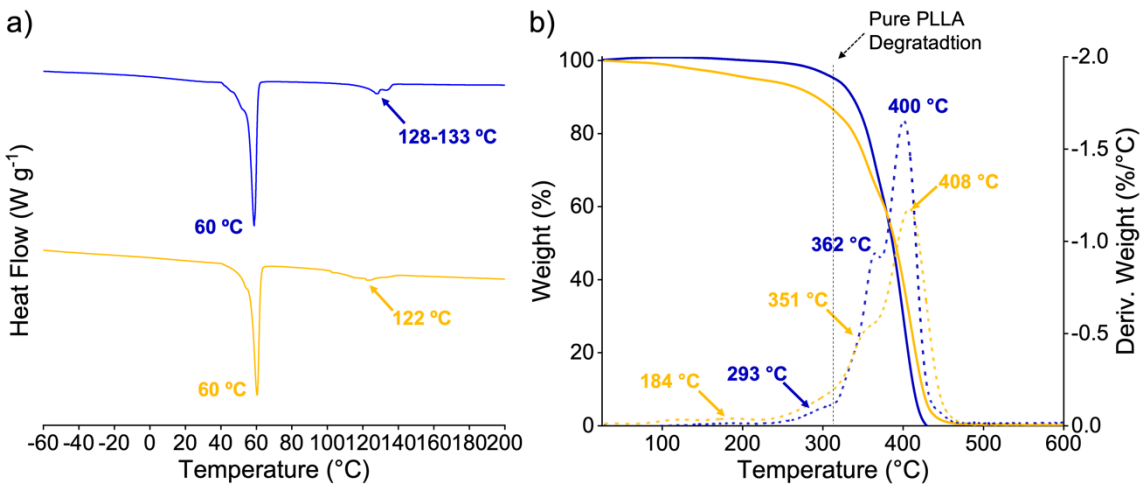

Figure 5. Thermal properties of branched PCL$_T$-*b*-PLLA/PCL (blue), and linear-PEG-*b*-PLLA (yellow) polyesters. (a) DSC thermograms during the first heating cycle, (b) TGA (solid lines) and DTGA (dotted lines) curves under nitrogen atmosphere.

The thermal stability of both products was studied by TGA. PCL$_T$-*b*-PLLA/PCL shows the first degradation at 293 °C with a mass loss of around 7.6%. The second decomposition temperature was observed at 362 °C with a mass loss of 30%. This decomposition is attributed to the PLLA degradation in the blend, which is higher than those reported for neat PLLA (321 °C).[28] The presence of PLLA blocks in the branched PCL$_T$-*b*-PLLA/PCL sample allowed for entanglement with the linear PCL homopolymer. This, in turn, increased the thermal stability of the copolymer. Linear PLLA, degraded at 321 °C,[28] and the thermal degradation of PCL occurs at approximately 400 °C. Conversely, block PEG, in sample linear PEG-*b*-PLLA/PCL, was observed at 184 °C, as reported in the literature.[28] Followed by the total decomposition of PLLA at 351 °C, the proportion of PLLA in the blend corresponded with ca. 30%, and finally the PCL degradation was at ca. 408 ºC. The degradation temperature of PLLA increased ca. 30 ºC compared with neat PLLA, thus the presence of PEG increased the compatibility of PLLA with PCL (**Figure 5b**).

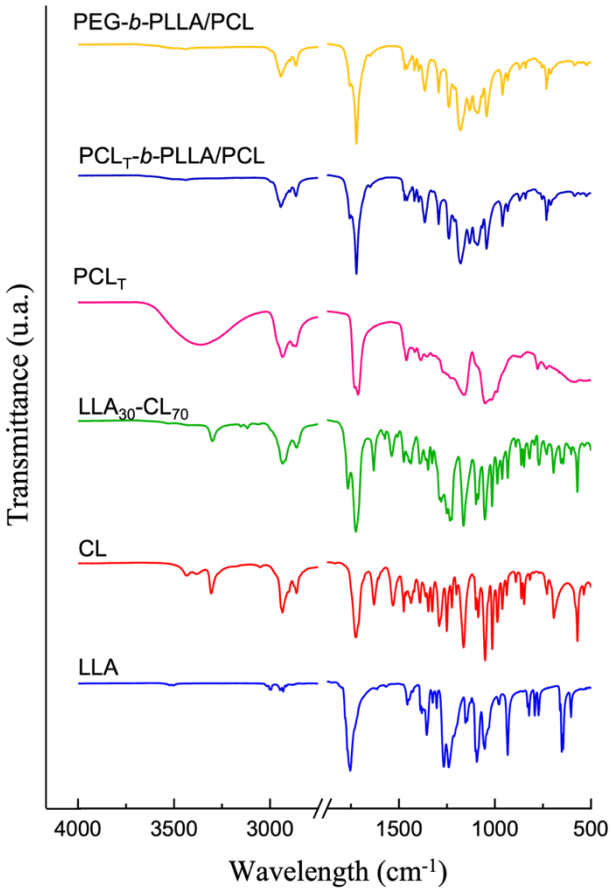

Figure 6. ATR-FTIR spectra of pure monomers LLA and CL, LLA_{30}-CL_{70} DESm and the branched PCL_T-*b*-PLLA/PCL and linear PEG-*b*-PLLA/PCL polyesters.

FTIR measurements were conducted on branched PCL_T-*b*-PLLA/PCL or linear PEG-*b*-PLLA/PCL to confirm the presence of PLLA and PCL. **Figure 6** shows the peaks at 2943 and 2864 cm^{-1} associated with (**-CH_3**) and (**-CH_2-**) groups present in PLLA and PCL.[28]The peak at 1757 cm^{-1} which is attributed to the (**C=O**) vibration in PLLA.[33]

The intensity of this peak is decreased in linear PEG-*b*-PLLA/PCL, suggesting the interaction of PEG counterpart of the block polymers with PLLA. While **C=O** peak attributed to PCL was observed at 1720 cm^{-1}.[34] Peak at 1474 cm^{-1} is attributed to the **C-H** stretching of PEG.[35] The peaks of **-C-O-** and **-COO-** that correspond to the presence of PLLA and PCL[34,36] in both PCL_T-*b*-PLLA/PCL or linear PEG-*b*-PLLA/PCL.

The crystalline character of PCL_T-*b*-PLLA/PCL and linear PEG-*b*-PLLA/PCL was further analyzed by X-ray diffraction (XRD). The spectra show semi-crystalline characteristics, with observed PLLA peaks at 2θ = 16.8° and 19.1°, and PCL peaks at 21.4 and 23.8°. XRD diffractogram of linear PEG-*b*-PLLA/PCL shows a characteristic peak of PEG at 19.3 and 23.3°. However, the first peak at 19.3° overlaps with PLLA peaks (**Figure 7**).[28,30,35]

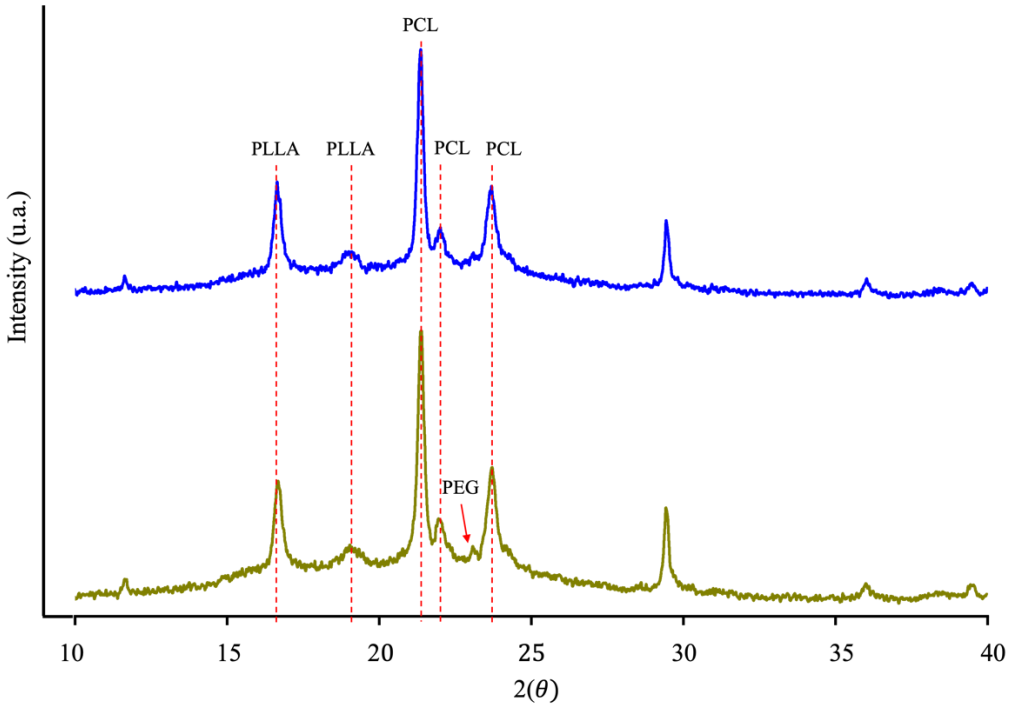

Figure 7. XRD scans of branched PCL_T-*b*-PLLA/PCL(blue) and linear PEG-*b*-PLLA/PCL (green) polyesters.

4.3.2 Kinetics study of the ROP LLA_{30}-CL_{70} DESm at 37 °C varying PCL_T or PEG as the macroinitiator of polyesters

The ROP kinetics of LLA_{30}-CL_{70} DESm varying the macroinitiator (PCL_T or PEG) were comparatively studied which the methodology and formulations that was previously reported[26] which was initiated by BnOH, pointing to the rapid polymerization of LLA during the first polymerization stage (1 min) followed by a steady polymerization of CL. This second stage follows a first-order kinetics associated with the slope of the curve corresponding to the initiation rate constant ($k_{p,CL1}^{app}$) (**Table 2**), showing that the polymerization presents the same behavior of the sequential ROP of LLA_{30}-CL_{70} DESm initiated by BnOH.

The relationship between the conversion of LLA_{30}-CL_{70} DESm and the polymerization time follows the same increasing trend regardless of the macroinitiator used, reaching up to 90% at 24 h. The synthesis of branched PCL_T-*b*-PLLA/PCL or linear PEG-*b*-PLLA/PCL polyesters was followed over time (after 6, 8, 12, 24, and 48 h) and the conversion was calculated by gravimetry. **Figure 8** shows the conversion of the PCL_T-*b*-PLLA/PCL sample. Within the first 6 h, the conversion reached around 80%, and full conversion was reached in 24 h. PLLA is formed rapidly in the first stage of the ROP. As the ROP continued, due to the conversion of CL into PCL, the viscosity increased.

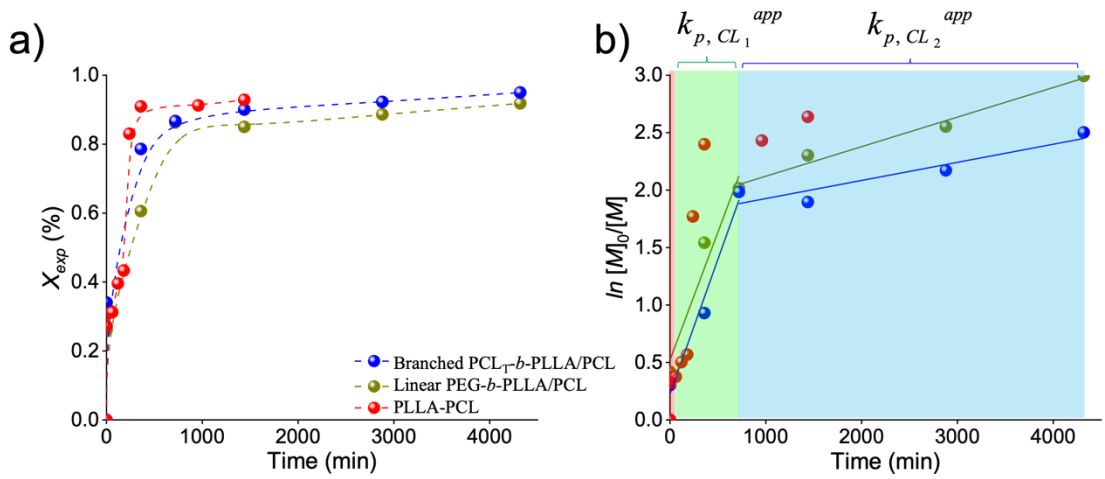

Figure 8. Evolution of the conversion profiles of branched PCL_T-*b*-PLLA/PCL and linear PEG-*b*-PLLA/PCL polyesters at 37 °C (Dashed lines denote tendencies, and solid lines are the linear regressions).

The reaction temperature (37 °C) was lower than the melting point of PCL in the macroinitiator and the subsequently formed PCL (60 °C); thus, the mobility of the CL monomer was constrained, and the polymerization rate decreased. Conversely, the polymerization of the linear PEG-*b*-PLLA/PCL sample was slower than PCL_T-*b*-PLLA/PCL; the conversion only reaches 60% after 6 h of reaction and finally reach maximum conversion after 12 h. Altogether, the conversion of both branched PCL_T-*b*-PLLA/PCL or linear PEG-*b*-PLLA/PCL reached similar values (ca. 80 %) at 12 h.

The total polymerization time was longer in comparison to the polyester synthesis reported by Perez-Garcia *et al.*,[19] which took only 6 h. While a similar DESm and organocatalysts were used, the difference was that BnOH was used as the initiator in Perez-García study. The macroinitiators used in this work, PCL_T and PEG, possessed higher molecular weights than BnOH, and the availability of hydroxyl groups, necessary for carrying out the ROP, was constrained. The resulting polyesters in this work possess higher molecular weights than those initiated by BnOH, thus, the viscosity of the reaction mixture was increased and limited the mobility of the monomers during the polymerization.

Table 2. Estimation of $k_{p,CL1}^{app}$ for LLA_{30}-CL_{70} DESm at 37 °C in bulk varying PCL_T or PEG as the macroinitiator of polyesters.

Sample	Macroinitiator	k_{p,CL_1}^{app} (s^{-1})	Ref.[7]
PLLA/PCL	BnOH	2.23×10^{-5}	Chapter 2
PCL_T-*b*-PLLA/PCL	PCL_T	3.70×10^{-5}	This work
linear PEG-*b*-PLLA/PCL	PEG	3.90×10^{-5}	This work

To study the role of initiators in PCL_T-*b*-PLLA/PCL and linear PEG-*b*-PLLA/PCL polymerization, the reaction was followed by ^{1}H NMR spectroscopy (6, 12, 24 and 48 h). **Figure 9a** shows the ROP of the DESm initiated by PCL_T, where PLLA presence was confirmed by the appearance of the repeating unit peaks at 5.17 and 1.60 ppm, and the methine end group peak at 4.38 ppm. This was observed within the first minute, as reported in literature.[19] The peak at 0.892 ppm corresponds to the methyl-methylene terminal group of PCL_T. While the peaks at 4.18 and 2.32 ppm are attributed to the PCL repeating methylene group, the polymerization was confirmed at 6 h, the polymerization was confirmed at 6 h, as reported in the literature.[19] The terminal methylene group of PCL at 3.66 ppm overlapped with the same terminal methylene groups presented in the PCL_T-*b*-PLLA/PCL used as macroinitiator.

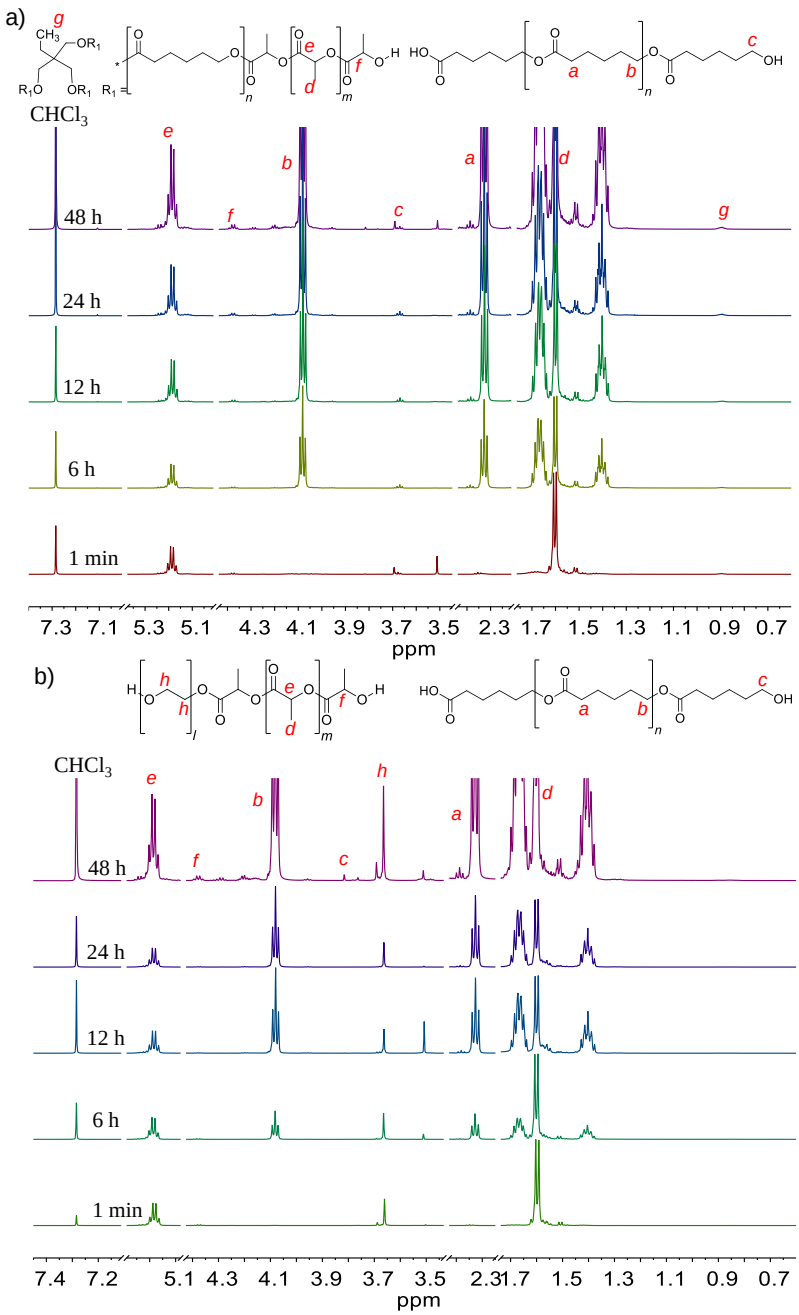

Figure 9. ^{1}H NMR spectra of the sequential ROP of (a) branched PCL_T-*b*-PLLA/PCL and (b) linear PEG-*b*-PLLA/PCL.

Figure 9b shows similar signals corresponding to PLLA and PCL. Additionally, the signal of PEG, that played the role of macroinitiator, at 3.67 ppm overlapped with the PCL end group. The presence of branched PLLA or PEG copolymers in blends with PLLA was reported to improve their properties, such as flow behavior or tensile strength, respectively.[31,37]

We compared the chromatographic profile of branched PCL_T-*b*-PLLA/PCL and linear PEG-*b*-PLLA/PCL with PLLA/PCL homopolymer blends and pure PLLA homopolymer by SEC. PLLA/PCL and PLLA were obtained from the method reported by Perez Garcia *et al*.[19] Size exclusion chromatography (SEC) was performed on PLLA, PLLA/PCL, branched PCL_T-*b*-PLLA/PCL and linear PEG-*b*-PLLA/PCL. **Figure 10** shows the unimodal SEC traces of PLLA. PCL and PLLA homopolymer mixtures show a bimodal curve representing PCL and PLLA.

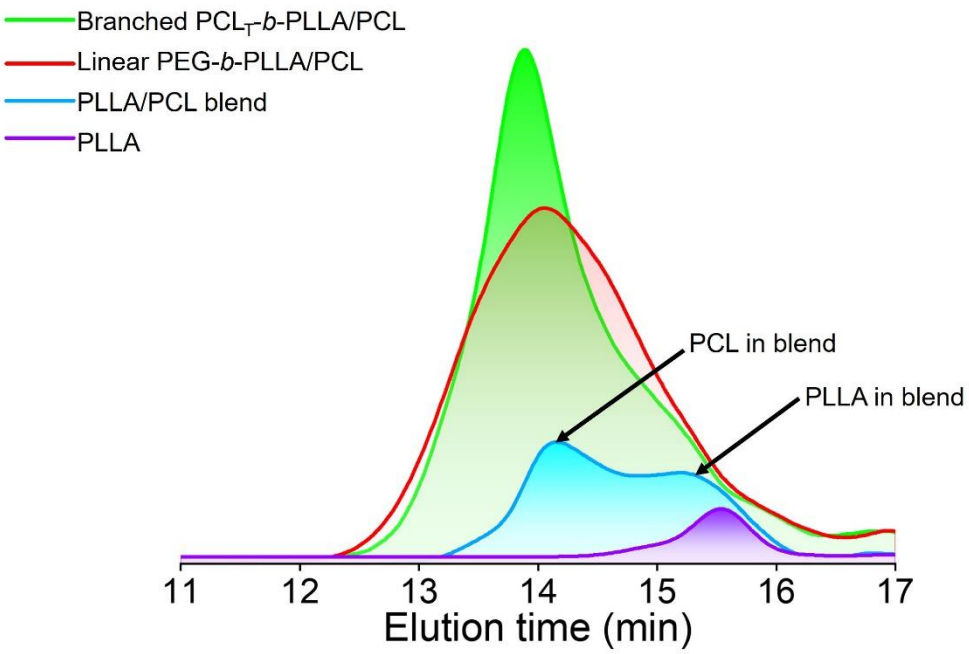

Figure 10. Comparative study of the SEC distribution for PLLA, PLLA/PCL blend, branched PCL_T-*b*-PLLA/PCL and linear PEG-*b*-PLLA/PCL polyesters.

The SEC of the branched PCL_T-*b*-PLLA/PCL and linear PEG-*b*-PLLA/PCL shows a unimodal peak at a lower retention volume compared to the PLLA/PCL linear blend. No peak was observed at the same elution time of neat PLLA, which suggested that PLLA obtained in branched PCL_T-*b*-PLLA/PCL and linear PEG-*b*-PLLA/PCL have higher molecular weight due to PCL_T and PEG-initiated ROP and are associated with the other polyesters (including the macroinitiators) as discussed in the ^{1}H NMR and DOSY results.

4.3.3 Linear PEG-*b*-PLLA/PCL amphiphilic properties

Linear PEG-*b*-PLLA/PCL exhibited amphiphilic properties due to the presence of hydrophilic PEG and more hydrophobic PLLA and PCL in the polymer blend. This amphiphilicity usually results in the self-assembly polymers into stable particles in aqueous media composed of a hydrophobic core covered by a hydrophilic shell, observed as a cloudy dispersion in the right side of (**Figure 11a**).[38]

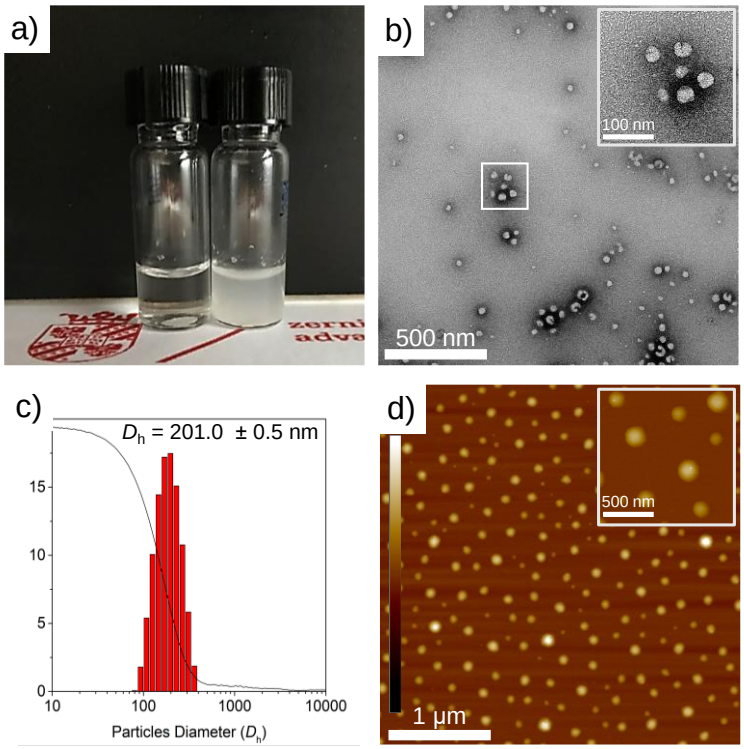

Figure 11. (a) PCL_T-*b*-PLLA/PCL precipitated (left vial) and linear PEG-*b*-PLLA/PCL (right vial) in water. (b) TEM images of uranyl acetate-stained self-assembly spheres of linear PEG-*b*-PLLA/PCL. (c) DLS histogram plot and cumulative function (solid line). (d) AFM height images of the self-assembled particles deposited on a freshly cleaved mica disk (AFM z-scale is ± 10 nm).

The morphology of the self-assembled structures resulting from linear PEG-*b*-PLLA/PCL in aqueous solution was studied by TEM and AFM. **Figure 11b** and **d** confirmed the presence of spherical structures of self-assembled linear PEG-*b*-PLLA/PCL in the range of ca. 100 nm. Furthermore, the polyester suspension (15 mg mL^{-1}) was studied by dynamic light scattering (DLS), revealing that the spherical structures possessed a hydrodynamic radius of 201 nm (**Figure 11c**).

To measure hydrophilicity/hydrophobicity properties of branched PCL_T-*b*-PLLA/PCL and linear PEG-b-PLLA/PCL, the water contact angle was conducted on films obtained from the casting of polymer monoliths. The contact angle value of water obtained is listed in **Table 1**. The contact angle of water of PLLA/PCL blends (BnOH-initiated) is 71°,[26] while for PEG-*b*-PLLA/PCL sample, the presence of PEG provides hydrophilic properties, as evidenced by a slightly lower contact angle value of 56° (**Inset Figure 12c and 12d respectively**).

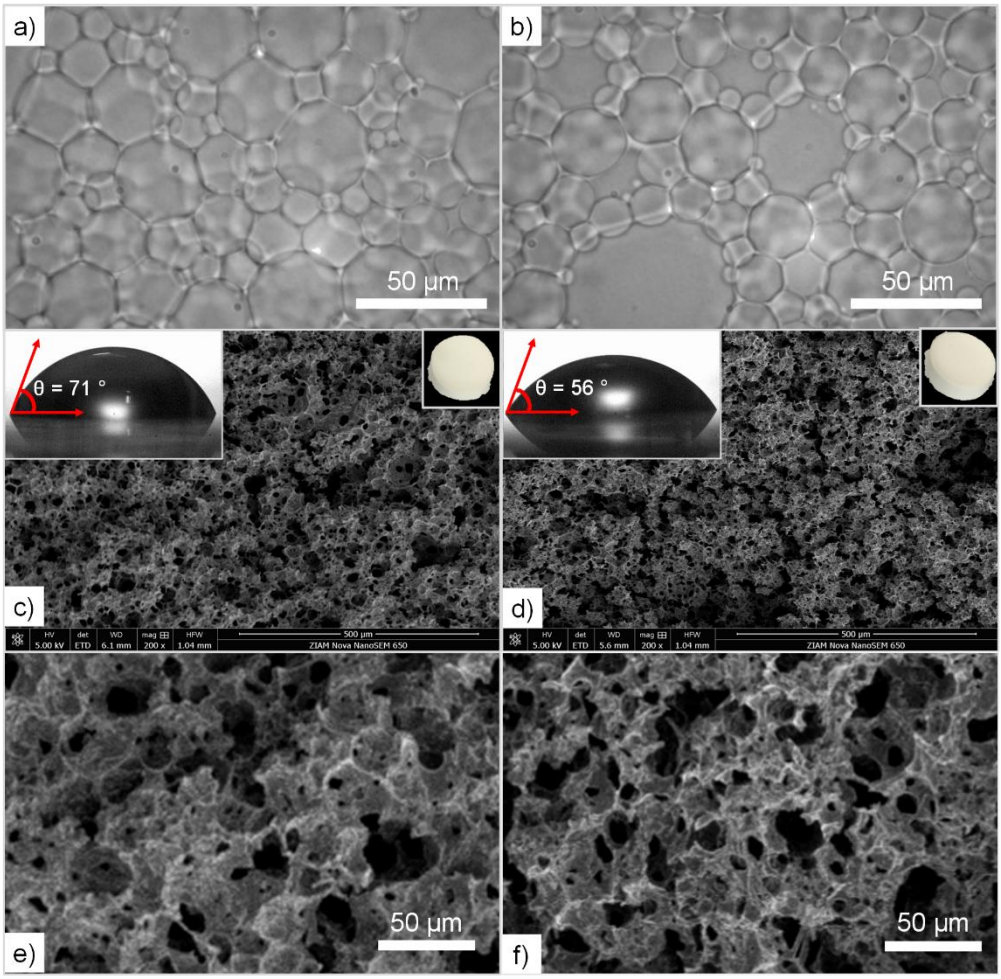

Figure 12. Optical micrographs of HIPEs containing different macroinitiators for the ROP of the continuous phase: (a) PCL_T and (b) PEG. SEM micrographs of polyHIPEs after extraction of the internal phase: (c) PH(branched PCL_T-*b*-PLLA/PCL), and (d) PH(linear PEG-*b*-PLLA/PCL); inset upper left side shows the water contact angle on polyHIPEs, and inset upper right side shows images of monoliths after purification. SEM micrographs at higher magnification of (e) PH(branched PCL_T-*b*-PLLA/PCL), and (f) PH(linear PEG-*b*-PLLA/PCL).

Conversely, the presence of PCL_T in the PCL_T-*b*-PLLA/PCL results in a more hydrophobic material because of the inherent properties of PCL, with a contact angle value of 71° (**Inset Figure 12c**). These results indicate that the macroinitiators can be utilized for tuning the hydrophilic characteristics of the polyesters either in bulk or as part of polyHIPEs as will be discussed in the next sections.

4.3.4 Synthesis of macroporous polyesters

PLLA and PCL polyesters are hydrophobic materials, which makes them suitable sorbents for the efficient separation of hydrophobic fluids from water, providing a porous structure is attained.[36,37] In this regard, Perez Garcia *et al*.,[19] reported the synthesis of degradable and macroporous 3D polymers by taking advantage of the liquid nature of LLA_{30}-CL_{70} DESm to formulate nonaqueous oil-in-DESm HIPEs. The ROP of the continuous phase and subsequent removal of the internal phase allows the preparation of degradable and macroporous 3D polymer replicas. In the same line, the synthesis of macroporous nanocomposites by incorporating non-functionalized nanohydroxyapatite exposed on their inner surface was reported.[39]

Herein, HIPEs were formulated with the LLA_{30}-CL_{70} DESm, containing PEG and PCL_T as macroinitiators, and Pluronic® F127 as surfactant to stabilized the oil-in-DESm emulsion, all composing the continuous phase, 20 vol% of the total emulsion.[19] The final product after *n*-hexane/ethanol purification and removal of the internal phase (tetradecane) and surfactant, appeared as white solids monoliths with a diameter of 12mm, and height of 7mm. (top right insets **Figure 12c** and **d**) and were named as PH(branched PCL_T-*b*-PLLA/PCL) and PH(linear PEG-*b*-PLLA/PCL), referring to the macroinitiator used in the ROP (PCL_T or PEG).

The morphology of the obtained HIPEs consists of polyhedral and polydisperse close-packed droplets (30 ± 2μm), separated by a characteristic thin film of continuous phase which macroscopically behave as highly viscous emulsions that do not flow upon inversion of the containing vials. Optical microscopy images of the obtained HIPEs are shown in **Figure 12a and b**.

The basic insights into the ROP of LLA_{30}-CL_{70} DESm using macroinitiators such as hydrophobicity, diffusion, or molecular weight of the final polyesters studied previously in bulk, served as the basis for the synthetic conditions translatable to polymerization of HIPEs. Therefore, the sequential ROP of the DESm catalyzed by DBU and MSA was followed for the ROP of the HIPEs, yielding high conversions of ca. 95 and 96% for PH(PCL_T-*b*-PLLA/PCL) and PH(linear PEG-*b*-PLLA/PCL), respectively, which is similar to the conversions achieved with the same DESm-based HIPEs but initiated with BnOH (94%).[19] **Figure 12c, d e, and f,** show the SEM images of the internal morphology of fractured monoliths after gold sputtering. The macroporous structure of the PH(branched PCL_T-*b*-PLLA/PCL) and PH(linear PEG-*b*-PLLA/PCL) consists of an interconnected pore network (33 - 42 ± 2 μm), similar in size to the droplet diameter of the parent emulsion, in the case of PH(linear PEG-*b*-PLLA/PCL), see in **Table 3**.

Table 3. Structural morphologies of PH(branched PCL_T-*b*-PLLA/PCL) and PH(linear PEG-*b*-PLLA/PCL).

Sample	Droplet diameter (μm)	Pore diameter (μm)	Pore throat (μm)
PH(branched PCL_T-*b*-PLLA /PCL)	30 ± 2	42 ± 2	12.0
PH(linear PEG-*b*-PLLA /PCL)	30 ± 2	33 ± 2	7.9

The HIPEs exhibited satisfactory shelf-life stability before the polymerization, allowing for the successful execution of the process. Both emulsions demonstrated adequate stability, enabling the ROP. Herein, ROP of the HIPEs led in a larger pore size in the case of PH(PCL_T-*b*-PLLA/PCL) (**Table 4)**. In contrast, PH(linear PEG-*b*-PLLA/PCL) exhibited better emulsion stability and less degree of openness. The presence of PEG block in the copolymer improved emulsion stability during polymerization thanks to its amphiphilic and self-assembling properties demonstrated above, which effectively prevented the emulsion from collapsing. Finally, the resulting δ_b and V_T values were similar for PH(branched PCL_T-*b*-PLLA/PCL) and PH(linear PEG-*b*-PLLA/PCL) consistent with other porous polyesters reported in the literature.[19,40]

^{1}H NMR spectra of PH(branched PCL$_T$-*b*-PLLA/PCL and PH(linear PEG-*b*-PLLA/PCL) is shown in **Figure 13**, and similar signals to the polyesters resulting from the ROP in bulk (PCL$_T$-*b*-PLLA/PCL and linear PEG-*b*-PLLA/PCL) were identified. The presence of PLLA blocks in branched PLLA or linear PEG-*b*-PLLA copolymers, and PCL homopolymer, was confirmed by the appearance of the characteristic peak at H_e, H_d for PLLA, H_a and H_b for PCL, as mentioned in section *4.3.1*.

Interestingly, the surfactant Pluronic® F-127 remained in PH(PCL$_T$-*b*-PLLA/PCL and PH(linear PEG-*b*-PLLA/PCL), as confirmed by the peak at 3.66 ppm (-C**H**$_2$-). Its presence was likely caused by the chains entangled in the branched PLLA and promoted by their affinity for the PEG, which was present in the linear PEG-*b*-PLLA copolymer.

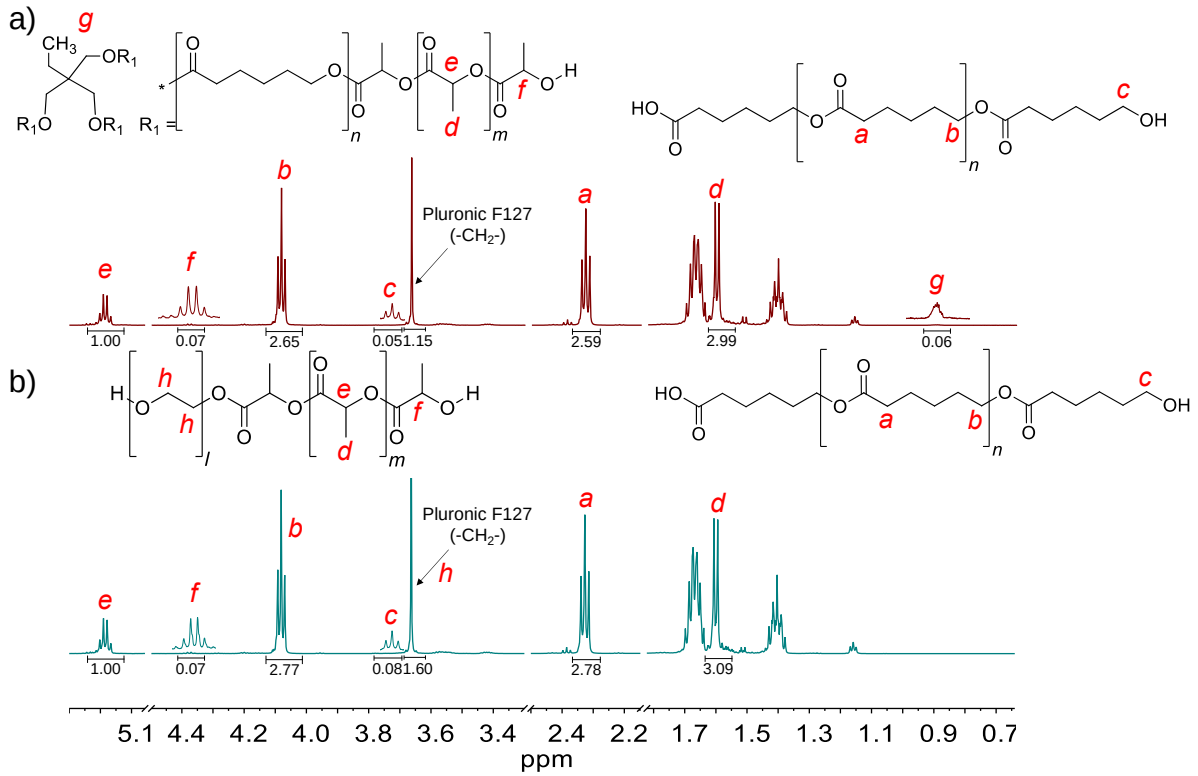

Figure 13. ^{1}H NMR spectra of polyHIPEs for (a) PH(branched PCL$_T$-*b*-PLLA/PCL), and (b) PH(linear PEG-*b*-PLLA/PCL).

^{13}C NMR spectra of PH(PCL$_T$-*b*-PLLA/PCL and PH(linear PEG-*b*-PLLA/PCL) also confirm PCL and PLLA ester groups corresponding to the carbon peaks C_1 =173 and C_8 = 169 ppm, respectively, and the peak at 70 ppm corresponding to (-**C**H$_2$-) group of the surfactant Pluronic® F-127 (**Figure 14**).

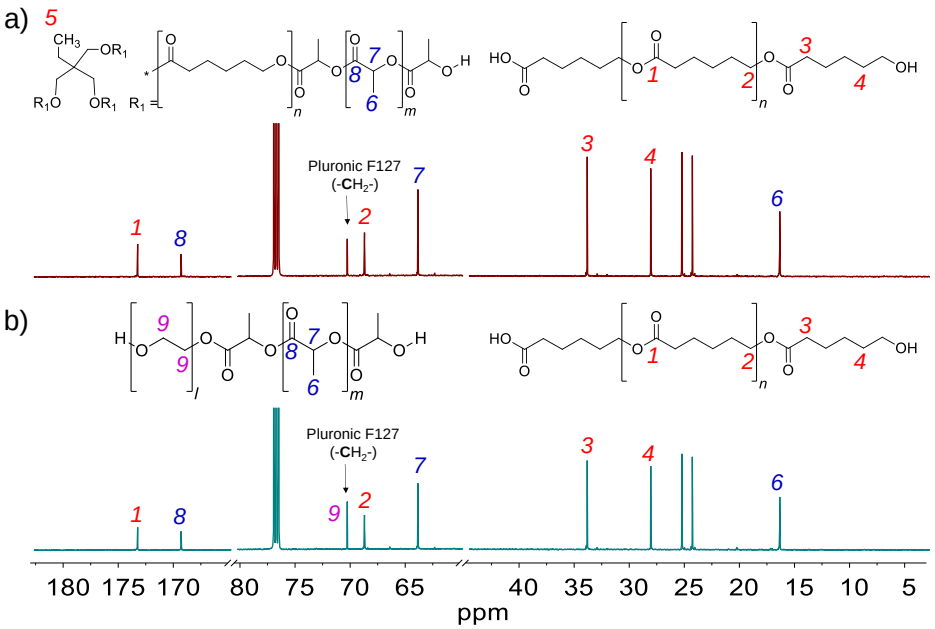

Figure 14. ^{13}C NMR spectra (a) PH(branched PCL$_T$-*b*-PLLA/PCL) and (b) PH(linear PEG-b-PLLA/PCL).

The mol fraction (F_i) of PLLA and PCL blocks in PH(branched PCL$_T$-*b*-PLLA/PCL and PH(linear PEG-*b*-PLLA/PCL), was calculated by ^{1}H NMR spectroscopy (**Table 4, Equations (1-3)** which also correspond to F_i of polyesters obtained in bulk.

The thermal behavior of the PH(branched PCL$_T$-*b*-PLLA/PCL) and PH(linear PEG-*b*-PLLA/PCL) were recorded during the first heating run (**Figure 15** and **Table 4**). The T_m of PLLA is higher in PH(linear PEG-*b*-PLLA/PCL) than that of linear PEG-*b*-PLLA/PCL obtained in bulk. The residual surfactant within the polyHIPE contributes to the increment in the melting point due to a favorable interaction with PLLA. In this regard, Athanasoulia *et al.*[37] observed an improvement in the melting point of PLLA in the presence of PEG at different ratios.

Table 4. Structural morphologies, molecular weight (M_n), and melting point (T_m) of PH(branched PCL_T-*b*-PLLA/PCL) and PH(linear PEG-*b*-PLLA/PCL).

Sample	F_{PLLA}:F_{PCL}[a]	Degree of Openness[b] (%)	δ_b[c] (g cm^{-3})	V_T[d] (cm^{-3} g)	M_n (g mol^{-1})[e]		T_m (ºC)[f]	
					PLLA	*PCL*	*PLLA*	*PCL*
PH(branched PCL_T-*b*-PLLA/PCL)	38:62	14	0.290	3.4	2 059	7 716	131	59
PH(linear PEG-*b*-PLLA/PCL)	42:58	10	0.281	3.6	2 059	7 904	133	60

[a] Mole fraction of monomers (F_i, were i = PLLA or PCL) was obtained by ^{1}H NMR by the **Equation (1-3)**.

[b] Degree of openness was estimated using the **Equation (7-10)** proposed by Pulko and Krajnc.[20]

[c] δ_b, monolith density

[d] V_T, total pore volume.

[e] M_n obtained by ^{1}H NMR.

[f] Thermal properties calculated by DSC.

Equations. PolyHIPE openness were estimated using by equation proposed by Pulko and Krajnc.[20]

In the sample PH (linear PEG-*b*-PLLA/PCL), the endothermic peaks were barely perceptible. However, the higher peak is attributed to the melting point of the PLLA blocks, which, in our case, was 133 °C, higher than the bulk counterpart. These results were obtained from the collective effect of PEG in the macroinitiator and the additional surfactant. However, the T_m of the surfactant (ca. 56 °C) in **Figure 15a** is not visible, suggesting that the surfactant chains were embedded in the polyester matrix thus overlapping with the thermal events of the polyesters.

Figure 15b displays the XRD patterns, where the PEG peaks may overlap with the PLLA and PCL patterns confirming a possible entanglement with the polyester´s chains. SEC traces of PH(branched PCL_T-*b*-PLLA/PCL) and PH(linear PEG-*b*-PLLA/PCL) were both observed as broad peaks with an additional peak at low elution times, consistent with the surfactant Pluronic® F-127 in the samples (**Figure 16**).

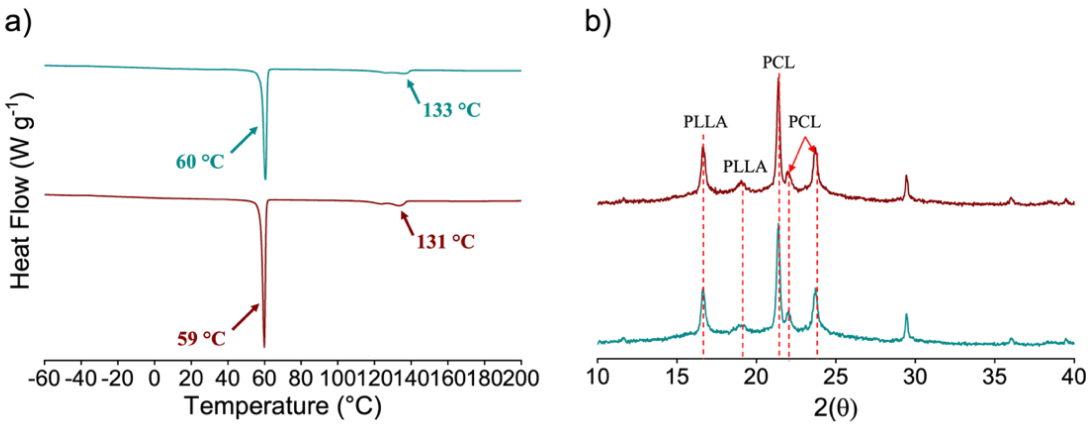

Figure 15. (a) DSC thermograms during the first heating cycle and (b) XRD pattern of PH(branched PCL_T-*b*-PLLA/PCL) [red]; and PH(linear PEG-*b*-PLLA/PCL) [blue] polyHIPES.

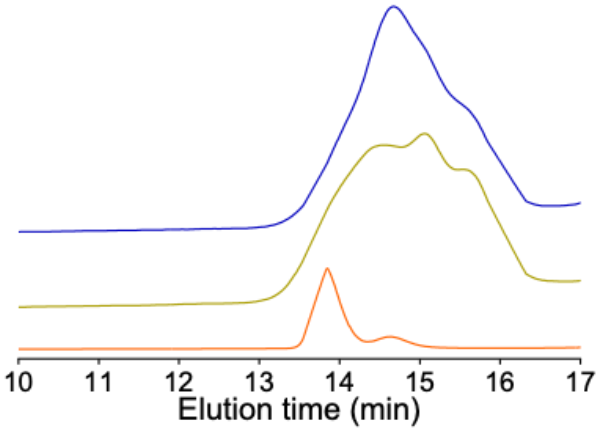

Figure 16. SEC scans of PH(branched PCL_T-*b*-PLLA/PCL) [blue]; PH(linear PEG-*b*-PLLA/PCL) [yellow]; and Pluronic® F-127 [orange].

4.3.5 Degradability test

We successfully obtained PH(branched PCL_T-*b*-PLLA/PCL) and PH(linear PEG-*b*-PLLA/PCL) macroporous polyesters, which were primarily composed of a blend of PCL homopolymer with their corresponding branched PCL_T-*b*-PLLA or linear PEG-*b*-PLLA, respectively.

These materials possess desirable properties such as biodegradability and biocompatibility due to the constituent polymers PCL, PLLA, and PEG blocks, along with the eco-friendly synthesis routes utilized. To assess the degradability of PH(branched PCL_T-*b*-PLLA/PCL and PH(linear PEG-*b*-PLLA/PCL), in vitro degradation profile tests were performed. The degradation assay of PH(branched PCL_T-*b*-PLLA/PCL) and PH(linear PEG-*b*-PLLA/PCL) was performed in parallel with the porous polyester composed by PLLA and PCL homopolymer blends, namely PH(PLLA/PCL).

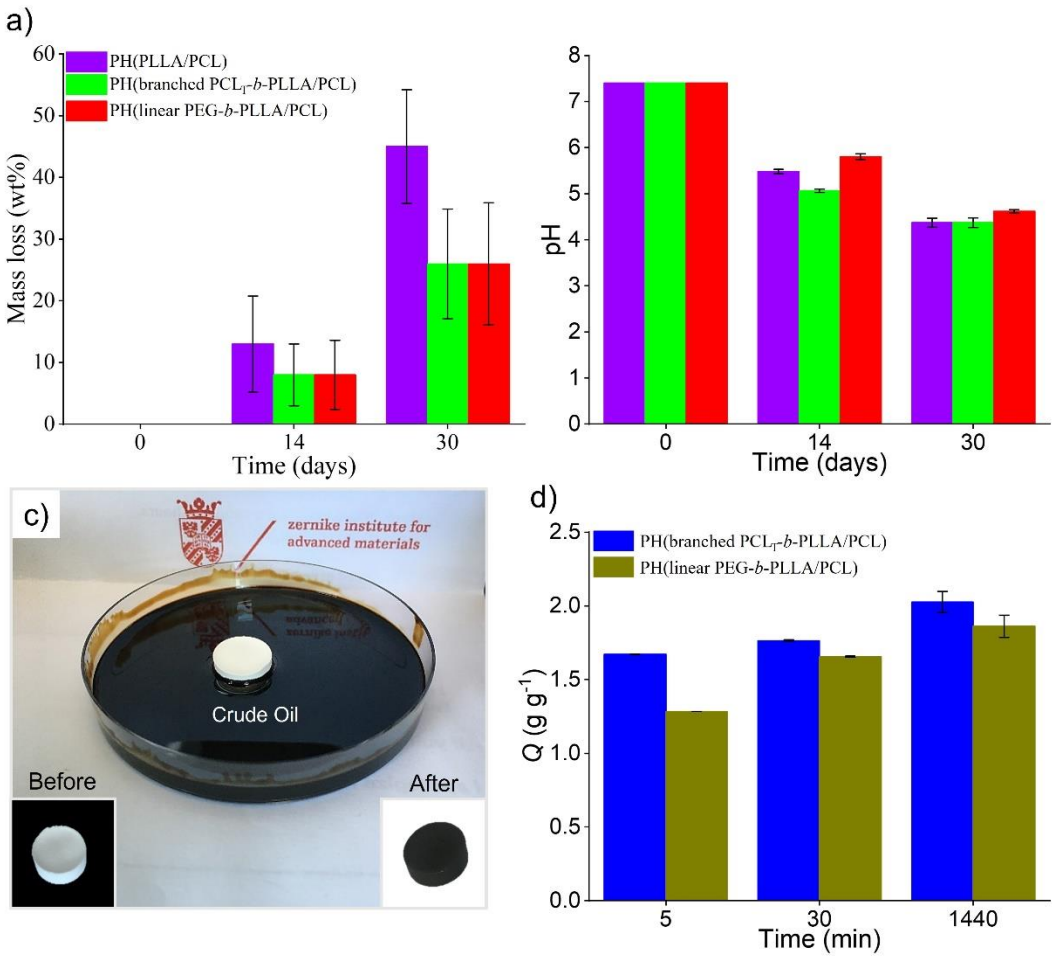

Figure 17. (a) Mass loss (wt%) and (b) pH values of PBS solution profiles degradations of the samples for 14 and 30 days at 37 °C of PH(PCL-PLLA), PH(branched PCL_T-*b*-PLLA/PCL) and PH(linear PEG-*b*-PLLA/PCL) polyHIPES. (c) Photographs of crude oil absorption (monolith before and after the test, left and right inset, respectively) (d) Oil absorption capacity using PH(branched PCL_T-*b*-PLLA/PCL) and PH(linear PEG-*b*-PLLA/PCL).

Degradation in polyesters in aqueous media can be caused by physical erosion or by cleavage of hydrolytic labile ester bonds. The latter shows an autocatalytic effect due to the hydrolysis of their acidic byproducts, which further accelerates the degradation process. **Figure 17a** illustrates the mass loss of the porous polyesters PH(branched PCL_T-*b*-PLLA/PCL), PH(linear PEG-*b*-PLLA/PCL) and PH(PLLA/PCL) after 14 and 30 days of the degradation assay. The degradation profile showed that the mass loss for all samples at 14 days and 30 days is 10% and 50% for PH(PLLA/PCL), respectively. While for PH(branched PCL_T-*b*-PLLA/PCL), PH(linear PEG-*b*-PLLA/PCL), the mass loss is 30% after 30 days.

Polyester mass loss is primarily due to physical erosion, and factors such as polymer architecture, molecular weight, hydrophobicity can alter the degradation profile. Therefore, the presence of branched PCL_T-*b*-PLLA or linear PEG-*b*-PLLA copolymer in PH(PCL_T-*b*-PLLA/PCL) and PH(linear PEG-*b*-PLLA/PCL), respectively, reduced erosion by improving the compatibility of the blends constituents.[41] The mass loss in polyesters was also accompanied by hydrolytic degradation due to acidification of the medium (initial pH of 7.4) causing a decrease of the pH to 4.5 as expected. PH(PCL_T-*b*-PLLA/PCL) and PH(linear PEG-*b*-PLLA/PCL) presented lower mass loss than sample PH(PLLA/PCL) after 30 days (**Figure 17b**). The presence of branched PCL_T-*b*-PLLA or the PEG block in the porous materials provided a higher compatibility among the polyester constituents confined within the thin layers of the porous structure, which was a replica of the high internal phase emulsion (HIPE). Consequently, the degradation rate of PCL and PEG is lower than that of PLLA. Therefore, the increase in the PCL content and the addition of PEG would retard degradation, resulting in decreased pH and exhibited lower mass loss, compared to PH(PLLA/PCL). Additionally, we also observed that PH(branched PCL_T-*b*-PLLA/PCL) and PH(linear PEG-*b*-PLLA/PCL) monoliths were able to maintain their structures after 30 days of the degradation test, whereas PH(PLLA/PCL) structure collapsed at the end of the test (**Figure 18**).

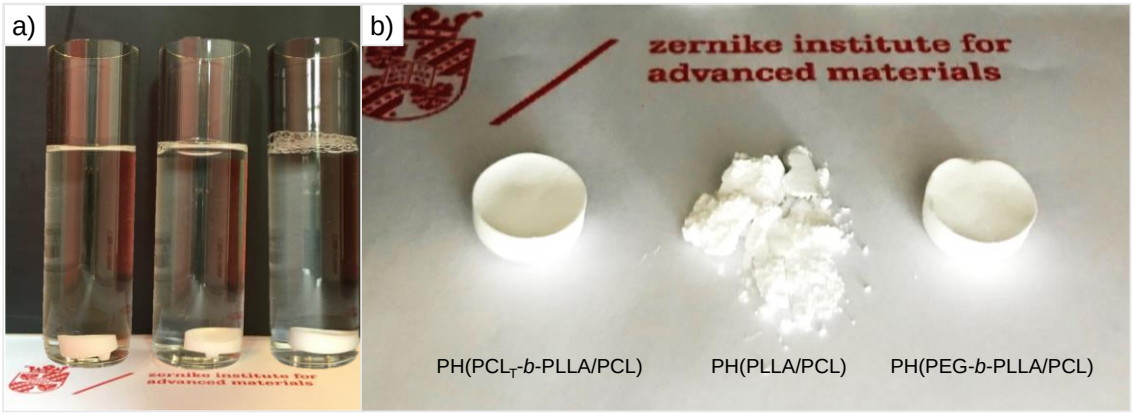

Figure 18. (a) PH(branched PCL$_T$-*b*-PLLA/PCL), PH(PLLA/PCL) and PH(linear PEG-*b*-PLLA/PCL) samples, respectively, placed in PBS solution first day. (b) Dried samples after 30 days of degradation test.

4.3.6 Oil adsorption

Macroporous polyesters, such as PH(PLLA/PCL), have been previously reported for removing hydrocarbons from water.[19] Other porous materials have also been utilized to remove various contaminants from water, such as oil spills.[15] However, addressing oil spill issues is complex and requires different methods for different scenarios, each with its own cost and time requirements, including environmental impact assessment. Although different materials have been used for crude oil removal, it is necessary to have different alternatives that preferably can be combined to improve their performance. In contrast to toxic and non-biodegradable materials currently being used, the importance of developing non-toxic and biodegradable materials for oil spill treatment cannot be overstated.[6,42]

Additionally, the vast majority of sorbents have some drawbacks in terms of lack of degradability; after fulfilling their function, they become another source of waste.[19] Thus, the development of degradable sorbents is current need, PH(branched PCL$_T$-*b*-PLLA/PCL) and PH(linear PEG-b-PLLA/PCL) porous polyesters, and synthesized without metal catalysts and at low temperature, represent a suitable class of sorbent materials for crude oil. Although some other porous polymers have been reported in the literature, the majority are not degradable;[40] for this reason, the porous polyesters suggested in this project constitutes a greener alternative.

The crude oil sorption test was performed as shown in **Figure 17c**. The capacities of crude oil sorption (*Q*), of PH(branched PCL_T-*b*-PLLA/PCL) and PH(linear PEG-*b*-PLLA/PCL), (*Q*, which represents the mass of crude oil after sorption per gram of dry monolith) were observed to be 1.86 ± 0.075 and 2.03 ± 0.071 g g^{-1} after 30 min and 1 440 min. (**Figure 17d**), respectively. Previous values were close as reported from chitosan aerogels or leaves residues which were apply as adsorbents for oily water.[11] The sorption process is the accumulation of sorbate on the internal surface and occurs through two phenomena: *i)* the internal diffusion onto the surface and *ii)* the retention of the oil molecules by capillarity.

PH(branched PCL_T-*b*-PLLA/PCL) sample had a higher degree of openness (**Table 4**), and the diffusion rate and retention capacity were higher in comparison to PH(linear PEG-*b*-PLLA/PCL). It is evident from the results that these materials, with their hydrophobic characteristics and significant surface area, have the capability to rapidly absorb crude oil, achieving a minimum absorption of 1 g g^{-1} within 5 minutes and potentially reaching up to 2 g g^{-1} in 24 hours. Nonetheless, further investigations into the absorption kinetics would provide valuable insights for a more comprehensive understanding of this rapid process. PH(branched PCL_T-*b*-PLLA/PCL) and PH(linear PEG-*b*-PLLA/PCL) an absorption capacity for crude oil, with a performance comparable to that of other biodegradable materials already reported in the literature such as Kapok fibers, lignin, cellulose foam, cotton, etc.[6] As previously discussed, the intrinsic biodegradability and high porosity of these materials, make them promising for potential applications in oil spills. They have been observed to degrade with a mass loss of approximately 30% in 30 days, indicating their prospective full compostability. Lastly, once they have fulfilled their function of absorbing oil, no additional steps would be necessary for their separation, and their components could become part of the final oil products.

4.4 Conclusions

In this study, multifunctional macroinitiators, specifically polycaprolactone triol (PCL_T) and polyethylene glycol (PEG), were successfully utilized in the ROP of the LLA_{30}-CL_{70} DESm to produce polyesters of diverse macromolecular architectures. The syntheses were performed at 37 °C through a sustainable approach employing organocatalysts such as DBU and MSA.

The resulting polyesters comprised blends of PCL homopolymer with branched PCL_T-*b*-PLLA or linear PEG-*b*-PLLA block copolymers, depending on the macroinitiator that selectively initiated the LLA in the DESm. These polymers exhibited different diffusion, hydrophobicity, and molecular weights, which are conducive to controlled degradability. The incorporation of macroinitiators in the ROP of LLA_{30}-CL_{70} DESm significantly improved the properties of the resulting polyesters, enabling the preparation of macroporous polyesters through emulsion templating.

Stable HIPEs oil-in-DESm sustained the efficient organocatalyzed ROP of the polymerizable continuous phase at low temperatures, achieving high conversions and yielding macroporous and interconnected polyesters replicas of the emulsions. The obtained macroporous polyesters are degradable while maintaining their macroporous structure for at least 30 days in the *in vitro* degradation test. Additionally, these macroporous materials demonstrated their ability to sorb crude oil, exhibiting competitive sorption capacity figures of 2 g g^{-1}. The bulk polyesters and their corresponding macroporous polyesters obtained through emulsion templating, synthesized using greener ROP under mild temperature conditions, represent alternative materials with promising applications in separation processes, scaffolds for cell culture, and drug delivery.

4.5 References

(1) Melchor-Martínez, E. M.; Macías-Garbett, R.; Alvarado-Ramírez, L.; Araújo, R. G.; Sosa-Hernández, J. E.; Ramírez-Gamboa, D.; Parra-Arroyo, L.; Alvarez, A. G.; Monteverde, R. P. B.; Cazares, K. A. S.; Reyes-Mayer, A.; Lino, M. Y.; Iqbal, H. M. N.; Parra-Saldívar, R. Towards a Circular Economy of Plastics: An Evaluation of the Systematic Transition to a New Generation of Bioplastics., *Polymers.* **2022**, *14*, 1–32.

(2) Nashawi, I. S.; Malallah, A.; Al-Bisharah, M. Forecasting World Crude Oil Production Using Multicyclic Hubbert Model. *Energy and Fuels.*, **2010**, *24*, 1788–1800.

(3) Barron, M. G. Ecological Impacts of the Deepwater Horizon Oil Spill: Implications for Immunotoxicity. *Toxicol. Pathol.*, **2012**, *40*, 315–320.

(4) Owens, E. H.; Reddy, C. M.; Eglinton, T. I.; Hounshell, A.; White, H. K.; Xu, L.; Gaines, R. B.; Frysinger, G. S. Comment on “The West Falmouth Oil Spill after Thirty Years: The Persistence of Petroleum Hydrocarbons in Marsh Sediments.” *Environ. Sci. Technol.*, **2003**, *37*, 2020–2021.

(5) Liu, H.; Wang, C.; Zou, S.; Wei, Z.; Tong, Z. Simple, Reversible Emulsion System Switched by PH on the Basis of Chitosan without Any Hydrophobic Modification. *Langmuir.*, **2012**, *28*, 11017–11024.

(6) Doshi, B.; Sillanpää, M.; Kalliola, S. A Review of Bio-Based Materials for Oil Spill Treatment. *Water Res.*, **2018**, *135*, 262–277.

(7) Evans, D. D.; Mulholland, G. W.; Baum, H. R.; Walton, W. D.; McGrattan, K. B. In Situ Burning of Oil Spills. *J. Res. Natl. Inst. Stand. Technol.*, **2001**, *106*, 231–278.

(8) Teas, C.; Kalligeros, S.; Zanikos, F.; Stournas, S.; Lois, E.; Anastopoulos, G. Investigation of the Effectiveness of Absorbent Materials in Oil Spills Clean Up. *Desalination.*, **2001**, *140*, 259–264.

(9) Azubuike, C. C.; Chikere, C. B.; Okpokwasili, G. C. Bioremediation Techniques–Classification Based on Site of Application: Principles, Advantages, Limitations and Prospects. *World J. Microbiol. Biotechnol.*, **2016**, *32*, 1–18.

(10) Mullin, J. V.; Champ, M. A. Introduction/Overview to in Situ Burning of Oil Spills. *Spill Sci. Technol. Bull.*, **2003**, *8*, 323–330.

(11) Gupta, S.; Tai, N. H. Carbon Materials as Oil Sorbents: A Review on the Synthesis and Performance. *J. Mater. Chem. A.*, **2016**, *4*, 1550–1565.

(12) Sabir, S. Approach of Cost-Effective Adsorbents for Oil Removal from Oily Water. *Crit. Rev. Environ. Sci. Technol.*, **2015**, *45*, 1916–1945.

(13) Wahi, R.; Chuah, L. A.; Ch,oong, T. S. Y.; Ngaini, Z.; Nourouzi, M. M. Oil Removal from Aqueous State by Natural Fibrous Sorbent: An Overview. *Sep. Purif. Technol.*, **2013**, *113*, 51–63.

(14) Yang, X.; Yin, Z.; Zhang, X.; Zhu, Y.; Zhang, S. Fabrication of Emulsion-Templated Macroporous Poly(ε-Caprolactone) towards Highly Effective and Sustainable Oil/Water Separation. *Polymer.*, **2020**, *204*, 122852.

(15) Silverstein, M. S. The Chemistry of Porous Polymers: The Holey Grail. *Isr. J. Chem.*, **2020**, *60*, 140–150.

(16) Pérez-García, M. G.; Carranza, A.; Puig, J. E.; Pojman, J. A.; del Monte, F.; Luna-Bárcenas, G.; Mota-Morales, J. D. Porous Monoliths Synthesized via Polymerization of Styrene and Divinyl Benzene in Nonaqueous Deep-Eutectic Solvent-Based HIPEs. *RSC Adv.*, **2015**, *5*, 23255–23260.

(17) Utroša, P.; Onder, O. C.; Žagar, E.; Kovačič, S.; Pahovnik, D. Shape Memory Behavior of Emulsion-Templated Poly(ε-Caprolactone) Synthesized by Organocatalyzed Ring-Opening Polymerization. *Macromolecules.*, **2019**, *52*, 9291–9298.

(18) Castillo-Santillan, M.; Torres-Lubian, J. R.; Martínez-Richa, A.; Huerta-Marcial, S. T.; Gutierrez, M. C.; Loos, K.; Peréz-García, M. G.; Mota-Morales, J. D. From Polymer Blends to a Block Copolymer: Ring-Opening Polymerization of L-Lactide/ε-Caprolactone Eutectic System. *Polymer.*, **2022**, *262*, 125432.

(19) Pérez-García, M. G.; Gutiérrez, M. C.; Mota-Morales, J. D.; Luna-Bárcenas, G.; Del Monte, F. Synthesis of Biodegradable Macroporous Poly(l -Lactide)/Poly(ϵ-Caprolactone) Blend Using Oil-in-Eutectic-Mixture High-Internal-Phase Emulsions as Template. *ACS Appl. Mater. Interfaces.*, **2016**, *8*, 16939–16949.

(20) Pulko, I.; Krajnc, P. High Internal Phase Emulsion Templating - A Path To Hierarchically Porous Functional Polymers. *Macromol. Rapid Commun.*, **2012**, *33*, 1731–1746.

(21) Coulembier, O. Nucleophilic Catalysts and Organocatalyzed Zwitterionic Ring-Opening Polymerization of Heterocyclic Monomers. In *Organic Catalysis for Polymerisation*; The Royal Society of Chemistry., **2018**; Vol. 31, pp 1–36.

(22) Coulembier, O.; Lemaur, V.; Josse, T.; Minoia, A.; Cornil, J.; Dubois, P. Synthesis of Poly(L-Lactide) and Gradient Copolymers from a L-Lactide/Trimethylene Carbonate Eutectic Melt. *Chem. Sci.*, **2012**, *3*, 723–726.

(23) Elomaa, L.; Teixeira, S.; Hakala, R.; Korhonen, H.; Grijpma, D. W.; Seppälä, J. V. Preparation of Poly(ε-Caprolactone)-Based Tissue Engineering Scaffolds by Stereolithography. *Acta Biomater.*, **2011**, *7*, 3850–3856.

(24) Torcasio, S. M.; Oliva, R.; Montesi, M.; Panseri, S.; Bassi, G.; Mazzaglia, A.; Piperno, A.; Coulembier, O.; Scala, A. Three-Armed RGD-Decorated StarPLA-PEG Nanoshuttle for Docetaxel Delivery. *Biomater. Adv.*, **2022**, *140*, 213043.

(25) Yu, Y.; Pang, Z.; Lu, W.; Yin, Q.; Gao, H.; Jiang, X. Self-Assembled Polymersomes Conjugated with Lactoferrin as Novel Drug Carrier for Brain Delivery. *Pharm. Res.*, **2012**, *29*, 83–96.

(26) Castillo-Santillan, M.; Maniar, D.; Gutierrez, M.; Quiñonez-Angulo, P.; Torres-Lubián, J. R.; Loos, K.; Mota-Morales, J. Low-Temperature and Solventless Ring-Opening Polymerization of Eutectic Mixtures of L-Lactide and Lactones for Biodegradable Polyesters. *ACS Appl. Polym. Mater.*, **2023**, 5, 5110-5121.

(27) Zhang, C.; Lan, Q.; Zhai, T.; Nie, S.; Luo, J.; Yan, W. Melt Crystallization Behavior and Crystalline Morphology of Polylactide/Poly(ε-Caprolactone) Blends Compatibilized by Lactide-Caprolactone Copolymer. *Polymers.*, **2018**, *10*, 1181.

(28) Li, R.; Wu, Y.; Bai, Z.; Guo, J.; Chen, X. Effect of Molecular Weight of Polyethylene Glycol on Crystallization Behaviors, Thermal Properties and Tensile Performance of Polylactic Acid Stereocomplexes. *RSC Adv.*, **2020**, *10*, 42120–42127.

(29) Broz, M. Structure and Mechanical Properties of Poly(L-Lactic Acid)/Poly(ε-Caprolactone) Blends. *Biomaterials.*, **2003**, *24*, 4181–4190.

(30) Yin, G.; Zhao, D.; Wang, X.; Ren, Y.; Zhang, L.; Wu, X.; Nie, S.; Li, Q. Bio-Compatible Poly(Ester-Urethane)s Based on PEG–PCL–PLLA Copolymer with Tunable Crystallization and Bio-Degradation Properties. *RSC Adv.*, **2015**, *5*, 79070–79080.

(31) Zhao, X.; Li, J.; Liu, J.; Zhou, W.; Peng, S. Recent Progress of Preparation of Branched Poly(Lactic Acid) and Its Application in the Modification of Polylactic Acid Materials. *Int. J. Biol. Macromol.*, **2021**, *193*, 874–892.

(32) Han, W.; Liao, X.; Yang, Q.; Li, G.; He, B.; Zhu, W.; Hao, Z. Crystallization and Morphological Transition of Poly(L-Lactide)–Poly(ε-Caprolactone) Diblock Copolymers with Different Block Length Ratios., *RSC Adv.* **2017**, *7*, 22515–22523.

(33) Yang, X.; Liu, S.; Yu, E.; Wei, Z. Toughening of Poly(L-Lactide) with Branched Polycaprolactone: Effect of Chain Length. *ACS Omega* **2020**, *5*, 29284–29291.

(34) Abdelrazek, E. M.; Hezma, A. M.; El-khodary, A.; Elzayat, A. M. Spectroscopic Studies and Thermal Properties of PCL/PMMA Biopolymer Blend. *Egypt. J. Basic Appl. Sci.*, **2016**, *3*, 10–15.

(35) Jayaramudu, T.; Raghavendra, G. M.; Varaprasad, K.; Reddy, G. V. S.; Reddy, A. B.; Sudhakar, K.; Sadiku, E. R. Preparation and Characterization of Poly(Ethylene Glycol) Stabilized Nano Silver Particles by a Mechanochemical Assisted Ball Mill Process. *J. Appl. Polym. Sci.*, **2016**, *133*, 1–8.

(36) Viral Tamboli; Mishra, G. P.; Mitra, A. K. Novel Pentablock Copolymer (PLA-PCL-PEG-PCL-PLA) Based Nanoparticles for Controlled Drug Delivery: Effect of Copolymer Compositions on the Crystallinity of Copolymers and in Vitro Drug Release Profile from Nanoparticles. *Colloid Polym Sci.*, **2013**, *291*, 1235–1245.

(37) Athanasoulia, I. G.; Tarantili, P. A. Preparation and Characterization of Polyethylene Glycol/Poly(L-Lactic Acid) Blends. *Pure Appl. Chem.*, **2017**, *89*, 141–152.

(38) Sedlacek, O.; Bardoula, V.; Vuorimaa-Laukkanen, E.; Gedda, L.; Edwards, K.; Radulescu, A.; Mun, G. A.; Guo, Y.; Zhou, J.; Zhang, H.; Nardello-Rataj, V.; Filippov, S.; Hoogenboom, R., Highly Porous and Drug-Loaded Amorphous Solid Dispersion Microfiber Scaffolds of Indomethacin Prepared by Melt Electrowriting, *Mater. Sci. Eng.*,**2022**, *18*, 2106251.

(39) García-Landeros, S. A.; Cervantes-Díaz, J. M.; Gutiérrez-Becerra, A.; Pelayo-Vázquez, J. B.; Landazuri-Gomez, G.; Herrera-Ordonez, J.; Soltero-Martínez, J. F. A.; Mota-Morales, J. D.; Pérez-García, M. G., Oil-in-eutectic mixture HIPEs co-stabilized with surfactant and nanohydroxyapatite: ring-opening polymerization for nanocomposite scaffold synthesis., *Chem. Commun.*, **2019**, *55*, 12292–12295.

(40) Johnson, D. W.; Langford, C. R.; Didsbury, M. P.; Lipp, B.; Przyborski, S. A.; Cameron, N. R., Fully biodegradable and biocompatible emulsion template polymer scaffolds by thiol-acrylate polymerisation of polycaprolactone macropolymers. *Polym. Chem.*, **2015**, *6*, 7256–7263.

(41) Woodard, L. N.; Grunlan, M. A. Hydrolytic Degradation and Erosion of Polyester Biomaterials. *ACS Macro Lett.*, **2018**, *7*, 976–982.

(42) Adebao, M. O.; Frost, R. L.; Kloprogge, J. T.; Carmody, O.; Kokot, S. J., Porous Materials for Oil Spill Cleanup: A Review of Synthesis and Absorbing Properties. *Porous Mater*. **2003**, *10*, 159–170.

Summary

Polymers have played an essential role in advancing humankind in areas such as agriculture, food, medicine, and telecommunications, mainly due to the versatility of compositions that translate to a wide gamut of properties. Polymers' technological progress has made it possible to improve specific properties such as resistance, durability, and lightness, enabling them to enter various areas that were previously restricted, such as aerospace and the automotive industries. Nevertheless, the poor management of their waste, coupled with their intrinsic properties of long-term degradation as well as the presence of additives, has caused polymers to be one of the primary sources of environmental pollution and health problems. One alternative to solve these issues is substituting current petroleum-based polymers with degradable ones. Examples of degradable and compostable polymers are polyesters such as polylactides and polylactones, whose biocompatibility enables their application in medicine. Due to the higher molecular weights obtained, the preferred mechanism to synthesize polylactides and polylactones is via ring opening-polymerization (ROP). Such a process can be performed in solution or in bulk. In Chapter 1, the environmental and health issues generated by polymers are described, as well as the world production of the main groups of polymers. In the same chapter, the properties, and applications of biodegradable polyesters, mainly polylactides and polylactones, are explained in more detail. Their main synthesis routes, advantages, and disadvantages are also underscored.

The production of polylactides and polylactones is generally performed in the industry by bulk ROP using metal catalysts. Usually, the ROP is effective and moderately sustainable by these routes, although the current trend pursues the replacement of metal catalysts. Organocatalysts are among the alternatives used to replace metal catalysts in some syntheses. However, organocatalysts' disadvantages include their poor thermal stability compared with the current tin-based catalysts. Some polymers have also been synthesized using organocatalysts at mild temperature conditions; nevertheless, they require organic solvents. Thus, ROP involving organocatalysts seeks improvements for their wide implementation. An ideal alternative for polyester synthesis is to produce them in the absence of metal catalysts, at mild temperature conditions, and excluding solvents with null or low toxicity.

Within this context, deep eutectic solvents (DESs) have been reported as a designer family of solvents that can be used for polymer synthesis. In chapter 1, different types of organocatalysts and DESs are discussed, including their classification, properties, advantages and drawbacks, and overall properties. In addition, this section also describes various polymerizations that can be performed using DESs as the reaction media. The application of DES in polymer science extends beyond their function as solvents for polymer synthesis. DES monomers (DESm), whose constituents can play the role of both inert solvent and monomer units, are able to polymerize by different mechanisms aided by catalysts and initiators. As an exciting subset of biodegradable polymers, some polyesters prepared via ROP are no exception, such as polylactide or polylactones.

In this regard, some polyesters can be produced by the ROP of their respective DESm. For instance, the copolymer of poly(L-lactide-*g*-trimethylene carbonate) was obtained by ROP of a DESm composed of L-lactide/trimethylene carbonate, while a homopolymers blend composed of poly(L-lactide) (PLLA) and poly(ε-caprolactone) (PCL) was produced by ROP of DESm comprising LLA/CL. In both cases, it can be highlighted that polymerization was carried out in the absence of solvents and metal catalysts. Furthermore, high conversion rates were obtained at low temperatures and in simple atmospheres. Thus, these works pose DESm as a sustainable alternative for producing biodegradable polyesters.

In chapter 1 we describe the synthesis of different DESm as reported in the literature, using polymerization mechanisms such as free radicals, polycondensation, and ROP. This part emphasizes the synthesis of the well-known PLLA and PCL, which are two biodegradable and biocompatible polyesters. State-of-the-art highlights the advantages of producing them by the ROP from their respective monomers in the form of a DESm. There are many challenges ahead with respect to the ROP of DESm. Examples include the generality of lactones and lactides transformation into DESm, the structure-properties relationships in these DESm, and the particular reaction conditions that allow for their ROP and application as biodegradable building blocks of biomaterials. With the general aim of filling these gaps, this thesis focuses on exploring the properties of a series of polyesters obtained from the ROP of DESm composed of lactides and lactones.

In the following chapters, details on new DESm rationally designed and their specific conditions for their ROP are presented. These DESm take the LLA/CL DESm as starting point and include stereoisomers of lactide and various lactones. Finally, the general kinetics of these ROP and a thorough characterization of their physicochemical properties like molecular weight, molecular architecture, crystallinity, thermal behavior, wettability, and biodegradability resulted from different organocatalysts and temperatures of polymerization are discussed.

The results presented in Chapter 2 revolve around two organocatalysts used for the sequential ROP of LLA/CL DESm. These included 1,8-diazabicyclo[5.4.0]undec-7-ene (DBU) and 1,5-diazabicyclo[4.3.0]non-5-ene (DBN) for LLA, and methanesulfonic acid (MSA) for CL, and benzyl alcohol as initiator. Through the adequate selection of these organocatalysts and mild temperatures, it was possible to modify the properties of PLLA and PCL, such as crystallinity, and molecular weight and architecture, either in the form of homopolymers or block copolymer. Thanks to the adequate selection of the amidine organocatalysts, the ROP of the eutectic mixture composed of LLA/CL could be carried out in a range temperature from 37 ºC to 92 ºC. This chapter also reports the modification of the stereochemistry of PLLA or the molecular weight of PCL by the incorporation of a lactide isomer and the controlled initiation taking advantage of the environmental water in the eutectic mixture, respectively.

The scope of DESm, able to undergo ROP, was then extended by exploring other lactones. In chapter 3, several DESm were produced by mixing LLA with lactones such as δ-valerolactone, δ-hexalactone, and δ-decalactone, providing DESm with different chemical structures. Furthermore, it was shown that the interaction between the DESm counterparts is through the protons of methine in L-lactide with the carbonyl groups of the lactones. Out of the DESm assayed, only LLA/δ-valerolactone (VAL) DESm produced polyesters with high conversions under the proposed conditions. Polymerization was carried out using DBU, DBN and MSA as organocatalysts and benzyl alcohol as initiator.

The final polyesters comprising mixtures of PLLA and poly-δ-valerolactone (PVAL) homopolymers exhibited properties such as hydrophobicity, crystallinity, and molecular weights that differed from the PLLA-PCL polyesters mentioned in chapter 2, thus expanding the palette of polyesters obtained through ROP of DESm. To enhance the final properties of PLLA/PCL, like the molecular weight and molecular architecture, in chapter 4, we introduced multifunctional macroinitiators, namely polyethylene glycol (PEG) and polycaprolactone triol (PCL-triol) in place of benzyl alcohol previously studied. PEG and PCL-triol served as efficient initiators of the LLA, yielding block copolymers in the case of PEG of 6000 $gmol^{-1}$, and branched copolymers in the case of PCL-triol with average Mn 900 $gmol^{-1}$. The resulting final polyesters comprised either a PLLA/PEG block copolymer or a poly(L-lactide) branched with the PCL-triol, which were blended with PCL coming from the ROP of CL counterpart of LLA in the DESm precursor. The two PLLA systems in the form of copolymer or branched PLLA together with PCL presented different properties, such as hydrophobicity and molecular weight, a consequence of the macroinitiators (PEG or PCL-triol) integrated into the PLLA chain.

The knowledge generated on the DESm and their ROP to produce polyesters with controlled molecular weight, crystallinity, polymer architecture, hydrophobicity, and degradability, was used to formulate stable high internal phase emulsions (HIPEs), oil-in-DESm, with the aid of a surfactant. The ROP of the continuous phase comprising the LLA/CL DESm and macroinitiators (PEG or PCL-triol), and subsequent removal of the internal phase, gave rise to macroporous and interconnected 3D self-standing polyesters (polyHIPEs). In addition, these porous materials showed mechanical stability for at least 30 days in a degradation assay in PBS solution under simulated physiological conditions, at pH 7.4 and 37 °C, and is estimated to fully degrade. Interestingly, thanks to their hydrophobicity and suitable surface area throughout the interconnected macroporosity, the polyHIPEs showed excellent performance in absorbing crude oil with a rate of 2 g g^{-1} at room temperature.

In summary, in this thesis, we demonstrate that it is feasible to modify the properties of polyesters obtained from the ROP of different DESm composed of lactides and lactones, which have not been reported in the literature.

The properties of the polyesters obtained by the ROP of DESm result from the interplay of the fine selection of the monomers composing the DESm, including macroinitiators and organocatalysts, and synthetic conditions, such as temperature and water content. ROP of DESm stands out as a sustainable alternative to obtain polyesters since metallic catalysts and volatile organic solvents are excluded.

In addition, a variety of polyester architectures can be obtained at mild temperature conditions, where the final products do not require complicated purification steps to remove the organocatalysts. Finally, the viscosity and polarity of eutectic mixtures of lactones and lactides are exploited to prepare macroporous, interconnected, and polyesters by emulsion templating via nonaqueous HIPEs. These findings are a significant advance in the path of the development of greener protocols for the creation of membranes or scaffolds composed of polyesters. The ROP of DESm carried out at low temperatures and in solventless conditions holds promise for a sustainable framework in preparing polymers which could be applied in some biomedical applications and separation technologies.

Resumen

Los polímeros han desempeñado un papel esencial en el avance de la humanidad en áreas como la agricultura, la alimentación, la medicina y las telecomunicaciones, y esto se debe principalmente a la versatilidad de sus propiedades, que se trasladan a una amplia gama de propiedades. El avance de la tecnología en los polímeros ha permitido mejorar propiedades específicas como resistencia, durabilidad y ligereza, lo que les ha permitido entrar en diversas áreas que antes estaban restringidas, como en la industria aeroespacial y automotriz. Sin embargo, la escasa gestión de sus residuos, junto con la propiedad intrínsecas de procesos de degradación a largo plazo, y la presencia de aditivos, ha provocado que los polímeros sean una de las principales fuentes de contaminación ambiental y de problemas de salud. Una alternativa para resolver estos problemas es mediante la sustitución de los polímeros actuales que son derivados del petróleo por otros biodegradables, actualmente estos representan el 1% de la producción total de polímeros. Ejemplos de polímeros biodegradables son los poliésteres, como las polilactidas y las polilactonas, cuya biocompatibilidad permite su aplicación en medicina. El mecanismo preferido para sintetizar polilactidas y polilactonas es la mediante la polimerización por apertura de anillo (ROP, ring-opening polymerization por sus siglas en inglés), debido a que se obtienen mayores pesos moleculares. Este proceso puede realizarse en solución o en bulto. En el Capítulo 1, se describen los problemas medioambientales y de salud generados por los polímeros, así como la producción mundial de los principales grupos de polímeros. En el mismo capítulo, se explican con más detalle las propiedades y aplicaciones de los poliésteres biodegradables, principalmente polilactidas y polilactonas. También se mencionan las principales rutas de síntesis, así como sus ventajas y desventajas.

La producción de polilactidas y polilactonas se realiza generalmente en la industria mediante ROP en bulto y mediante el uso de catalizadores metálicos. En general, la ROP es un mecanismo eficaz y moderadamente sostenible, aunque la tendencia actual busca la sustitución de los catalizadores metálicos. Los organocatalizadores se encuentran como alternativas para sustituir a los catalizadores metálicos en algunas síntesis. Sin embargo, una desventaja de los organocatalizadores se encuentra su baja estabilidad térmica en comparación con los catalizadores actuales con los derivados de estaño.

También se han sintetizado algunos polímeros utilizando organocatalizadores en temperaturas ambientales; sin embargo, requieren disolventes. Así pues, la ruta de la ROP con organocatalizadores busca ampliar sus aplicaciones. Una alternativa sostenible para la síntesis de poliésteres es producirlos sin catalizadores metálicos, en condiciones de temperatura suaves y utilizando disolventes de nula o escasa toxicidad.

En este contexto, las mezclas eutécticas profundas (DES, por sus siglas en inglés deep eutectic solvents) se han considerado una familia de disolventes que pueden utilizarse para la síntesis de polímeros. En el capítulo 1, se analizan distintos tipos de organocatalizadores y DES, incluyendo su clasificación, propiedades, ventajas e inconvenientes y así como sus propiedades generales. Además, en esta sección también se describen diversas polimerizaciones que pueden realizarse utilizando DES cuando funge como medio de reacción. La aplicación de los DES en la ciencia de los polímeros va más allá funcionar como disolventes para la síntesis de polímeros. Los llamados DES monómeros (DESm), cuyos constituyentes pueden desempeñar el papel tanto de disolvente inerte como monómeros, y son capaces de polimerizar mediante diferentes mecanismos ayudados por catalizadores e iniciadores. Los poliésteres preparados mediante la ROP constituyen un interesante subconjunto de polímeros biodegradables. En este sentido, algunos poliésteres pueden producirse mediante la ROP de sus respectivos DESm. Por ejemplo, el copolímero de poli(L-lactida-*g*-trimetilencarbonato) se obtuvo por la ROP de un DESm compuesto de L-lactida y trimetilencarbonato, así mismo se obtuvo la mezcla de homopolímeros compuesta de poli(L-lactida) (PLLA) y poli(ε-caprolactona) (PCL) mediante la ROP del DESm compuesto por LLA/CL (L-lactida y ε-caprolactona, respectivamente). En ambos casos, es importante destacar que la polimerización se llevó a cabo en ausencia de disolventes y de catalizadores metálicos. Además, se obtuvieron altas tasas de conversión a bajas temperaturas y en atmósferas sencillas. Así, estos trabajos plantean a los DESm como una alternativa sostenible para producir poliésteres biodegradables. En la primera sección se describe la síntesis de diferentes DESm (también se conocen como mezclas eutécticas polimerizables) descritos en la bibliografía, mediante mecanismos de polimerización por radicales libres, policondensación y por ROP. Esta parte hace hincapié en la síntesis de los poliésteres muy estudiados, polilactida (PLA) y policaprolactona (PCL), que además son biodegradables y biocompatibles.

El estado del arte resalta las ventajas de producirlos mediante ROP a partir de sus respectivos monómeros cuando forman parte de DESm. Hay muchos desafíos con respecto a la ROP de los DESm. Por ejemplo, las diferentes combinaciones de lactonas y lactidas para producir un DESm, estudiar las relaciones entre estructura y propiedades en estos DESm, así como las condiciones específicas de reacción que permitan su ROP e incluido su aplicación en el diseño de bloques para la construcción biomateriales biodegradables. Con el objetivo general de cubrir estas brechas, esta Tesis se centra en explorar las propiedades de una serie de poliésteres obtenidos a partir de la ROP de DESm compuestos por lactidas y lactonas. En los capítulos siguientes, se presentan detalles de nuevos DESm diseñados racionalmente, incluido sus condiciones para su ROP. Estos DESm se basan en el DESm de LLA/CL también se incluyen estereoisómeros de lactida con diversas lactonas. Por último, se analiza sus cinéticas de cada una de su ROP, así como su caracterización de sus propiedades fisicoquímicas como el peso molecular, la arquitectura molecular, la cristalinidad, el comportamiento térmico, la hidroafinidad y la biodegradabilidad resultante de diferentes organocatalizadores y temperaturas de polimerización.

Los resultados en el Capítulo 2 se enfocan a dos organocatalizadores utilizados para la ROP secuencial de LLA/CL DESm. Estos incluían 1,8-diazobiciclo[5.4.0]undec-7-eno (DBU) y 1,5-diazobiciclo[4.3.0]non-5-eno (DBN) para LLA, ácido metanosulfónico (MSA) para la CL, y alcohol bencílico como iniciador. Mediante la adecuada selección de estos organocatalizadores y a bajas temperaturas, fue posible modificar las propiedades de la poli(L-lactida) PLLA y el PCL, como la cristalinidad, peso y arquitectura molecular, ya sea en forma de homopolímeros o de copolímeros en bloque. También debido a la adecuada selección de los organocatalizadores (amidina), la ROP de la mezcla eutéctica compuesta por LLA/CL pudo llevarse a cabo en un rango de temperaturas de 37 ºC a 92 ºC.

En este capítulo también se incluye la modificación de la estereoquímica de la PLLA o el peso molecular de la PCL mediante la incorporación de isómeros de lactida y la iniciación controlada aprovechando el agua ambiental de la mezcla eutéctica, respectivamente. Más adelante, se amplió el alcance de los DESm, en los que puede realizarse la ROP, mediante la incorporación de otras lactonas.

En el capítulo 3, se produjeron varios DESm mezclando LLA con lactonas como δ-valerolactona, δ-hexalactona y δ-decalactona, obteniendo DESm con diferentes estructuras químicas. Además, se demostró que la interacción entre los DESm homólogos se produce a través de los protones del metil en la L-lacttida con los grupos carbonilo de las lactonas. De los DESm ensayados, sólo el DESm LLA/δ-valerolactona (VAL) produjo poliésteres con altas conversiones en las condiciones propuestas. La polimerización se llevó a cabo utilizando DBU, DBN y MSA como organocatalizadores y alcohol bencílico como iniciador. Los poliésteres finales, compuestos por mezclas de homopolímeros de PLLA y poli-δ-valerolactona (PVAL), presentaban propiedades tales como hidrofobicidad, cristalinidad y pesos moleculares diferentes a los poliésteres de PLLA-PCL mencionados en el capítulo 2, ampliando así la serie de poliésteres obtenidos mediante ROP de DESm.

Para optimizar las propiedades de PLLA/PCL, como el peso y la arquitectura molecular, en el capítulo 4 incluimos macroiniciadores multifuncionales, concretamente polietilenglicol (PEG) y policaprolactona triol (PCL-triol) en lugar del alcohol bencílico estudiado anteriormente. El PEG y el PCL-triol sirvieron como iniciadores eficientes de la LLA, dando lugar a copolímeros en bloque en el caso del PEG de 6000 g mol^{-1}, y a copolímeros ramificados en el caso del PCL-triol promedio de Mn 900. Los poliésteres finales resultantes comprendían un copolímero en bloque PLLA/PEG o un poli(L-lactida) ramificada con el PCL-triol, que se mezclaron con la PCL procedente del ROP de la CL contraparte de la LLA en el DESm precursor. Los dos sistemas de PLLA en forma de copolímero o PLLA ramificado junto con PCL presentaron propiedades diferentes, como la hidrofobicidad y el peso molecular, consecuencia de los macroiniciadores (PEG o PCL-triol) integrados en la cadena de la PLLA.

Los conocimientos generados sobre los DESm y su ROP para obtener poliésteres con peso molecular, cristalinidad, arquitectura polimérica, hidrofobicidad y degradabilidad controlados, se utilizaron para formular emulsiones alta mente concentradas estables (HIPE, high internal phase emulision por sus siglas en inglés), aceite-en-DESm, con la ayuda de un tensioactivo. La ROP de la fase continúa compuesta por LLA/CL DESm junto con los macroiniciadores (PEG o PCL-triol), y la posterior eliminación de la fase interna, dieron lugar a poliésteres macroporosos en 3D y con porosidad interconectados (poliHIPEs).

Además, estos materiales porosos mostraron estabilidad mecánica durante al menos 30 días en un ensayo de degradación en solución PBS (phosphate buffer solution por sus siglas en inglés) en condiciones fisiológicas simuladas, a pH 7,4 y 37 °C, y se estima que se degradan completamente en 14 semanas. Importante es que gracias a su hidrofobicidad y su adecuada superficie en toda la macroporosidad interna, los poliHIPEs mostraron un excelente rendimiento en la absorción de petróleo crudo con una. tasa de 2 g g^{-1} a temperatura ambiente.

En resumen, en esta Tesis, demostramos que es factible modificar las propiedades de los poliésteres obtenidos a partir de la ROP de diferentes DESm compuestos por lactidas y lactonas, que no han sido reportados en la literatura. Las propiedades de los poliésteres obtenidos por ROP de DESm resultan de la interacción de la adecuada selección de los monómeros que componen el DESm, incluyendo macroiniciadores y organocatalizadores, y las condiciones de síntesis, como temperatura y el contenido de agua. La ROP de DESm destaca como una alternativa sostenible para obtener poliésteres biodegradables, ya que se excluyen los catalizadores metálicos y los solventes orgánicos volátiles. Además, se puede obtener una variedad de arquitecturas de poliésteres en condiciones a bajas temperaturas, además los productos finales no requieren adicionales etapas de purificación específicos para eliminar los organocatalizadores. Por último, se aprovechan la viscosidad y la polaridad de las mezclas eutécticas de lactonas y lactidas para preparar poliésteres macroporosos, interconectados y biodegradables mediante las emulsiones concentradas no acuosas utilizadas como molde HIPEs. Estos hallazgos suponen un avance significativo en el camino del desarrollo de protocolos más sustentables para la creación de membranas o andamios compuestos por poliésteres. Así, la ROP de DESm llevada a cabo a bajas temperaturas y en ausencia de solventes orgánicos, lo que hace prometedora como marco sostenible en la preparación de polímeros biodegradables para aplicaciones biomédicas y tecnologías de separación.

Acknowledgments

Thank you, God, for allowing me to complete this journey, please guide me to the next step.

I am in the last stage of completing my Doctorate, which has been a personal dream that I always wished to achieve. During my time in the Academy, I have received support, assistance, advice, encouragement, and learned new skills that will help me be better in the following stages of my life.

My deepest gratitude to my supervisors, Dr. Josué David Mota Morales and Prof. dr. Katja Loos, and my co-supervisor, Dr. Dina Maniar, who worked with me throughout the project. All three supported me every step of the project and without their help and guidance I would not have been able to complete this project.

Josué, you have supported me during my entire PhD, since the moment we selected the topic, you supported me in setting the scope and definition. We discussed progress constantly and I always got feedback from you. I admired the quickness with which you processed information whereas I sometimes was unable to keep up with you. Thank you for giving me the flexibility to explore the project and create new results. Moreover, you not only helped me in the academic part, you were also there in the administrative bits, where we often encountered setbacks. Finally, thank you for giving me your friendship, and opening the doors of your house to me, together, with the members of the "Laboratorio de polímeros", we had a lot of fun. The thing I can say for certain is that I learnt a lot from you.

Katja, thank you for allowing me to be part of the “Macromolecular Chemistry and New Polymeric Materials” research group this year. Thank you for the confidence you showed when including my project in your group. Despite my limited time, we were able to achieve excellent results, and with this experience I was able to enrich myself with new ideas and skills. I feel that with more time we could produce more outstanding results.

Dina, you were there during the final stage of my project, but you still helped me a lot. You were a great support and gave me a lot of focus. You understood how hard it was for me to be away from my family. I am thankful that Katja selected you as my co-supervisor, from the first meeting, you explained to me the requirements of my degree. I admire your serenity and patience. I would have liked to continue in Zernike, and I think we could have come up with further projects.

I would also like to express my gratitude to my committee at UNAM, Dr. Larissa Alexandrova and Dr. Jorge Herrera Ordoñez, who were always aware of my progress, sending feedback and comments on my project. I thank them for all their time and efforts throughout this project.

This thesis has received great help from many colleagues, collaborators, and technical support in both research groups. To the esteemed technical staff of UNAM, at the Center for Applied Physics and Advanced Technology (CFATA), I wish to express my sincere appreciation for the invaluable technical assistance provided by Dra. Beatriz Marcela Millán Malo (National Laboratory of Materials Characterization with ISO 9001:2015 Certification), Dra. Blanca Edith Millán Chiu, Dr. Mario Enrique Rodríguez García, M.Sc. Manuel Aguilar Franco and Guillermo Vázquez. Their unconditional support in the fields of optical microscopy, X-ray diffraction, use of FTIR equipment and scanning electron microscopy, respectively, has been fundamental to the success of my research efforts.

In addition, I would like to express my sincere thanks to my study center director, Dr. José Luis Aragón Vera, for his invaluable guidance and support throughout my PhD. His expertise and encouragement have been indispensable in shaping my academic and professional growth.

To my beloved administrative staff: Diana Arias, Concepción Arellano, Esther Carrillo and Luisa Resendiz, who always accompanied me. To Dr. Luis Enrique Sansores, coordinator of the graduate program, who has always been a very important support in the double degree program and Dr. Remy Avila, coordinator of the graduate program in my faculty, as well as the Coordinación General de Estudios de Posgrado.

This project would not have been possible without the technical support of Zernike. Jur J.van Dijken, thank you very much for all your technical help with the thermal analysis techniques such as TGA and DSC. Albert J.J. Woortman, you assisted me greatly with the GPC measurements, for which I am very thankful, as well as Pieter van der Meulen who aided me with NMR spectroscopy.

Technical support was also provided by Antonio Martínez-Richa for his contributions in thermal analysis, Dr. José Román Torres Lubián who always had time to talk, give advice, and contribute to the project in NMR analysis, and Dra. María Concepción Gutiérrez Pérez who assisted a lot with MALDI-TOF analysis, and our email conversations were always very enlightening.

Of course, this project was possible thanks to those who helped me adapt and guided me during the early days in Groningen. Karin, you were always so nice and supportive, guiding me in all the administrative matters, in getting access to the facilities and the equipment, I really admire the cheerfulness you transmitted. I would also like to thank my colleagues such as Fitrila, who helped me adapt easily during the beginning of my stay in the lab, I thank you very much for your help. Lena, you were a great support all the time. Julian, I appreciate your friendship and warm welcome, thank you for your help with UV-VIS spectroscopy, my family is very grateful for all you did for me. Aldo, you were my partner in the lab, and we always supported each other. Chongnan, you were always there for me in the lab. Theophile, thank you very much for helping me with different topics including research talks and characterization techniques, not forgetting your help in TEM, DLS and AMF techniques, you are a very sincere person. Dina, Julian and Teo, all of you knew how difficult it was for me to be away from my family and the health issues I faced, helping me overcome those hardships.

To my colleagues in the Polymer group at CFATA, Saul, Elizabeth, Griselda, Priscila, Angelo, Silvia and Kaori. I am grateful that we have been able to work together during our projects and often work in parallel, messages you sent never fail to make me smile, I realized that Josue has changed with you. One thing I know for sure is that you have chosen the best advisor.

In Groningen I met my roommate, Raneem. The first time we got in touch was by video conference, afterwards, I spoke to her about my family, and she also knew about the struggles I faced being far away from them. As time passed, she became my friend, confident and finally I considered her as my sister. I am extremely grateful that she always cared about me. It hurt for me to leave her, knowing that my sister is staying alone.

Prof. Marleen Kamperman and Prof. Giuseppe Portale, you were always very kind and always greeted me with a smile. Albeit, I did not have the opportunity to work directly with you, there was a possibility to begin a collaboration with Gosia and Gianni, which I unfortunately did not have the time to move forward with.

Piotr, Gianni, Renato, and Gosia thank you very much for your confidence, I regret not having enough time to collaborate, I hope one day we meet again to fulfill this unfinished project. In that sense, I would like to apologize to my colleagues from the polymer group for not being able to participate in so many activities, but I did not have enough time. I want to express my gratitude to Eleonora, Xiaohong Lan, Laura, Mokun Chen, Qi Chen, Luan, Corniek, Xia, Antonis, Adrivit, and Roberto.

Thanks to my colleagues in Mexico: Angel, Alejandro, Brenda, Dinorah, Diego, Raul, Gustavo, Ana Laura, for all your support. But I am particularly grateful to three Mexicans: Martha, you were attentive when I was sick, you also helped guide me in the development of my dissertation. It is funny that we never met personally, and all communication happened through the phone, many thanks for your help. Lina, you always helped me with the guidelines of my dissertation, you also gave me tips on how to adapt easily in Groningen, otherwise it would have been much more complicated. Huitzi, many thanks for being my family doctor here in Groningen. I apologize to all of you because I have not been able to join you in your reunions and enjoy the experience. However, time was limited for me. I appreciate your messages, inquiring about how I was doing, and how many of you were keeping an eye on me. I believe there is a very small Mexico here in Groningen.

Finally, to the person I love with all my heart and whom I thank for having shared with me this path called life. Erendira, my wife, you are the only person who believed in me and helped me fulfill this dream. I am very grateful to you and thanks to you I know that true love exists. My children Emmanuel and Vania, you were always the engine that pushed me forward, many times I thought about giving up but when I thought I would fail you made me keep going, I love you all with all my heart, thank you for having me as your father.

To my dad, my mom, my sisters Ely and Mireya, thank you for supporting me during this journey. To my brothers Aaron and Josué, thank you for worrying about me and Israel, thank you for trusting me.

This project has been funded by the Mexican Government through CONAHCYT, with additional financial support from UNAM through PAEP-UNAM and PAPIIT-UNAM, specifically through grant IA206022. Furthermore, we would like to express our sincere appreciation to the University of Groningen and the Faculty of Science and Engineering for their generous contributions to this endeavor. Crude oil was kindely provided by Nederlandse Aardolie Maatschappij (NAM).

List of publications

Gachuz E. J., **Castillo-Santillán M.,** Juarez-Moreno K., Maya-Cornejo J., Martinez-Richa A., Andrio A., Compañ V., Mota-Morales J. D. Electrical conductivity of an all-natural and biocompatible semi-interpenetrating polymer network containing a deep eutectic solvent. Green Chemistry, 2020, **17**, 22, 5785-5797. https://doi.org/10.1039/D0GC02274H

Castillo-Santillán M., Torres-Lubian J. R., Martinez-Richa A., Huerta-Marcial S. T., Gutierrez M. C., Loos K., Peréz-García M. G., Mota- Morales J. D. From polymer blends to a block copolymer: ring-opening polymerization of l-lactide/ε- caprolactone eutectic system. Polymer., 2022, **262**, 125432. https://doi.org/10.1016/j.polymer.2022.125432

Castillo-Santillán M., Maniar D., Torres-Lubian J. R., Gutierrez M. C., Quiñonez-Angulo P., Loos K., Mota-Morales J. D. Low-temperature and solventless ring-opening polymerization of eutectic mixtures of L- lactide and lactones for biodegradable polyesters. ACS Appl. Polym. Mater., 2023, **5**, 5111-5121. https://doi.org/10.1021/acsapm.3c00591.

Castillo-Santillán M., Quiñonez-Angulo P., Maniar D., Torres-Lubian J. R., Gutierrez M.C., Pelras T., Woortman A. J. J, Quiñonez-Angulo P., Chen Q., Peréz-García M. G., Loos K., Mota-Morales J. D. Ring-opening polymerization of emulsion-templated deep-eutectic system monomer for macroporous polyesters with controlled degradability. (Submitted).